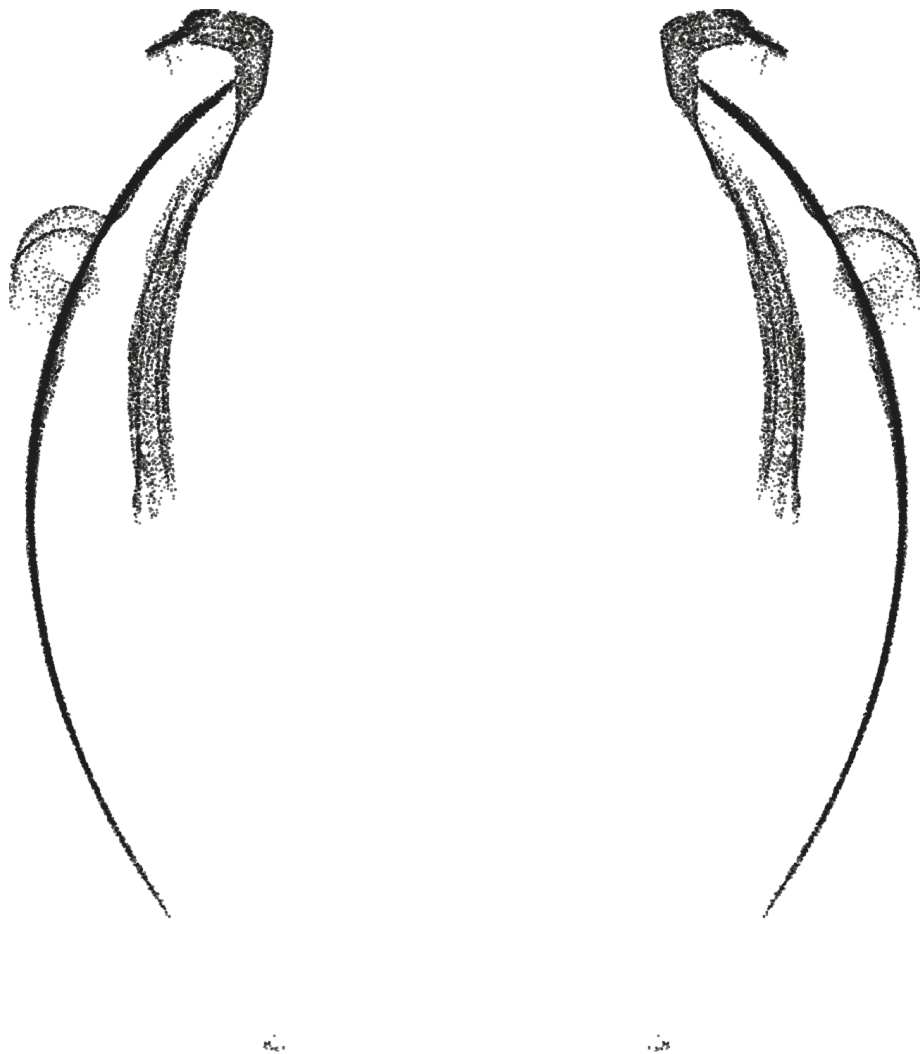


MV015c - Globular Ovoid Jar

An Exploration of Precision



Author: Stine Gerdes, arcsai.org

License: Creative Commons BY-NC-SA 4.0

Date: 2025-07-21

Version: 01.20



Petrie Museum, CC BY-NC-SA

Contents

Artifact Information 2

Alignment In The Cartesian Coordinate System 3

Statistics used throughout the report 5

Precision 6

 Circularity 6

 Concentricity 30

 Coaxiality 43

 Surface Variability 47

 Precision Score Of The Artifact 56

Analysis Roadmap 58

Appendix A - Comparison Of Circularity Measurements (Z-plane vs. surface-perpendicular) 59

Appendix B - Comparison Of Concentricity Measurements (Z-plane vs. surface-perpendicular) 69

Artifact Information

Artifact Data

| | |
|--------------------------|--|
| Collection | Petrie Museum of Egyptian Archaeology |
| Provenance ¹ | Petrie Museum of Egyptian Archaeology (London), recovered by Flinders Petrie |
| Provenience ² | Naqada Tomb T 16 (Naqada II) - Petrie Excavation |
| Attribution | Naqada II |

Museum information

| | |
|-------------|--|
| Ref. | LDUCE-UC4354 |
| Description | Stone vase, identified in museum register as black and white syenite, perhaps hornblende diorite (?), barrel-shaped type 39. From Naqada Tomb T 16 |
| URL | https://collections.ucl.ac.uk/Details/collect/6836 |

Maijers vessel classification³

| | |
|----------------------|--|
| Short classification | Globular Ovoid Jar |
| Long classification | The vessel is created in a closed form classified as a globular jar with a ovoid shape, a rounded rim. |

Physical properties

| | |
|------------------------------|---|
| Precision score ⁴ | 52 |
| Height (approximate) | 72 mm 2.83 in |
| Width (approximate) | 63 mm 2.48 in |
| Material | Black & White Syenite, perhaps Hornblende Diorite |
| Mohs Hardness ⁵ | 5.5 - 7 (Diorite) |
| Weight | |

Scan information

| | |
|------------------------------|--|
| Source | Max Fomitchev-Zamilov, 3D Scans of the Naqada Period Stone Vessels from the Petrie Museum of Egyptian and Sudanese Archeology, 2025. |
| Source file name | UC4354-hi.stl |
| Scan method | CMM |
| Scanner | Keyence VL -500 |
| Rated scan accuracy | 10 µm 0.41 thou |
| Scan date | 2025-05-12 |
| Scanned by | Max Fomitchev-Zamilov |
| Mesh decimation | None, raw scan file used in the analysis |
| Number of vertices | 293 330 |
| Mesh density ⁶ | 145 µm 5.70 thou |
| Max vertex distance | 1102 µm 43.371 thou |
| Min vertex distance | 22 µm 0.853 thou |
| Vertices per cm ² | 1912 (approximated) |
| Vertices per in ² | 12 335 (approximated) |

¹The verifiable chain of custody of an artifact

²The location or site where an artifact was recovered

³Vessel artifact classification developed by W. Arnold Maijer and described in his publication Masters of Stone, ISBN 978-90-829212-0-5

⁴The precision score metric is described in Precision Score Of The Artifact, p. 57

⁵The Mohs scale is an ordinal scale, from 1 to 10, describing the materials resistance to abrasion (the ability of harder material to scratch softer material)

⁶Median distance between vertices

Alignment In The Cartesian Coordinate System

For precise and valid measurements of the vessel's geometry to be possible, the points of the scanned dataset must first and foremost be placed optimally in a Cartesian coordinate system. Several alignment methods and algorithms have been tested on a number of different vessels to determine the best way to achieve optimal alignment.

Any misalignment of the artifact will increase the error of the precision measurements, due to the distortion/wobble effect caused by the misaligned object. To visualize this distortion, we can consider a representation of the three-dimensional point cloud data, folded to a two-dimensional plane. This folded representation is obtained by rotating all scanned points around an assumed center axis to $y = 0, x > 0$, thus resulting in a two-dimensional profile representation of all scanned vertices in the object.

Figure 1 illustrates this effect on a ideal ellipsoid. In the first image, the ellipsoid is perfectly aligned, resulting in a narrow and precise two-dimensional folded profile. As misalignments are introduced, the two-dimensional profile increases in width, visually showing the distortion, causing the error in the precision measurements to increase. While easy to understand visually, this distortion can also be objectively quantified, and as such used to compare the fitness of different assumed center axes against each other, and further to create an automated and solid process for optimal Cartesian alignment of the scan data.

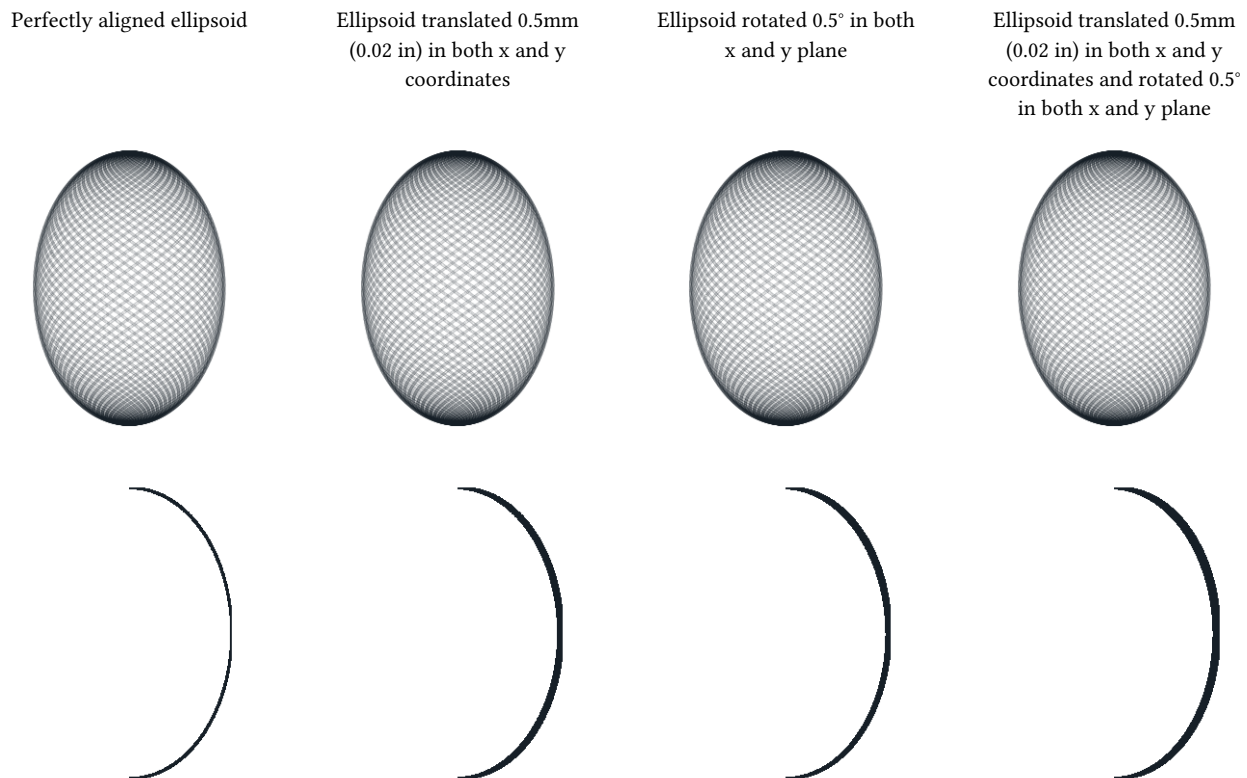


Figure 1: Distortion caused by a misalignment of the artifact

In contemporary metrology analysis of modern production objects, it is common to align the object in a Cartesian coordinate system by fitting a flat surface of the object to a reference plane in the coordinate system, cylindrical features to an ideal cylinder etc., or by using specific markers placed on the object in the design process. This methodology, however, is inadequate for the ancient objects in question. Most scanned artifacts, do not have a valid flat surface which could be aligned to a plane in the Cartesian coordinate system; most surfaces seem to be curved. Some artifacts do have a flat base, however this is often a worn area of the artifact and practical tests have shown that alignment to such surfaces will not produce optimal alignment of the scan data.

As conventional methods of alignment do not always yield good results with these types of artifacts, a more adequate method of alignment has been developed to enable precise measurements and statistical analysis of the scan data.

To find the optimal position of the vessel in the coordinate system, a range of rotation and translation tests are carried out to find the best fit of the central axis.

Based on the assumption that the analyzed object was created using a rotational process, and thus have symmetry around a central axis, the alignment of the artifact is carried out in a two-step process. An overview of this process is given below.

The artifact is placed in a Cartesian coordinate system, in an initially unaligned state. The first step in the alignment process estimates the central rotational axis of the vessel, by analyzing the coaxiality of thin cross-section slices of the vessel. The slices will be as thin as possible based on the mesh density of the scan, while still ensuring enough data points in each slice to be statistically valid.

For each slice, circular regression⁷ (estimate of best fit circle) is used to estimate the center point of this slice. Combined over the total Z-axis range of the vessel, these center points provide us with an indicator of the incline and position of the vessel's central axis.

The next step will optimize the center axis alignment by progressively minimizing the deviation (perpendicular to the surface curvature) of the two-dimensional profile, see Figure 1. By ascertaining and comparing the resulting fit of many thousands of different potential rotations, the best fit alignment of the scan data can be estimated, and an optimal center axis (in relation to the data points) can be reconstructed. The actual three-dimensional point-cloud is then aligned to this axis, by rotating and translating the scanned data points to match the Z-axis of the Cartesian coordinate system.

To enable extensive analysis of the full surface of the artifact, the mesh is split into exterior and interior surfaces. The exterior surface is aligned independently of interior data points, providing a baseline for exterior quality assessment. The interior surface is represented by two alignments:

- Aligned with the exterior mesh to analyze concentricity, and
- Aligned separately to assess its precision and compare the true tilt/displacement between interior and exterior surfaces.

⁷Circle regression algorithm used: Kenichi Kanatani, Prasanna Rangarajan, "Hyper least squares fitting of circles and ellipses" Computational Statistics & Data Analysis, Vol. 55, pages 2197-2208, (2011)

Statistics used throughout the report

This section provides an overview of the key statistical and model-evaluation metrics employed throughout the report to analyze dataset variability, model fit, and predictive accuracy.

Each measure is introduced with its mathematical formulation, practical interpretation, and explicit reference to how it is calculated in the context of the evaluated models and residuals. Together, these metrics quantify:

- Data variability (e.g., MAD, Standard Deviation, Range).
- Model accuracy (e.g., MSD, RMSD).
- Robustness vs. sensitivity to extreme values and central tendencies.

Mean Squared Deviation (MSD), also known as Mean Squared Error (MSE).

$$\text{MSD} = \frac{\sum_{i=1}^n (y_i - \hat{y})^2}{n}$$

The Mean Squared Deviation (MSD) measures the average magnitude of squared differences between observed (y_i) and predicted (\hat{y}) values, calculated as the mean of squared residuals, and is used as a measure of discrepancy in regression and model-fitting contexts.

This measure amplifies the influence of larger deviations through squaring, emphasizes imperfections in the observed data, but retains sensitivity to outliers.

Root Mean Squared Deviation (RMSD), also known as Root Mean Squared Error (RMSE).

$$\text{RMSD} = \sqrt{\frac{\sum_{i=1}^n (y_i - \hat{y})^2}{n}}$$

The Root Mean Square Deviation (RMSD) measures the magnitude of differences between observed (y_i) and predicted (\hat{y}) values by calculating the square root of the average of squared residuals.

RMSD is a commonly used measure of discrepancy in regression and model-fitting contexts. It quantifies the average magnitude of residuals while retaining sensitivity to larger deviations (via squaring), making it particularly useful for evaluating model accuracy.

Standard Deviation (SD)

$$s = \sqrt{\frac{\sum_{i=1}^n (y_i - \bar{y})^2}{n - 1}}$$

The Standard Deviation measures the spread of data (y_i) around the mean (\bar{y}) by calculating the square root of the average of squared differences between each value and the mean.

It is sensitive to outliers as it amplifies their influence through squaring, in contrast to MAD.

Throughout this report, the Standard Deviation is calculated using the absolute residuals from regression models.

Median Absolute Deviation (MedianAD)

$$\text{MedianAD} = \text{median}(|y_i - \text{median}(y)|)$$

The Median Absolute Deviation (MAD) measures the spread of data around the median by calculating the median of absolute differences between each value and the median.

MAD is a robust measure of spread, analogous to the interquartile range (a robust measure centered on the middle 50% of data), and differs from the standard deviation in that it minimizes the impact of outliers.

Throughout this report, the MAD is calculated using the absolute values of residuals from regression models.

Range

$$\max(y_i) - \min(y_i)$$

The Range measures the spread of a dataset by calculating the difference between the maximum and minimum values.

The Range is a simple measure of spread, capturing the full extent of variability. Range is very sensitive to extreme values, as it is entirely determined by the two most extreme data points.

Throughout this report, the Range is calculated using the full range of residuals from regression models.

Precision

To explore the manufacturing precision of the artifact in depth, the following analysis have been carried out:

- Circularity around the axis of symmetry is examined in detail at selected cross-sections.
- Overall circularity around the axis of symmetry is measured for the full height of the vessel (areas of the vessel with extensive damage are not taken into account for this metric).
- Concentricity of the vessel between selected cross-sections are examined in detail to determine if the existence of an axis of rotation in the manufacture of the object can be established.
- The coaxiality of the vessel is analyzed to explore the precision of the central axis of the object.
- The surface variability is analyzed and visualized on through a heatmap.

Circularity

Circularity is the measurement of how round the surface of an object is, optionally in reference to a datum axis. The *circularity tolerance* is the radial distance of two circles, each with their centers in the datum axis, and each of them conforming, respectively, to the minimum and maximum deviations of the data-set to a true circle, see Figure 2.

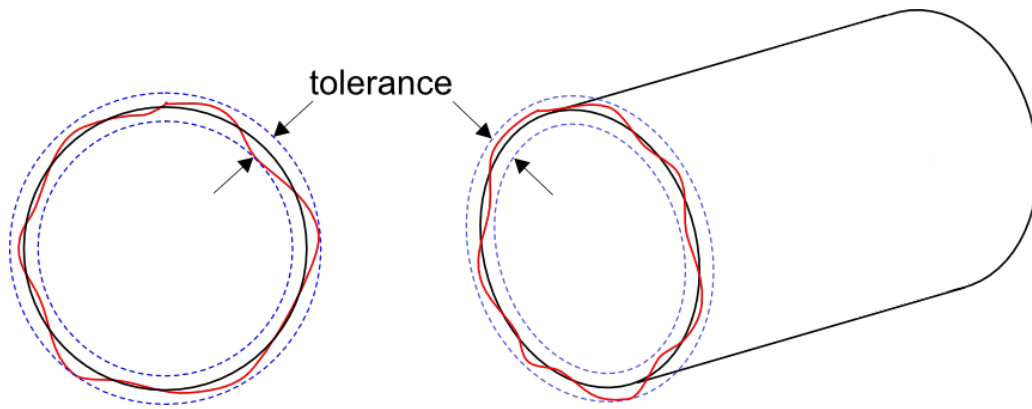


Figure 2: Circularity tolerance.

Circularity is examined at different cross-sections of the vessel, using the established Z-axis as the datum axis (axis of symmetry). The distance between the scanned points in the local datum plane is measured to determine the range between the two concentric circles encompassing the measured points, see Figure 3.

Referencing all of the individual circularity measurements to the global (reconstructed) axis of symmetry of the object, allows us to ascertain not only circularity of local features of the object, but how well circularity was *maintained* over the entire manufacturing process. This is an important distinction, which may be able to provide valuable insights into requirements of the construction methods. For reference, and seeing that the variance in local circularity also holds interest, measurements of circularity of the vessel without reference to the axis of symmetry can additionally be found in the Concentricity, p. 31.

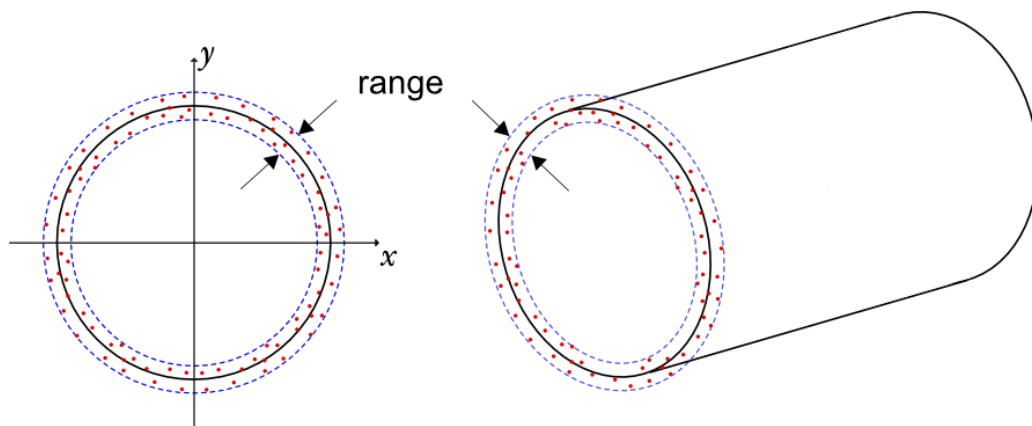


Figure 3: Circularity measurements.

If the circularity is determined from slices of the vessel exclusively in the *Z-plane* (actually measuring the cylindricity of a very thin slices of the vessel, in an attempt to approximate circularity), this would - in some areas - introduce significant distortion (increasing measurement errors) in the samples, due to the curvature of the vessel's surface.

Each sample slice of the vessel is therefore obtained perpendicular to the surface curvature, see Figure 6 to Figure 16. The measurements are taken conservatively without filtration of potential outliers.

To explore the potential distortion caused by obtaining samples in the Z-plane only, please refer to Appendix A, where measurements in the Z-plane and measurements perpendicular to surface curvature are compared side by side.

Detailed circularity measurements of selected points

Circularity measurements across a range of selected slices of the vessel (see Table 1) have been analyzed in-depth, and detailed plots of each measurement is provided. Furthermore, full circularity measurements are shown for each available scanned surface including a detailed plot to visualize the circularity of all areas of the vessel.

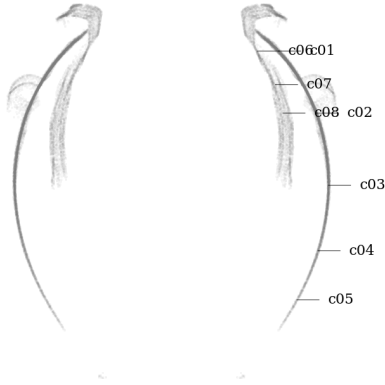


Figure 4: Circularity measurement sample locations, full mesh aligned with exterior surface

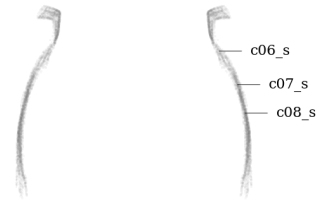


Figure 5: Circularity measurement sample location, separately aligned interior mesh

Metric

| Tag | Area | Measured deviation ⁸ | Residuals | | | | Sample size | Slice | | |
|-------|---------------|---------------------------------|-----------|-------------------|-------------------|-------|-------------|--------|----------|----------------------|
| | | | Range | RMSD ⁹ | MAD ¹⁰ | SD | | Height | Z coord. | Radius ¹¹ |
| | | mm | mm | mm | mm | mm | | mm | mm | mm |
| c01 | exterior | Ø42.631±0.411 | 0.796 | 0.163 | 0.060 | 0.099 | 2099 | 0.200 | 64.672 | 21.316 |
| c02 | exterior | Ø57.616±0.608 | 0.976 | 0.161 | 0.053 | 0.108 | 2204 | 0.200 | 52.303 | 28.808 |
| c03 | exterior | Ø62.507±0.269 | 0.503 | 0.112 | 0.046 | 0.068 | 1756 | 0.200 | 37.904 | 31.254 |
| c04 | exterior | Ø58.321±0.244 | 0.463 | 0.117 | 0.051 | 0.060 | 901 | 0.200 | 24.858 | 29.160 |
| c05 | exterior | Ø49.929±0.218 | 0.406 | 0.090 | 0.034 | 0.054 | 334 | 0.200 | 15.082 | 24.965 |
| c06 | interior sep. | Ø34.082±0.745 | 1.411 | 0.324 | 0.187 | 0.191 | 556 | 0.200 | 64.672 | 17.041 |
| c06_s | interior sep. | Ø34.082±0.745 | 1.411 | 0.324 | 0.187 | 0.191 | 556 | 0.200 | 64.672 | 17.041 |
| c07 | interior sep. | Ø41.386±0.727 | 1.275 | 0.287 | 0.123 | 0.175 | 1104 | 0.200 | 58.007 | 20.693 |
| c07_s | interior sep. | Ø41.386±0.727 | 1.275 | 0.287 | 0.123 | 0.175 | 1104 | 0.200 | 58.007 | 20.693 |
| c08 | interior sep. | Ø44.340±0.589 | 0.945 | 0.209 | 0.080 | 0.123 | 1307 | 0.200 | 52.303 | 22.170 |
| c08_s | interior sep. | Ø44.340±0.589 | 0.945 | 0.209 | 0.080 | 0.123 | 1307 | 0.200 | 52.303 | 22.170 |

Imperial

| Tag | Area | Measured deviation ⁸ | Residuals | | | | Sample size | Slice | | |
|-------|---------------|---------------------------------|-----------|-------------------|-------------------|--------|-------------|--------|----------|----------------------|
| | | | Range | RMSD ⁹ | MAD ¹⁰ | SD | | Height | Z coord. | Radius ¹¹ |
| | | in | in | in | in | in | | in | in | in |
| c01 | exterior | Ø1.6784±0.0162 | 0.0314 | 0.0064 | 0.0024 | 0.0039 | 2099 | 0.0079 | 2.5461 | 0.8392 |
| c02 | exterior | Ø2.2684±0.0239 | 0.0384 | 0.0063 | 0.0021 | 0.0043 | 2204 | 0.0079 | 2.0592 | 1.1342 |
| c03 | exterior | Ø2.4609±0.0106 | 0.0198 | 0.0044 | 0.0018 | 0.0027 | 1756 | 0.0079 | 1.4923 | 1.2305 |
| c04 | exterior | Ø2.2961±0.0096 | 0.0182 | 0.0046 | 0.0020 | 0.0024 | 901 | 0.0079 | 0.9786 | 1.1480 |
| c05 | exterior | Ø1.9657±0.0086 | 0.0160 | 0.0036 | 0.0014 | 0.0021 | 334 | 0.0079 | 0.5938 | 0.9829 |
| c06 | interior sep. | Ø1.3418±0.0293 | 0.0555 | 0.0128 | 0.0074 | 0.0075 | 556 | 0.0079 | 2.5461 | 0.6709 |
| c06_s | interior sep. | Ø1.3418±0.0293 | 0.0555 | 0.0128 | 0.0074 | 0.0075 | 556 | 0.0079 | 2.5461 | 0.6709 |
| c07 | interior sep. | Ø1.6294±0.0286 | 0.0502 | 0.0113 | 0.0048 | 0.0069 | 1104 | 0.0079 | 2.2838 | 0.8147 |
| c07_s | interior sep. | Ø1.6294±0.0286 | 0.0502 | 0.0113 | 0.0048 | 0.0069 | 1104 | 0.0079 | 2.2838 | 0.8147 |
| c08 | interior sep. | Ø1.7457±0.0232 | 0.0372 | 0.0082 | 0.0031 | 0.0048 | 1307 | 0.0079 | 2.0592 | 0.8728 |
| c08_s | interior sep. | Ø1.7457±0.0232 | 0.0372 | 0.0082 | 0.0031 | 0.0048 | 1307 | 0.0079 | 2.0592 | 0.8728 |

Table 1: Detailed circularity measurements at selected samples of MV015c.

Figure 6 to Figure 16 shows a detailed plots of each circularity measurement.

⁸Sample diameter Ø± maximum measured deviation from measured radius

⁹Root mean square deviation (RMSD) also called Root mean square error (RMSE)

¹⁰Median absolute deviation

¹¹Median sample radius from z-axis

Graphical overview of circularity measurement c01

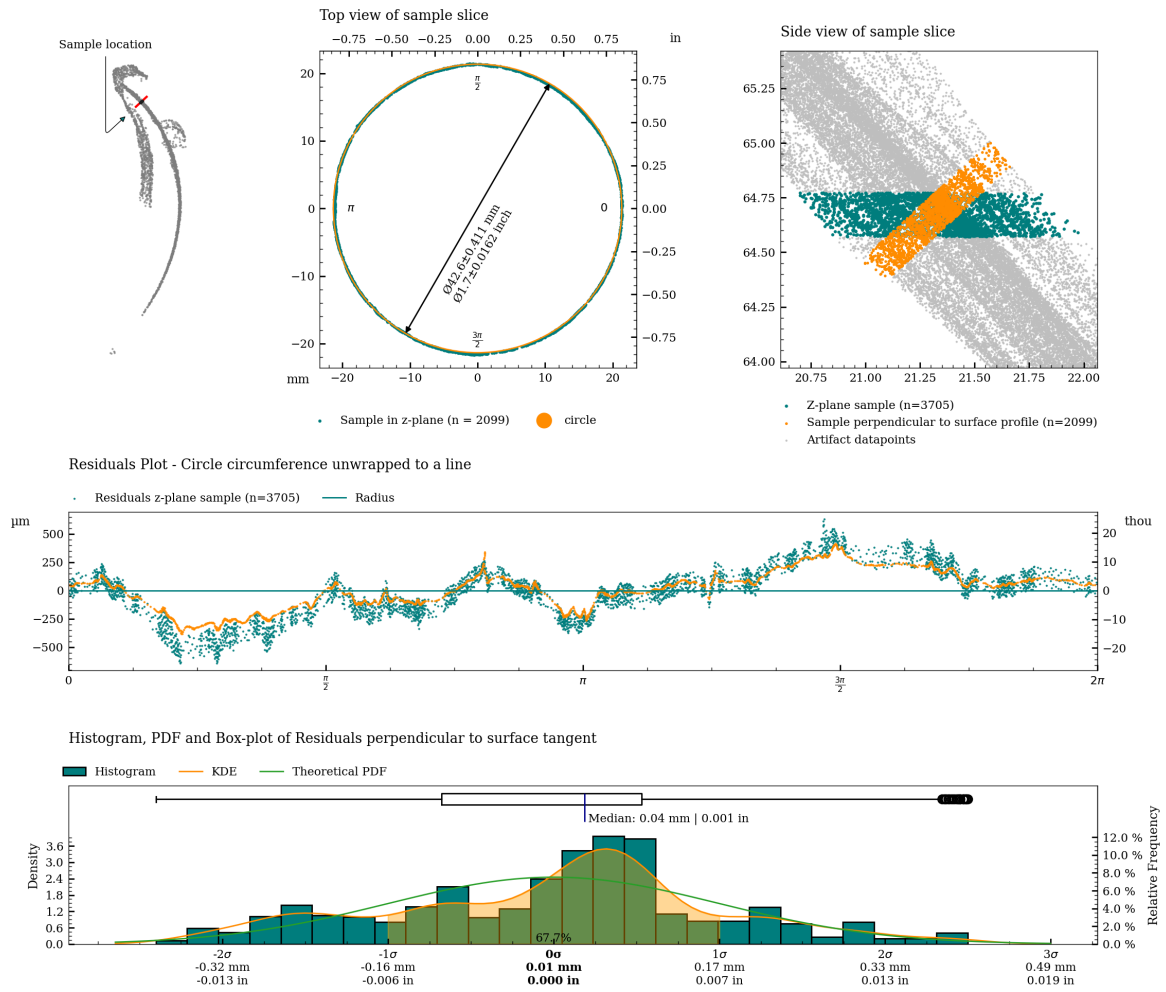


Figure 6: Charts with statistics for the measurement of c01.

Graphical overview of circularity measurement c02

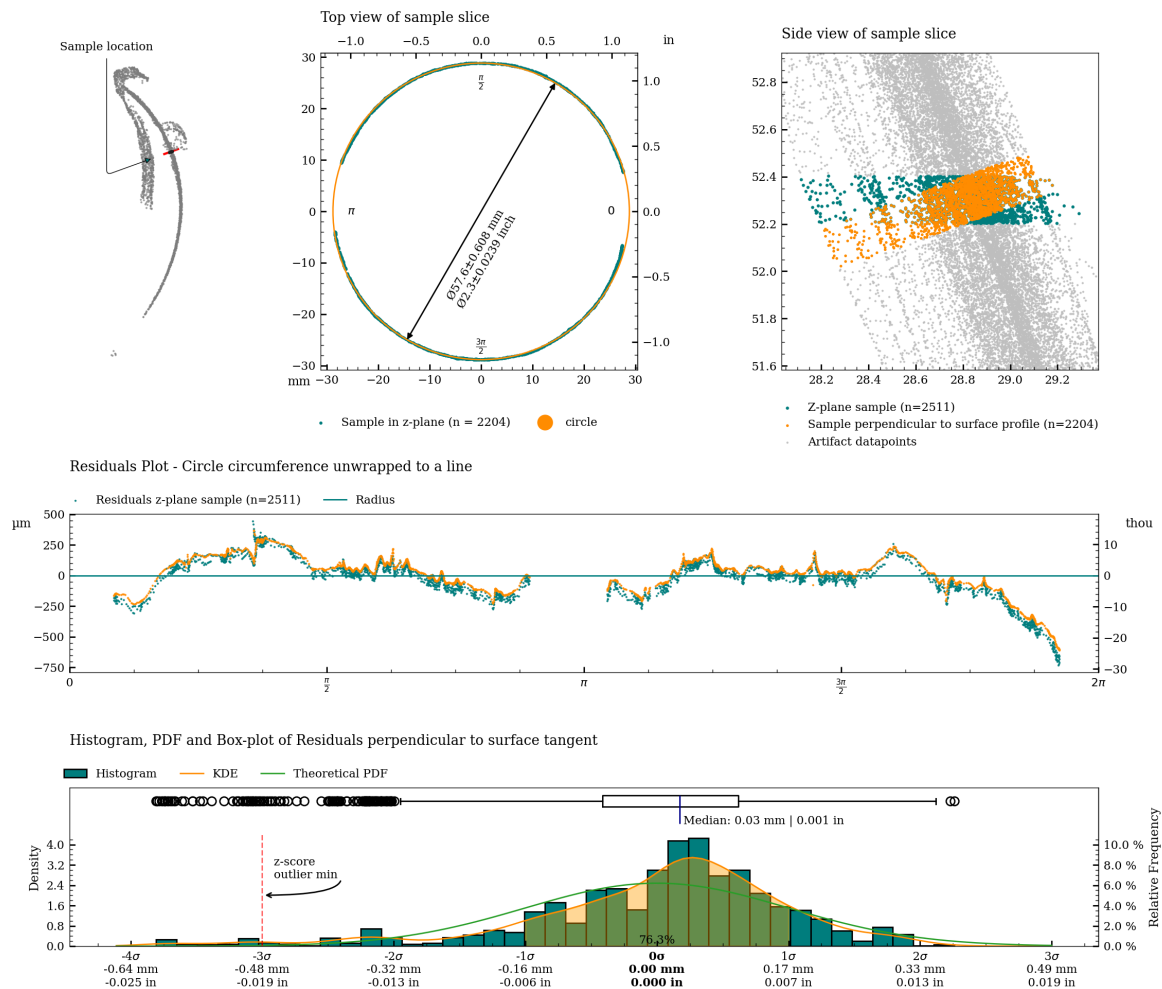


Figure 7: Charts with statistics for the measurement of c02.

Graphical overview of circularity measurement c03

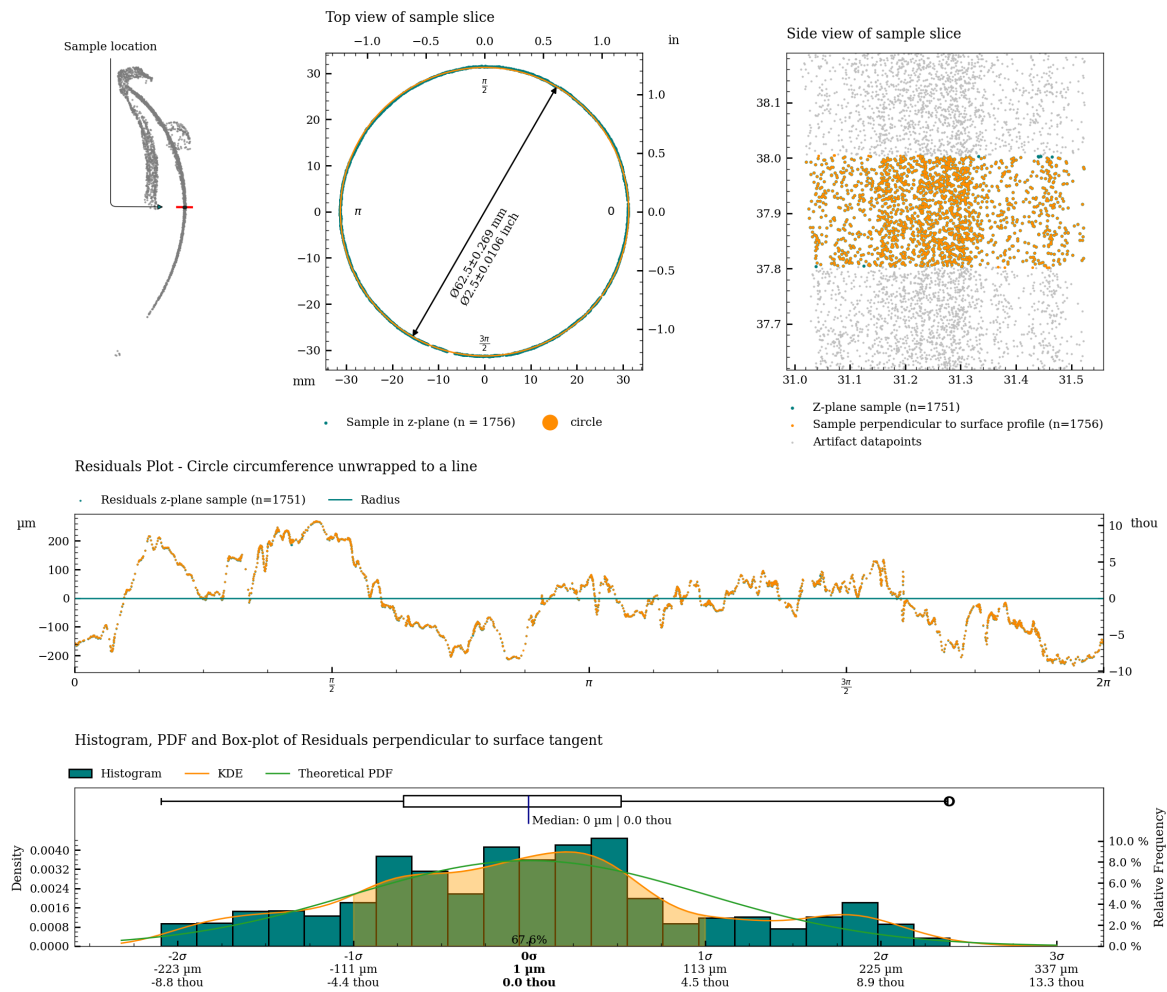


Figure 8: Charts with statistics for the measurement of c03.

Graphical overview of circularity measurement c04

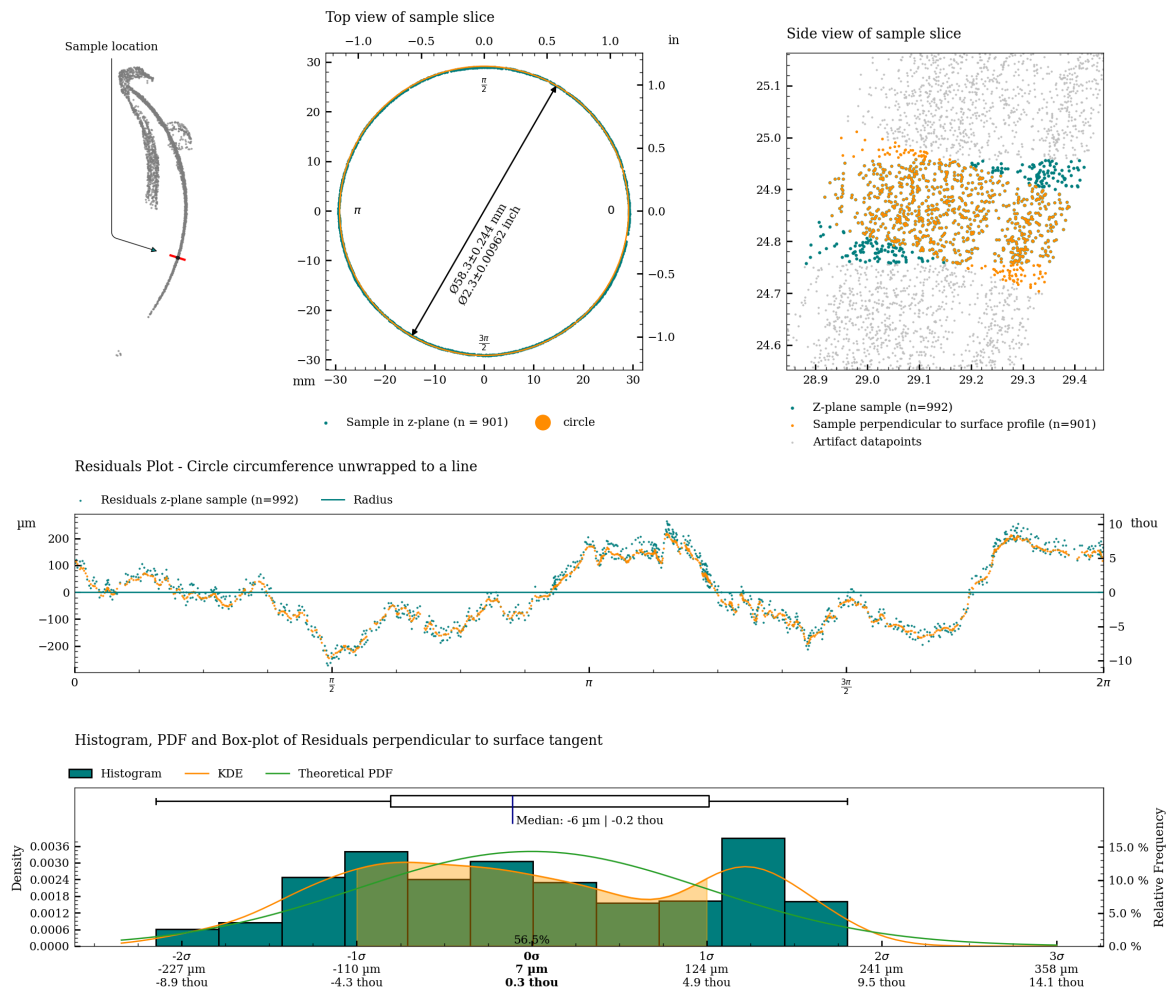


Figure 9: Charts with statistics for the measurement of c04.

Graphical overview of circularity measurement c05

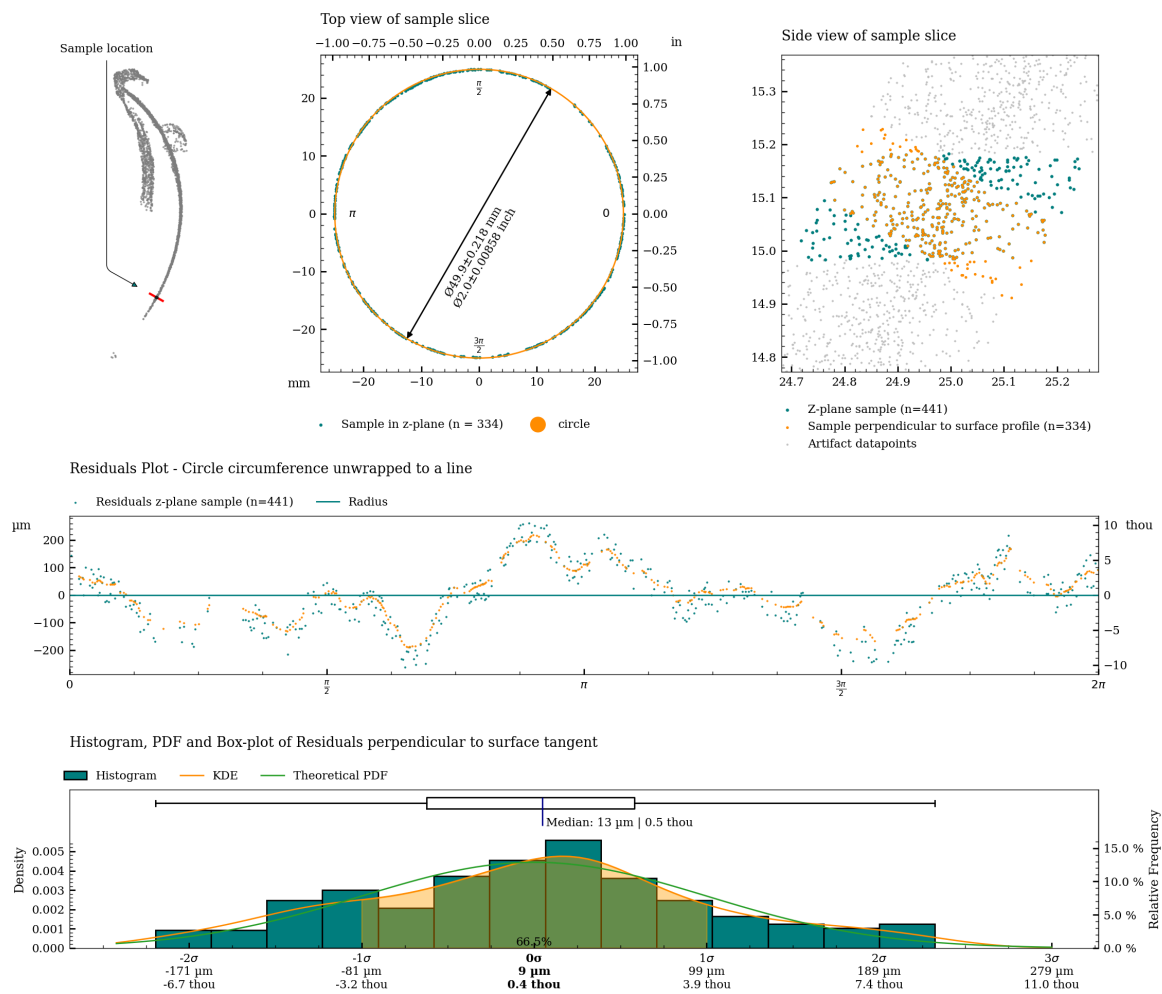


Figure 10: Charts with statistics for the measurement of c05.

Graphical overview of circularity measurement c06

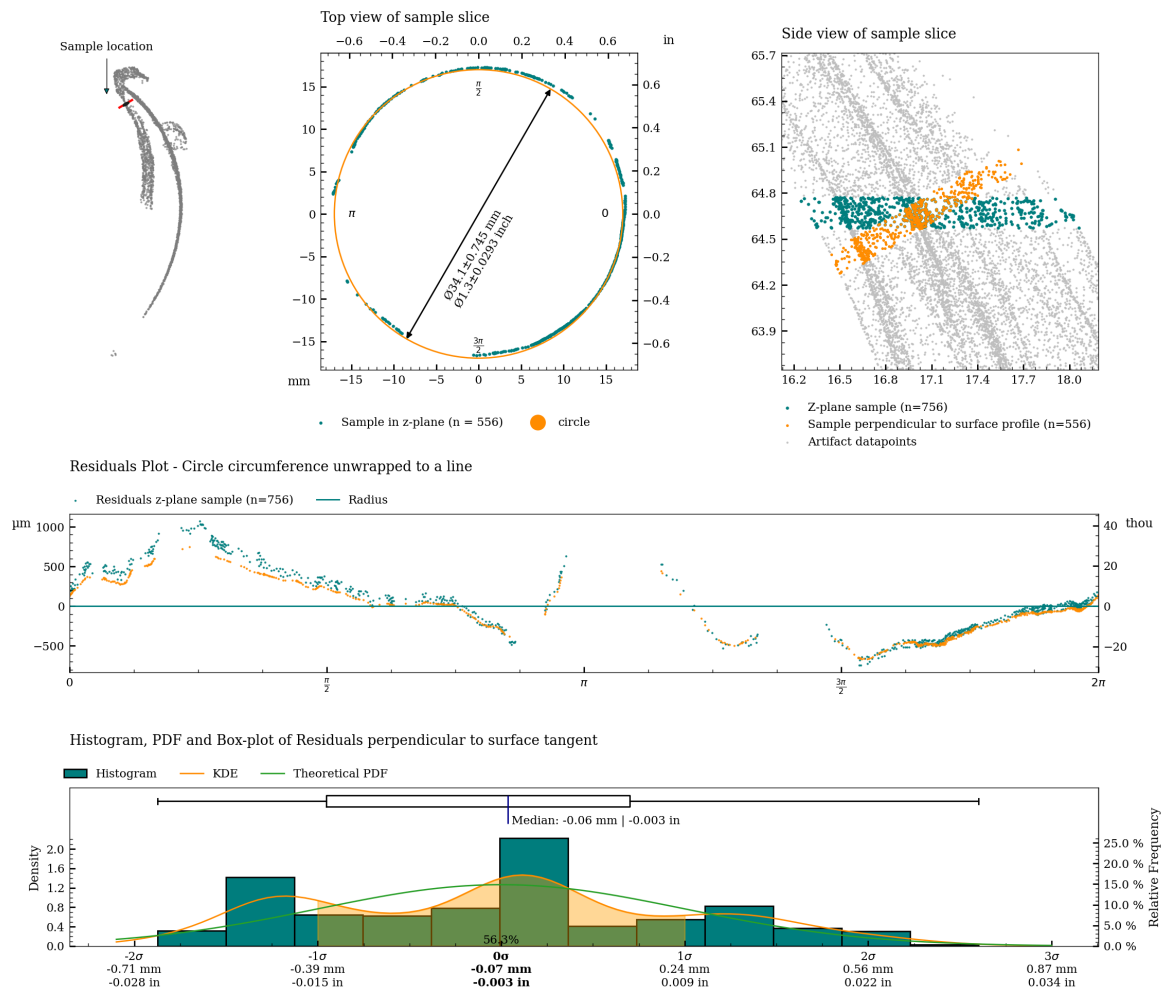


Figure 11: Charts with statistics for the measurement of c06.

Graphical overview of circularity measurement c06_s

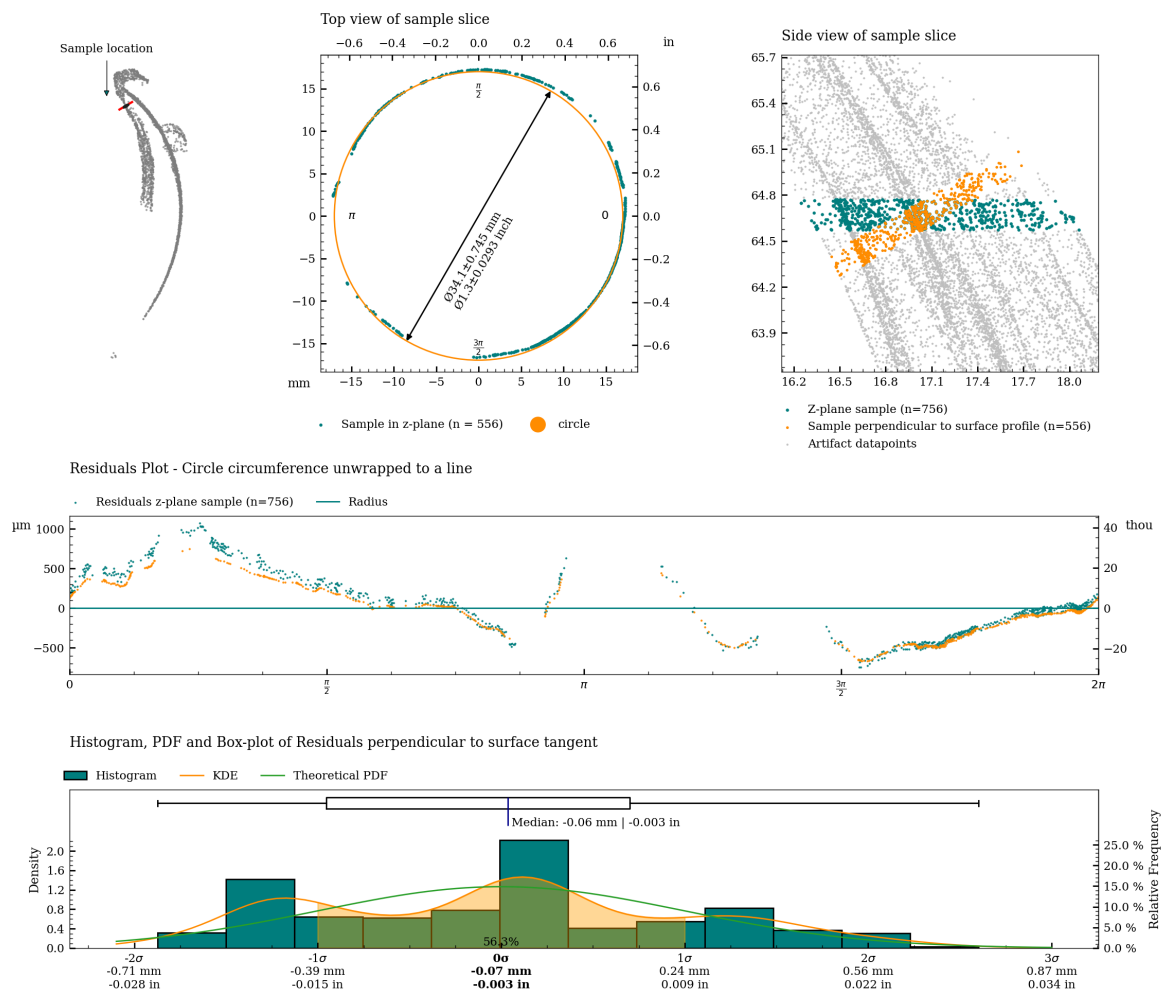


Figure 12: Charts with statistics for the measurement of c06_s.

Graphical overview of circularity measurement c07

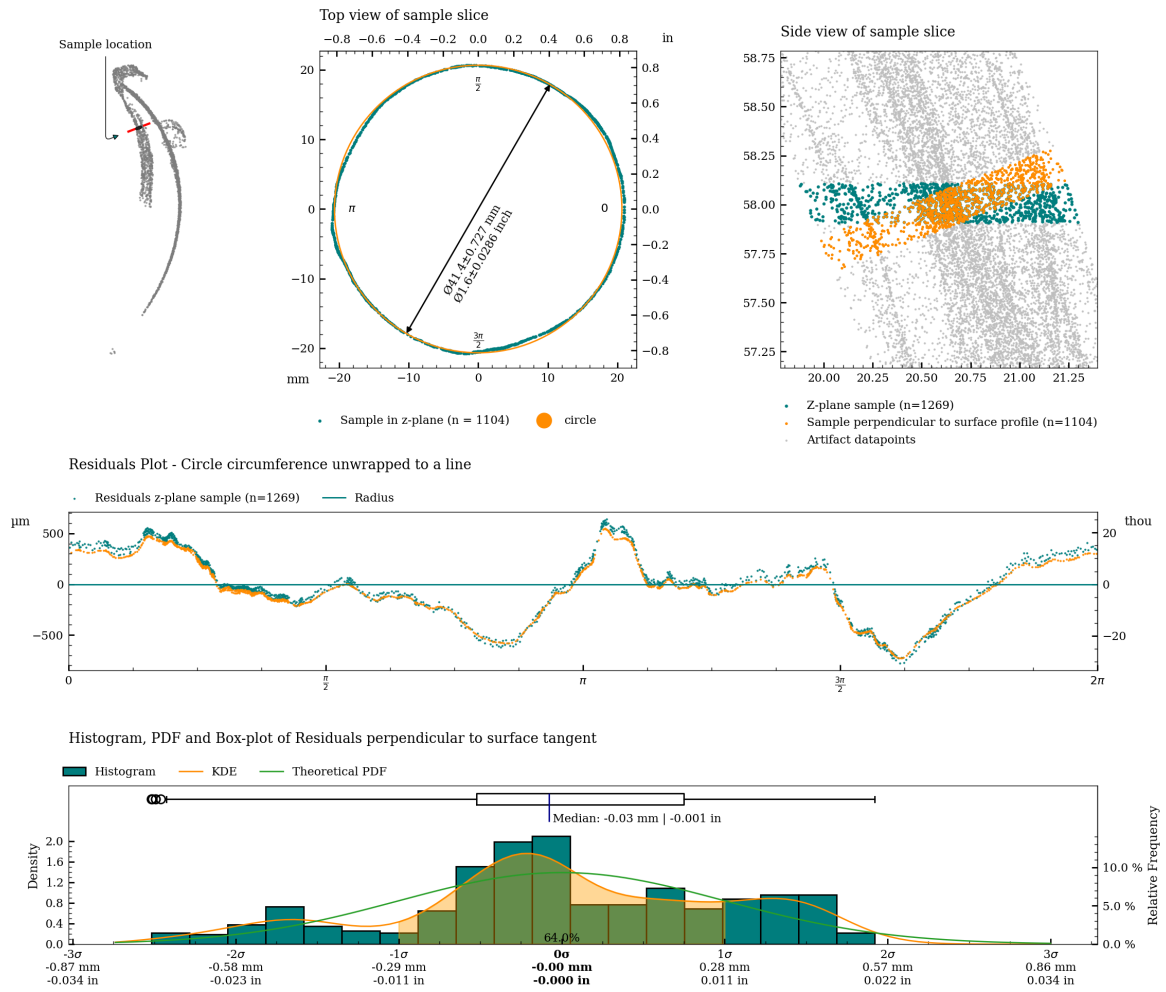


Figure 13: Charts with statistics for the measurement of c07.

Graphical overview of circularity measurement c07_s

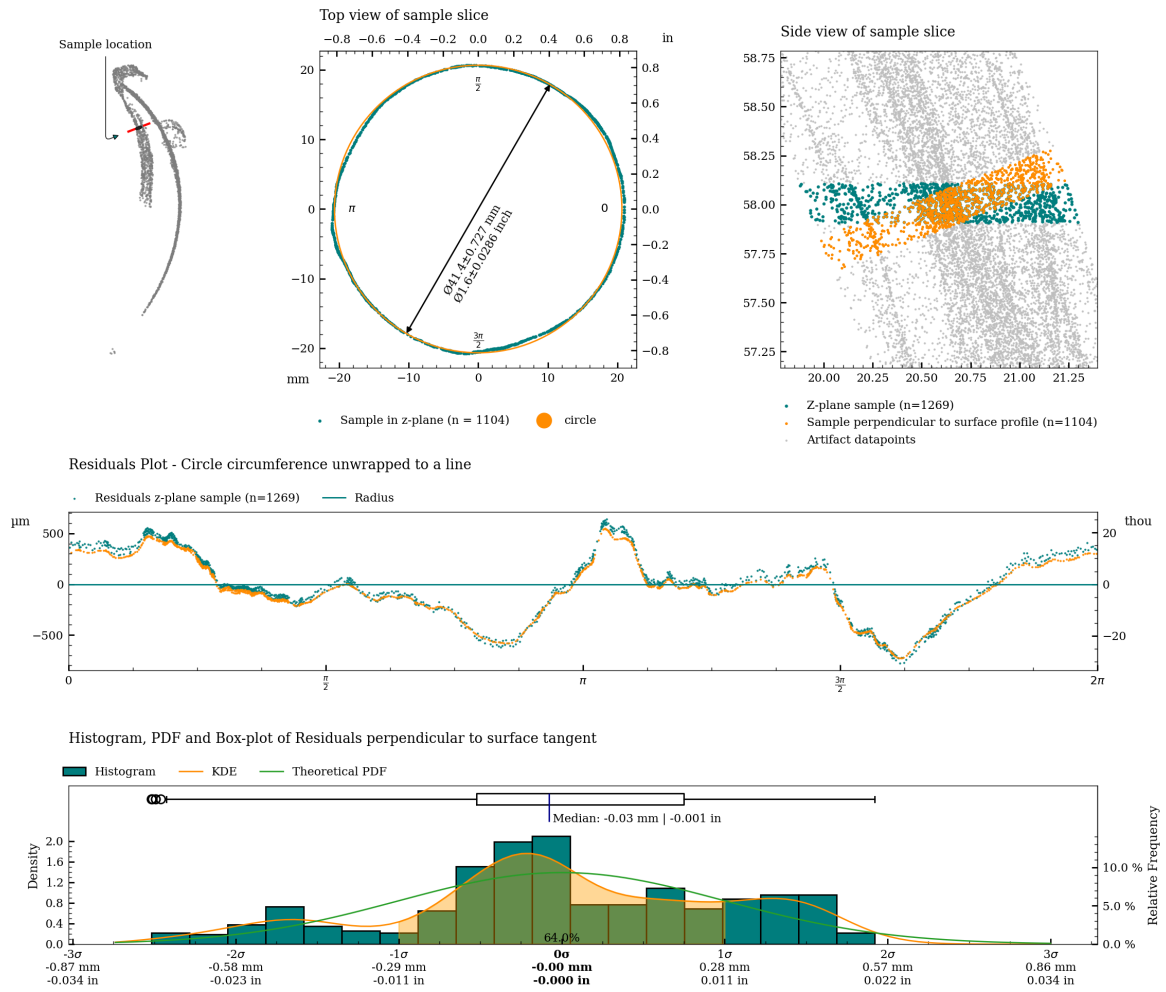


Figure 14: Charts with statistics for the measurement of c07_s.

Graphical overview of circularity measurement c08

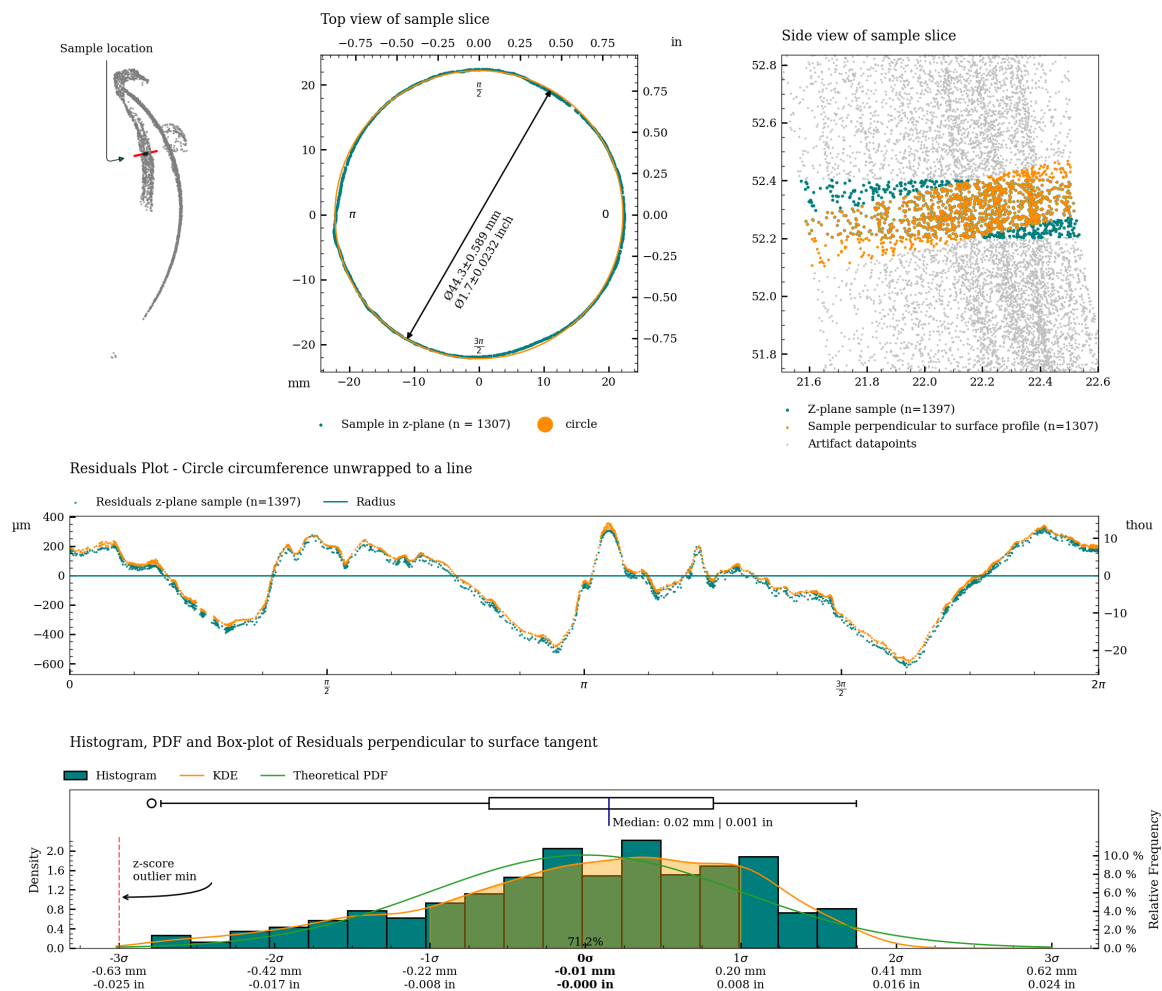


Figure 15: Charts with statistics for the measurement of c08.

Graphical overview of circularity measurement c08_s

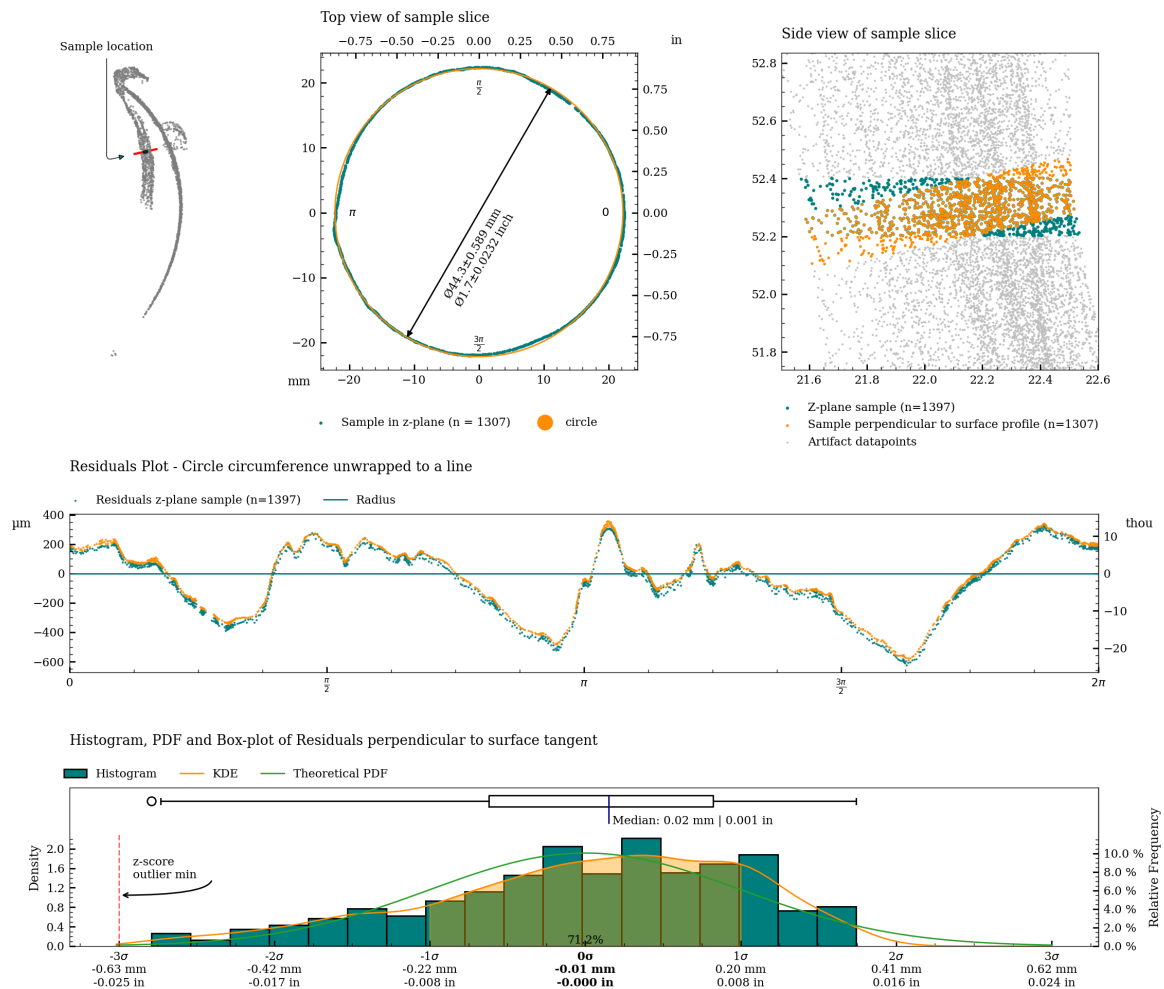


Figure 16: Charts with statistics for the measurement of c08_s.

Table 2 shows statistical measures of the circularity of the vessel, measured along the full height (areas on the artifact scan containing damaged parts have been removed to the best extent possible to reduce the influence of the measurement).

| Metric | | | | | | | | | | | |
|-------------------|--------|-------|-------|--------------------|-------|-------|--------|-------|-------|--------|--------------|
| Area | Range | | | Standard Deviation | | | RMSD | | | Slices | Slice height |
| | Median | Min. | Max. | Median | Min. | Max. | Median | Min. | Max. | | |
| | mm | mm | mm | mm | mm | mm | mm | mm | mm | | |
| Exterior | 0.564 | 0.345 | 1.152 | 0.068 | 0.044 | 0.161 | 0.117 | 0.070 | 0.215 | 275 | 0.200 |
| Interior | 2.340 | 1.038 | 2.991 | 0.308 | 0.097 | 0.437 | 0.690 | 0.123 | 0.964 | 118 | 0.200 |
| Interior separate | 1.243 | 0.942 | 2.050 | 0.152 | 0.086 | 0.298 | 0.254 | 0.131 | 0.566 | 118 | 0.200 |

| Imperial | | | | | | | | | | | |
|-------------------|--------|-------|-------|--------------------|-------|-------|--------|-------|-------|--------|--------------|
| Area | Range | | | Standard Deviation | | | RMSD | | | Slices | Slice height |
| | Median | Min. | Max. | Median | Min. | Max. | Median | Min. | Max. | | |
| | in | in | in | in | in | in | in | in | in | | |
| Exterior | 0.564 | 0.345 | 1.152 | 0.068 | 0.044 | 0.161 | 0.117 | 0.070 | 0.215 | 275 | 0.200 |
| Interior | 2.340 | 1.038 | 2.991 | 0.308 | 0.097 | 0.437 | 0.690 | 0.123 | 0.964 | 118 | 0.200 |
| Interior separate | 1.243 | 0.942 | 2.050 | 0.152 | 0.086 | 0.298 | 0.254 | 0.131 | 0.566 | 118 | 0.200 |

Table 2: Perpendicular Circularity analysis of MV015c.

Circularity analysis of exterior surface

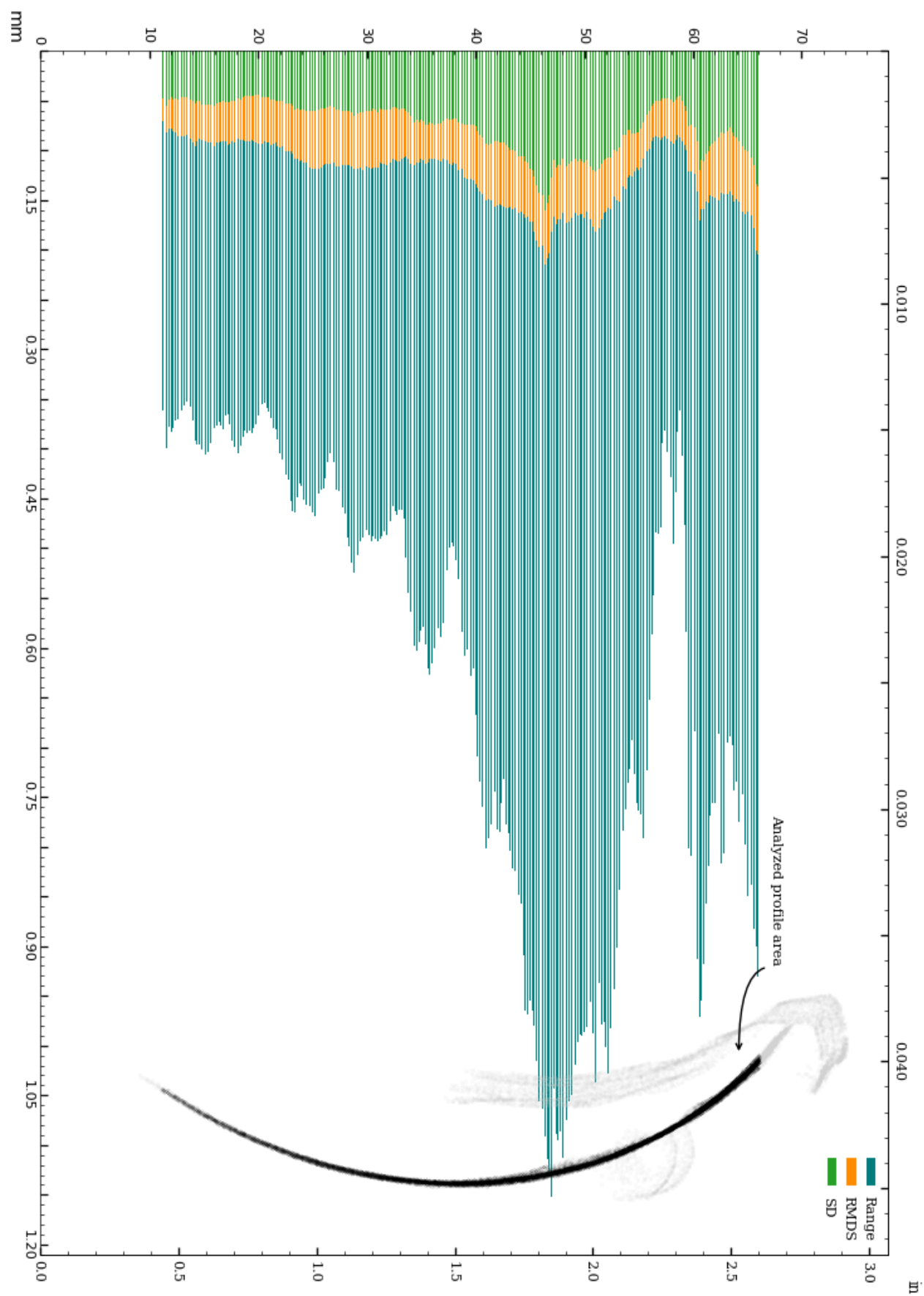


Figure 17: Circularity of exterior surface.

Circularity analysis of exterior surface, Standard Deviation and Root Mean Squared Deviation

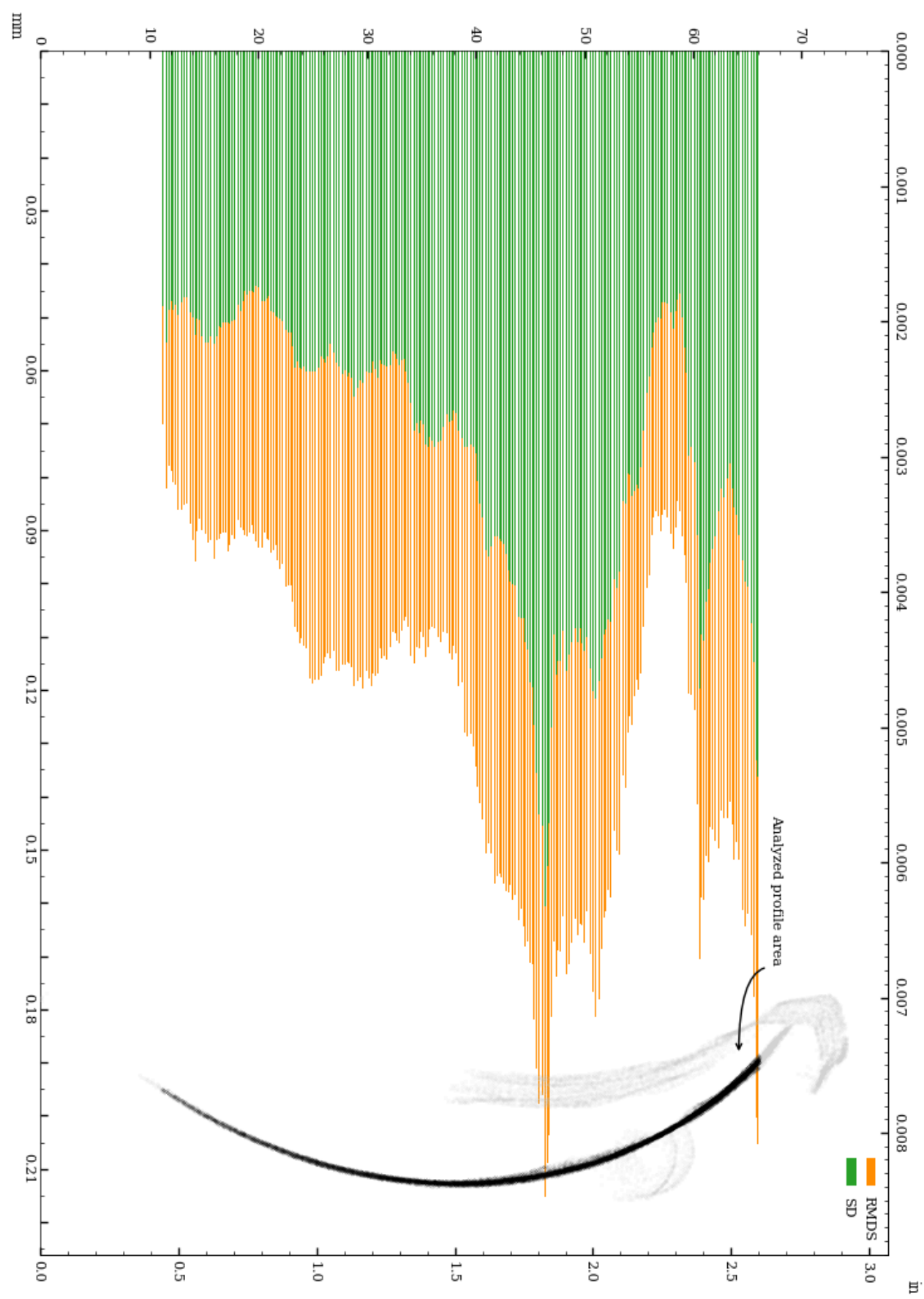


Figure 18: Vessel circularity of exterior surface, standard deviation and median absolute deviation.

The distributions of the circularity measurements across 275 slices of the exterior surface are shown below.

Range measurement distribution across 275 slices of exterior surface

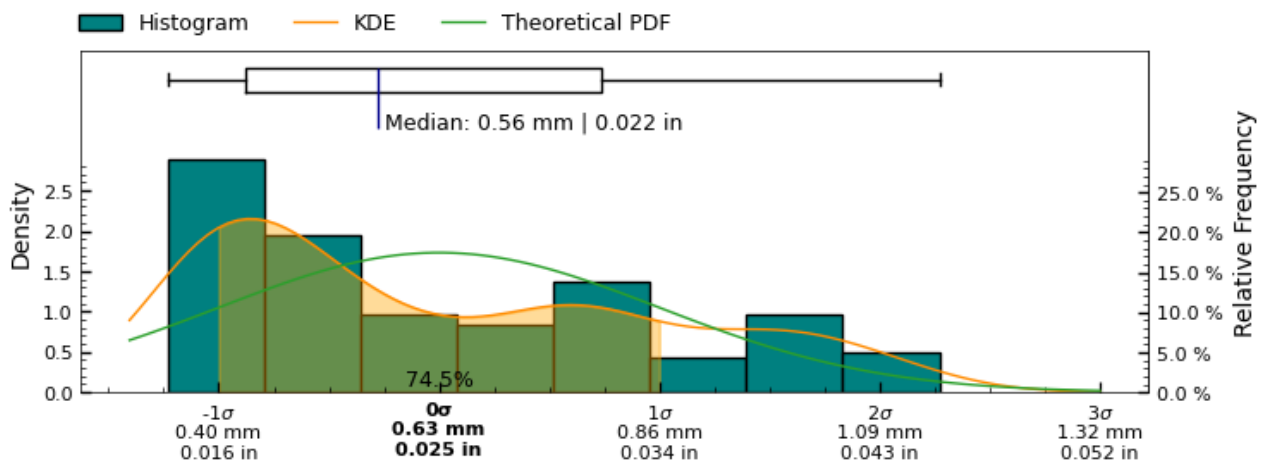


Figure 19: Range measurement distribution across measured slices of exterior surface

Standard Deviation measurement distribution across 275 slices of exterior surface

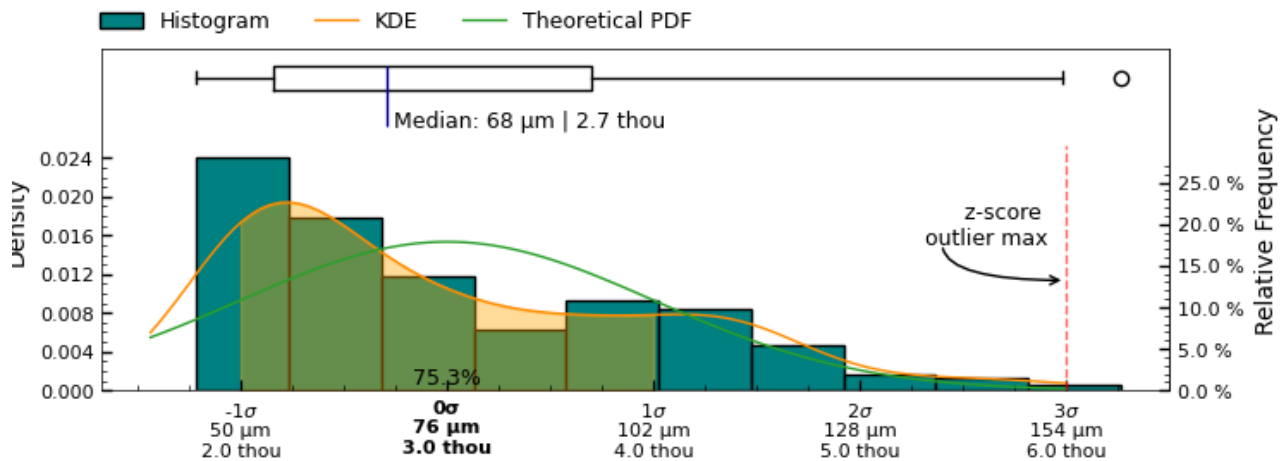


Figure 20: Standard Deviation measurement distribution across measured slices of "+ exterior +" surface

Root Mean Squared Deviation measurement distribution across 275 slices of exterior surface

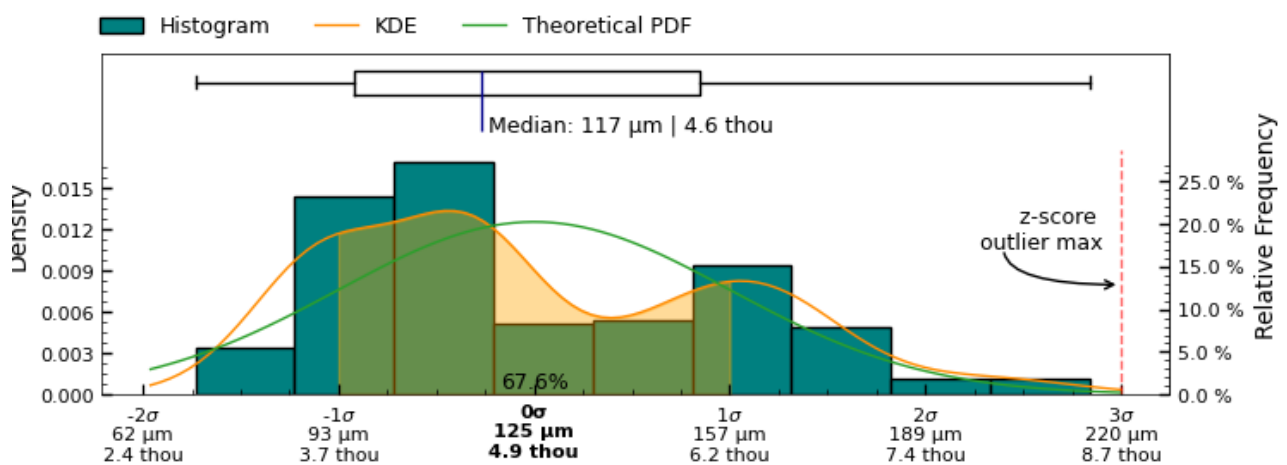


Figure 21: Root Mean Squared Deviation measurement distribution across measured slices of exterior surface

Circularity analysis of interior surface

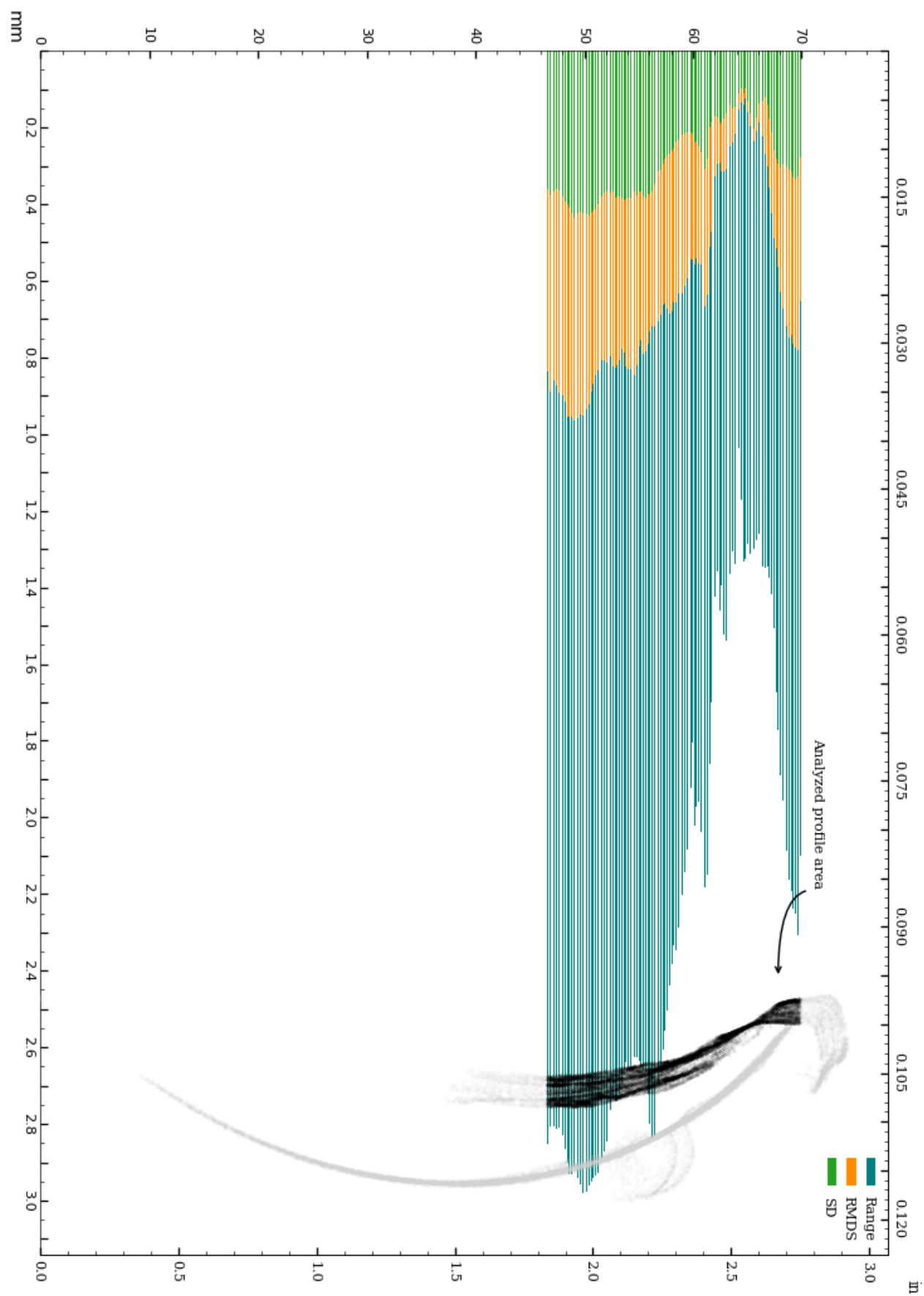


Figure 22: Circularity of interior surface.

Circularity analysis of interior surface, Standard Deviation and Root Mean Squared Deviation

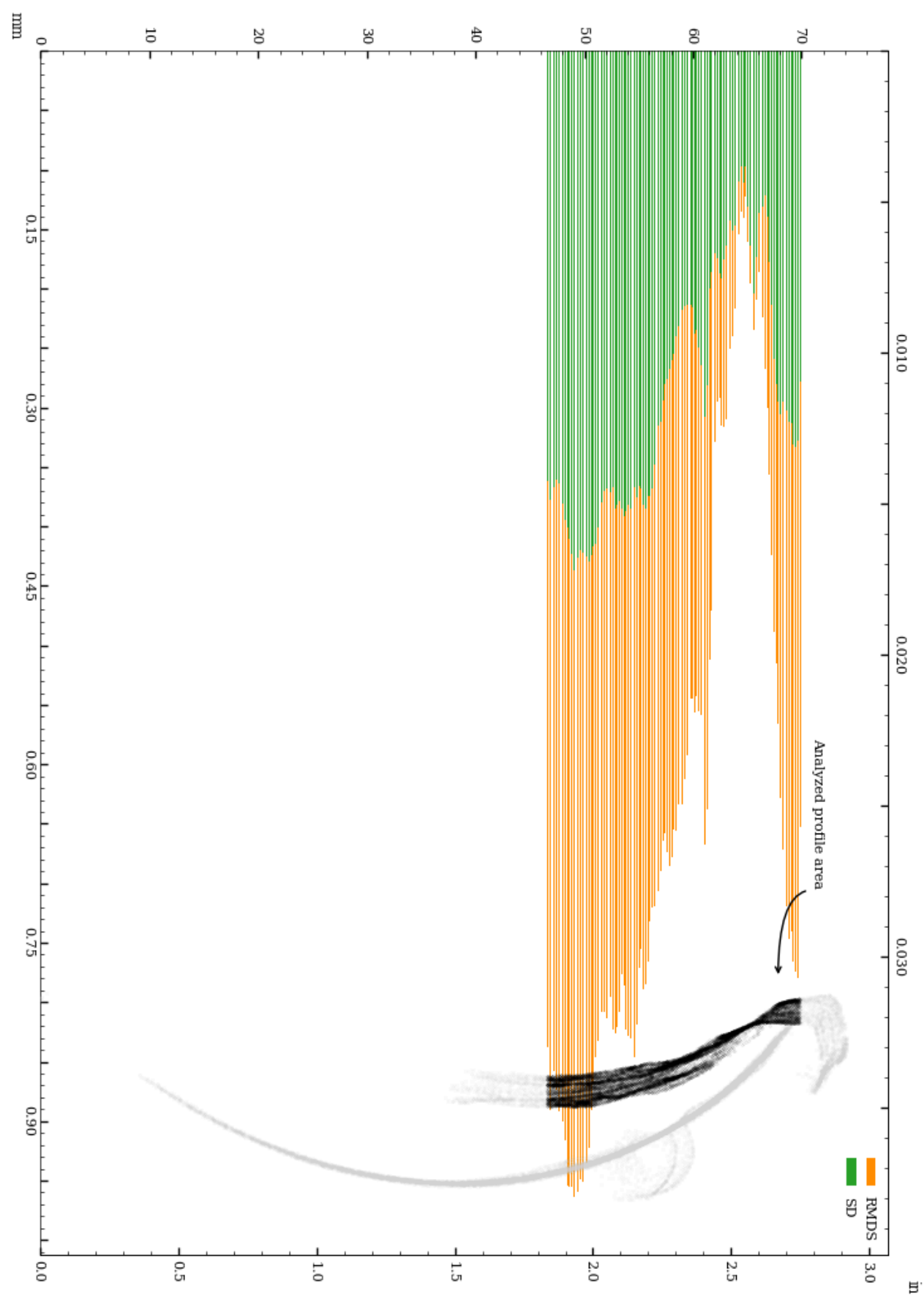


Figure 23: Vessel circularity of interior surface, standard deviation and median absolute deviation.

The distributions of the circularity measurements across 118 slices of the interior surface are shown below.

Range measurement distribution across 118 slices of interior surface

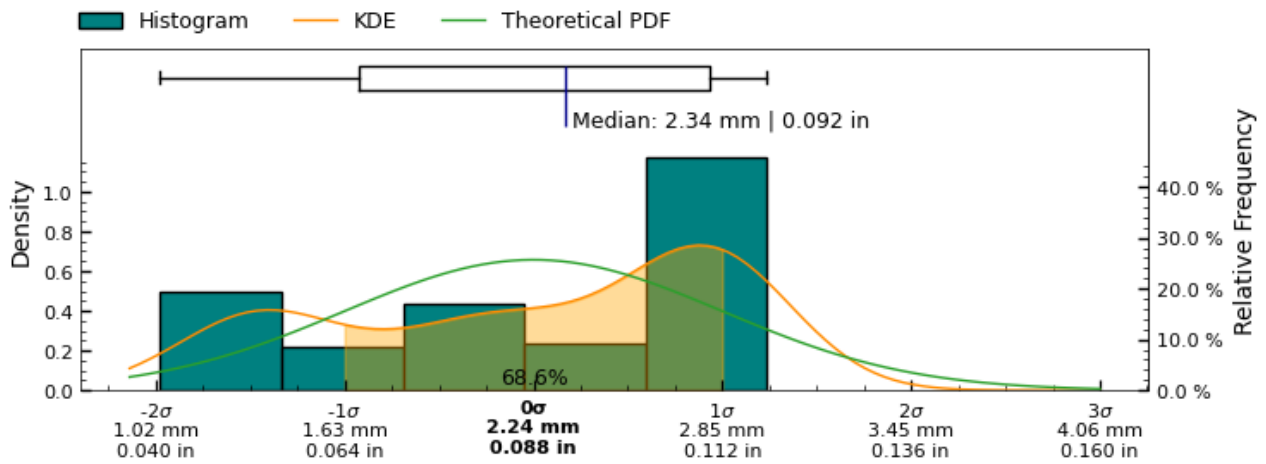


Figure 24: Range measurement distribution across measured slices of interior surface

Standard Deviation measurement distribution across 118 slices of interior surface

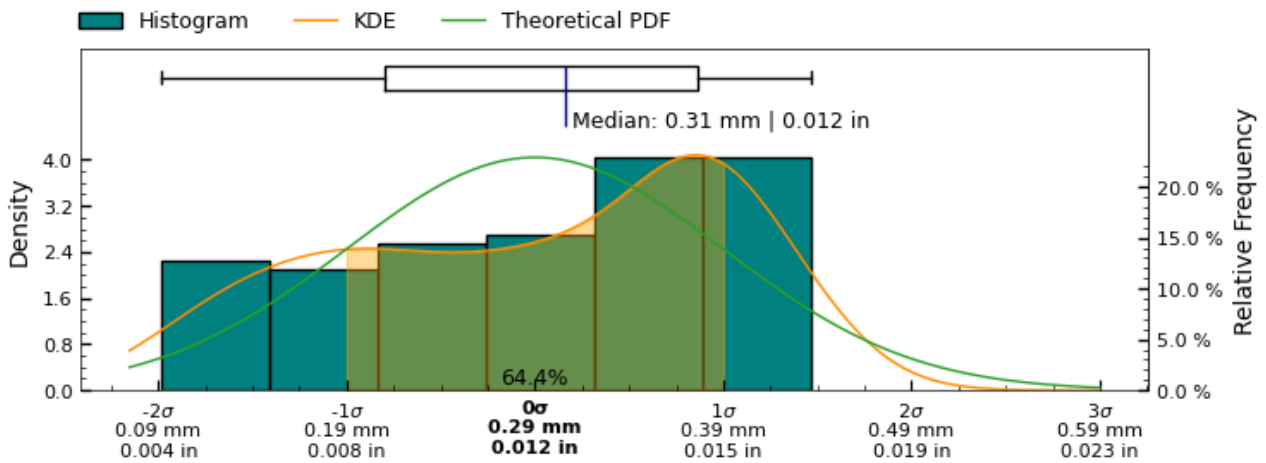


Figure 25: Standard Deviation measurement distribution across measured slices of " + interior + " surface

Root Mean Squared Deviation measurement distribution across 118 slices of interior surface

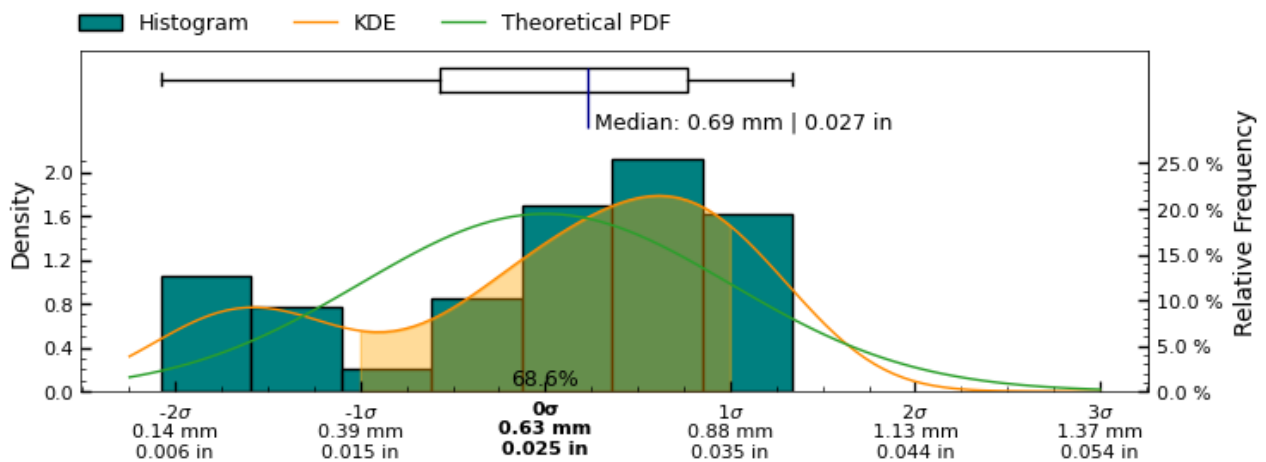


Figure 26: Root Mean Squared Deviation measurement distribution across measured slices of interior surface

Circularity analysis of interior separately aligned surface

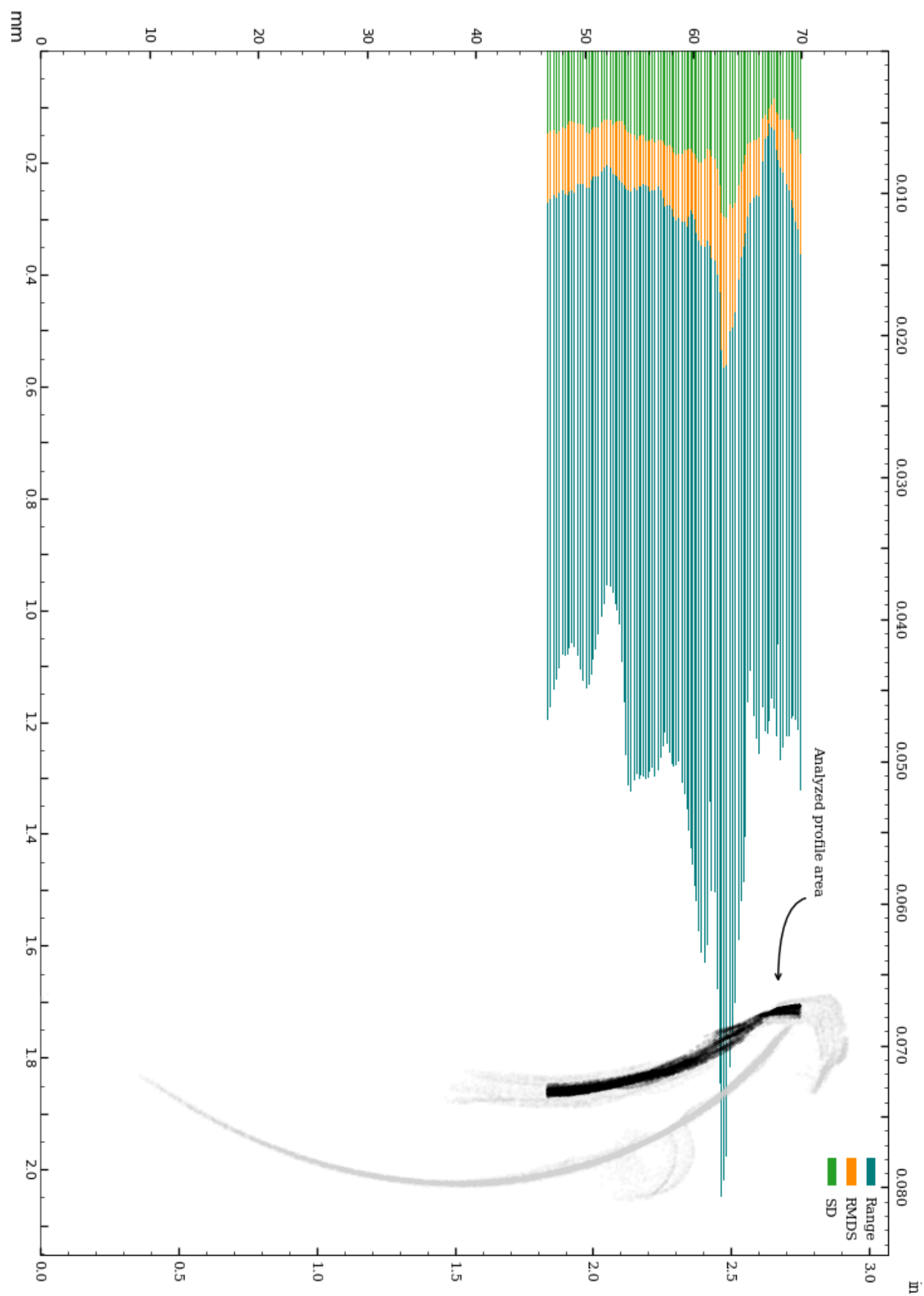


Figure 27: Circularity of interior_separate surface.

Circularity analysis of interior separately aligned surface, Standard Deviation and Root Mean Squared Deviation

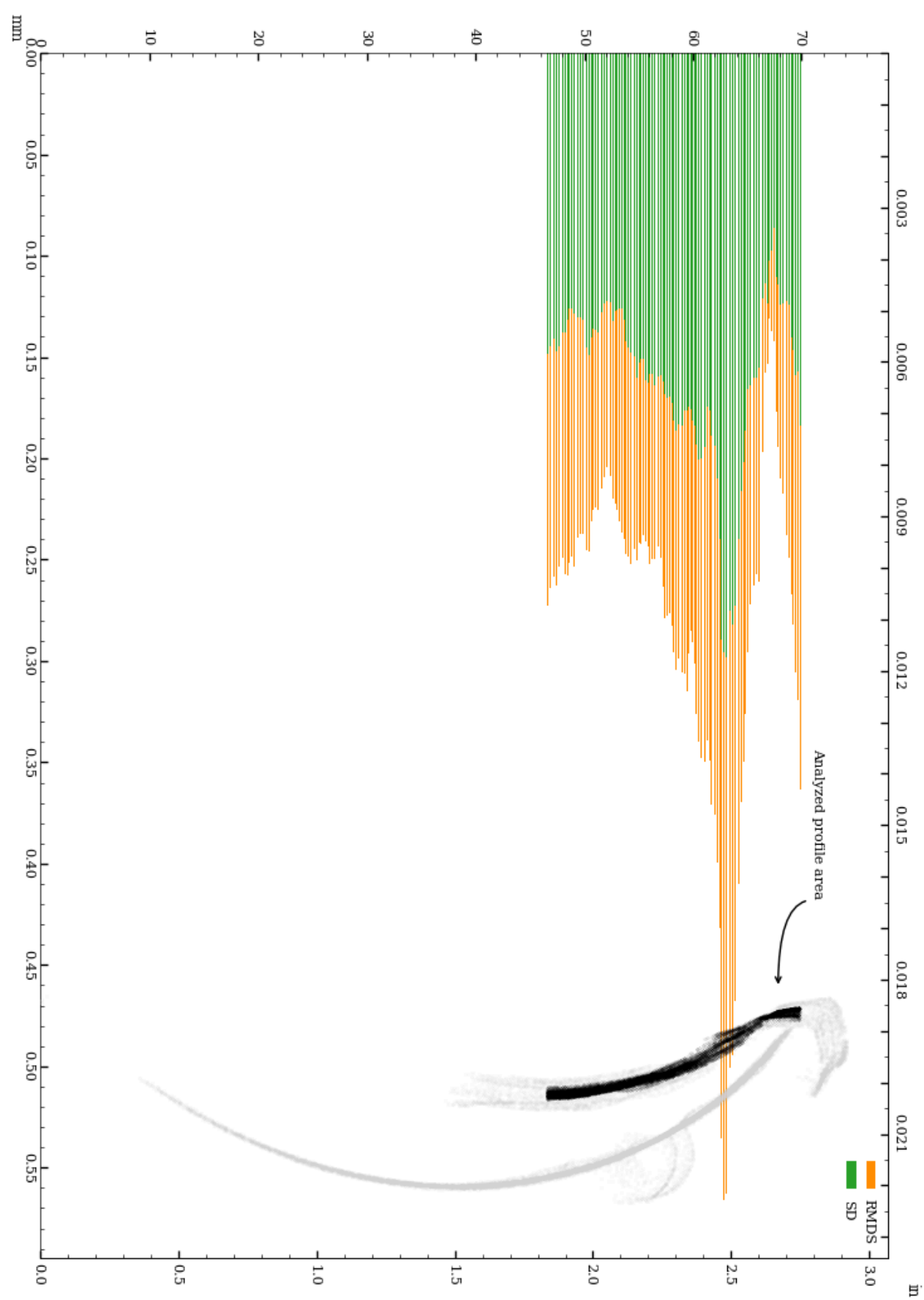


Figure 28: Vessel circularity of interior_separate surface, standard deviation and median absolute deviation.

The distributions of the circularity measurements across 118 slices of the interior_separate surface are shown below.

Range measurement distribution across 118 slices of interior separately aligned surface

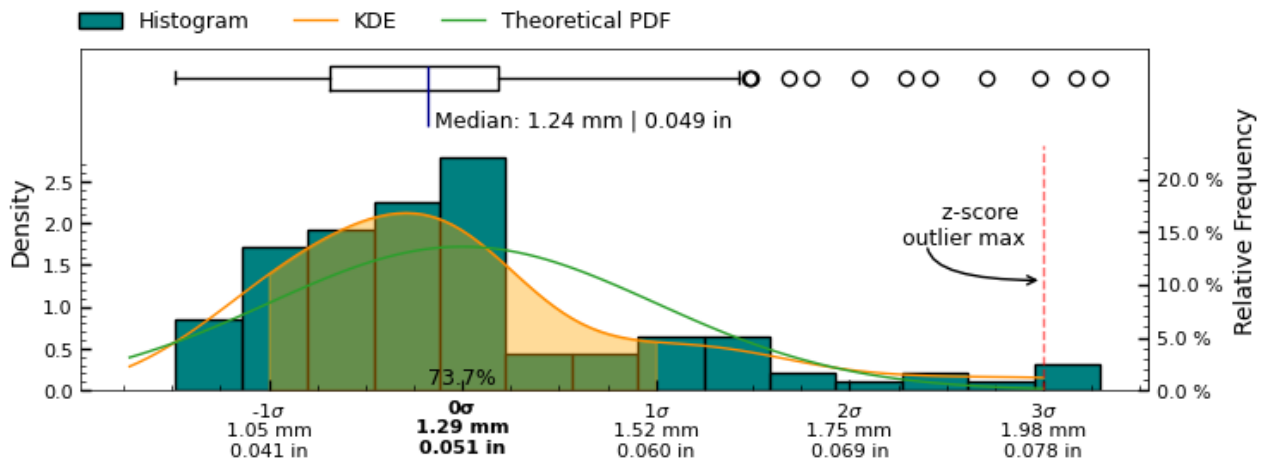


Figure 29: Range measurement distribution across measured slices of interior_separate surface

Standard Deviation measurement distribution across 118 slices of interior separately aligned surface

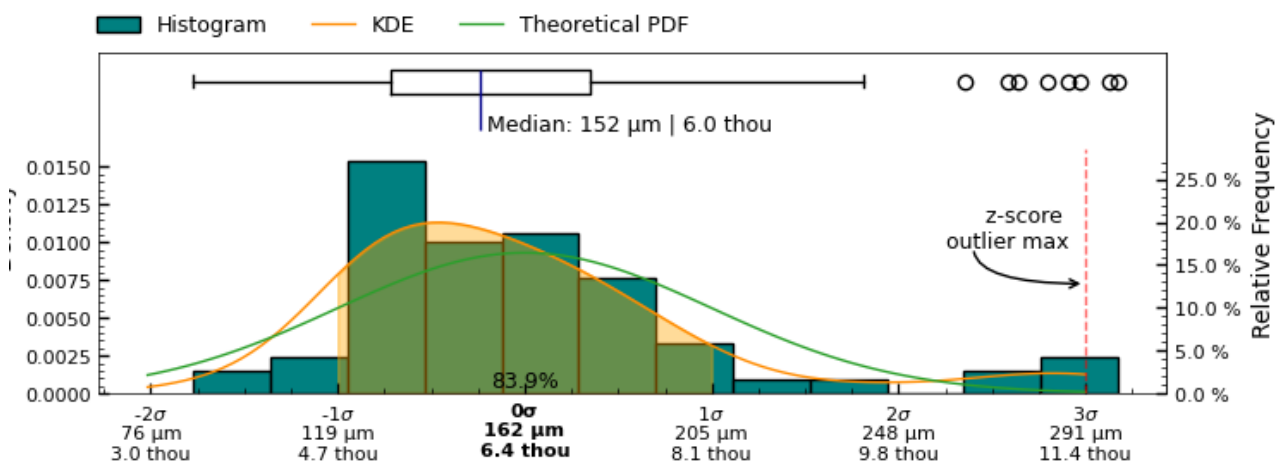


Figure 30: Standard Deviation measurement distribution across measured slices of " + interior_separate + " surface

Root Mean Squared Deviation measurement distribution across 118 slices of interior separately aligned surface

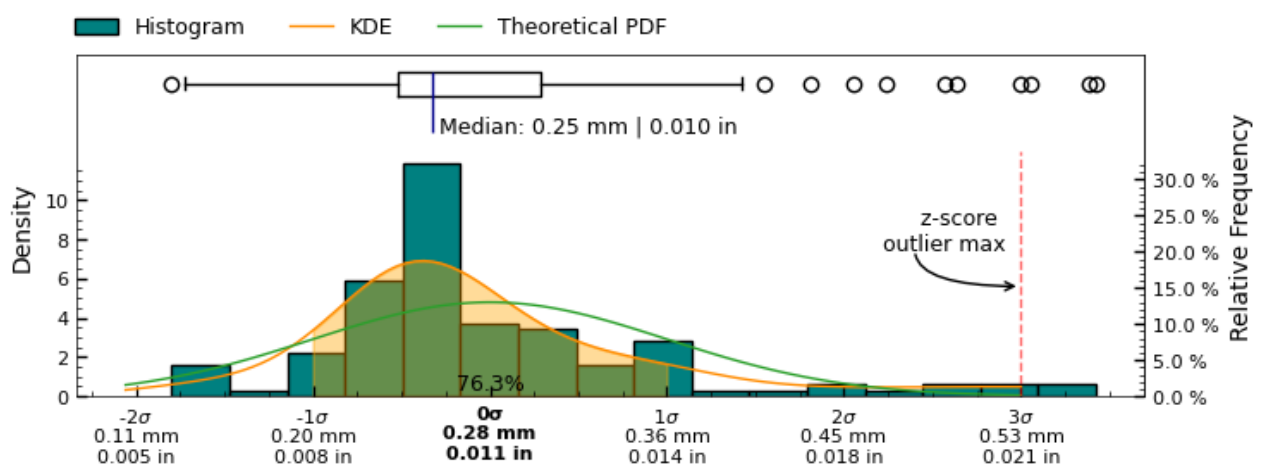


Figure 31: Root Mean Squared Deviation measurement distribution across measured slices of interior separately aligned surface

Concentricity

The concentricity metric describes the deviation in the center-point of the referenced features. As such, it is a measure to determine if several features of the object share the same center point/axis, and how closely. See Figure 32 for a visual representation of this metric.

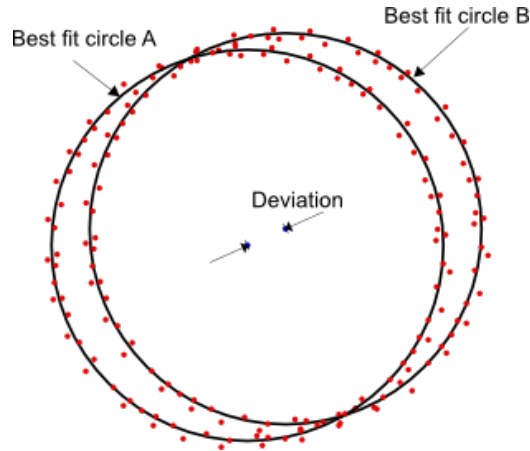


Figure 32: Concentricity measures the deviation (distance) between the center of two circles.

Determination of concentricity has been carried out by establishing the best fit circles of sample slices, using RANSAC (Random sample consensus) algorithm for outlier detection of a least squares circle regression on the scanned data-points at each cross-section, to estimate centers of each cross-section.

The concentricity between both the interior and exterior circular cross-sections is explored for cross-section measurements with the same Z-coordinates.

Additionally, the concentricity between each cross-section measurement defined in Figure 4 and the datum axis $(x, y) = (0, 0)$ has been calculated to establish the deviation of the feature center from the datum axis.

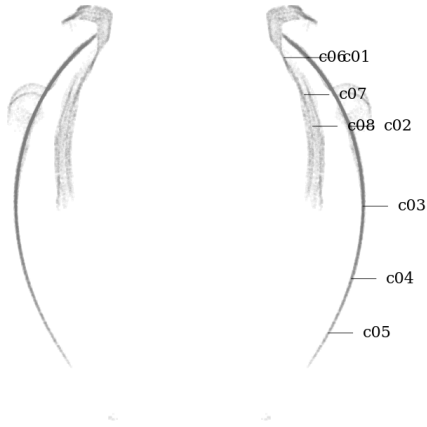


Figure 33: Circularity measurement sample locations, full mesh aligned to exterior surface

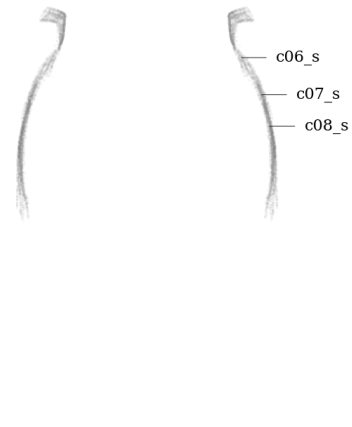


Figure 34: Circularity measurement sample location, separately aligned interior mesh

Metric

| Tag | Reference | Deviation | Sample size | Circle fit residuals analysis for sample listed in Tag column | | | | | | |
|-------|-----------|-----------|-------------|---|---------------|-----------|--------------|---------|------------|--------------|
| | | | | Range full | Range inliers | RMSD full | RMDS inliers | SD full | SD inliers | Center (x,y) |
| | | mm | | mm | mm | mm | mm | mm | mm | µm |
| c01 | z-axis | 0.124 | 2099 | 1.018 | 1.018 | 0.223 | 0.223 | 0.130 | 0.130 | −7, −124 |
| c02 | z-axis | 0.051 | 2204 | 0.999 | 0.885 | 0.167 | 0.152 | 0.111 | 0.097 | −31, 41 |
| c03 | z-axis | 0.046 | 1756 | 0.549 | 0.549 | 0.127 | 0.127 | 0.078 | 0.078 | −10, 45 |
| c04 | z-axis | 0.033 | 901 | 0.536 | 0.536 | 0.125 | 0.125 | 0.067 | 0.067 | 4, −33 |
| c05 | z-axis | 0.027 | 334 | 0.421 | 0.421 | 0.094 | 0.094 | 0.057 | 0.057 | −22, −16 |
| c06 | z-axis | 0.461 | 556 | 2.200 | 2.075 | 0.564 | 0.550 | 0.293 | 0.276 | 238, 395 |
| c06_s | z-axis | 0.460 | 556 | 2.198 | 2.073 | 0.564 | 0.548 | 0.292 | 0.274 | 237, 394 |
| c07 | z-axis | 0.093 | 1104 | 1.328 | 1.328 | 0.315 | 0.315 | 0.198 | 0.198 | 62, 69 |
| c07_s | z-axis | 0.093 | 1104 | 1.328 | 1.328 | 0.315 | 0.315 | 0.198 | 0.198 | 62, 69 |
| c08 | z-axis | 0.049 | 1307 | 0.973 | 0.973 | 0.219 | 0.219 | 0.123 | 0.123 | 29, 40 |
| c08_s | z-axis | 0.049 | 1307 | 0.973 | 0.973 | 0.219 | 0.219 | 0.123 | 0.123 | 29, 40 |
| c01 | c06_s | 0.573 | | | | | | | | −244, −518 |
| c02 | c08_s | 0.060 | | | | | | | | −60, 1 |
| c07 | c07_s | 0.000 | | | | | | | | 0, 0 |

Imperial

| Tag | Reference | Deviation | Sample size | Circle fit residuals analysis for sample listed in Tag column | | | | | | |
|-------|-----------|-----------|-------------|---|---------------|-----------|--------------|---------|------------|--------------|
| | | | | Range full | Range inliers | RMSD full | RMDS inliers | SD full | SD inliers | Center (x,y) |
| | | in | | in | in | in | in | in | in | thou |
| c01 | z-axis | 0.0049 | 2099 | 0.0401 | 0.0401 | 0.0088 | 0.0088 | 0.0051 | 0.0051 | −0.3, −4.9 |
| c02 | z-axis | 0.0020 | 2204 | 0.0393 | 0.0349 | 0.0066 | 0.0060 | 0.0044 | 0.0038 | −1.2, 1.6 |
| c03 | z-axis | 0.0018 | 1756 | 0.0216 | 0.0216 | 0.0050 | 0.0050 | 0.0031 | 0.0031 | −0.4, 1.8 |
| c04 | z-axis | 0.0013 | 901 | 0.0211 | 0.0211 | 0.0049 | 0.0049 | 0.0026 | 0.0026 | 0.1, −1.3 |
| c05 | z-axis | 0.0011 | 334 | 0.0166 | 0.0166 | 0.0037 | 0.0037 | 0.0022 | 0.0022 | −0.9, −0.6 |
| c06 | z-axis | 0.0182 | 556 | 0.0866 | 0.0817 | 0.0222 | 0.0216 | 0.0115 | 0.0109 | 9.4, 15.6 |
| c06_s | z-axis | 0.0181 | 556 | 0.0865 | 0.0816 | 0.0222 | 0.0216 | 0.0115 | 0.0108 | 9.3, 15.5 |
| c07 | z-axis | 0.0036 | 1104 | 0.0523 | 0.0523 | 0.0124 | 0.0124 | 0.0078 | 0.0078 | 2.4, 2.7 |
| c07_s | z-axis | 0.0036 | 1104 | 0.0523 | 0.0523 | 0.0124 | 0.0124 | 0.0078 | 0.0078 | 2.4, 2.7 |
| c08 | z-axis | 0.0019 | 1307 | 0.0383 | 0.0383 | 0.0086 | 0.0086 | 0.0048 | 0.0048 | 1.1, 1.6 |
| c08_s | z-axis | 0.0019 | 1307 | 0.0383 | 0.0383 | 0.0086 | 0.0086 | 0.0048 | 0.0048 | 1.1, 1.6 |
| c01 | c06_s | 0.0225 | | | | | | | | −9.6, −20.4 |
| c02 | c08_s | 0.0023 | | | | | | | | −2.3, 0.0 |
| c07 | c07_s | 0.0000 | | | | | | | | 0.0, 0.0 |

Table 3: Concentricity analysis of MV015c.

Concentricity analysis of c01

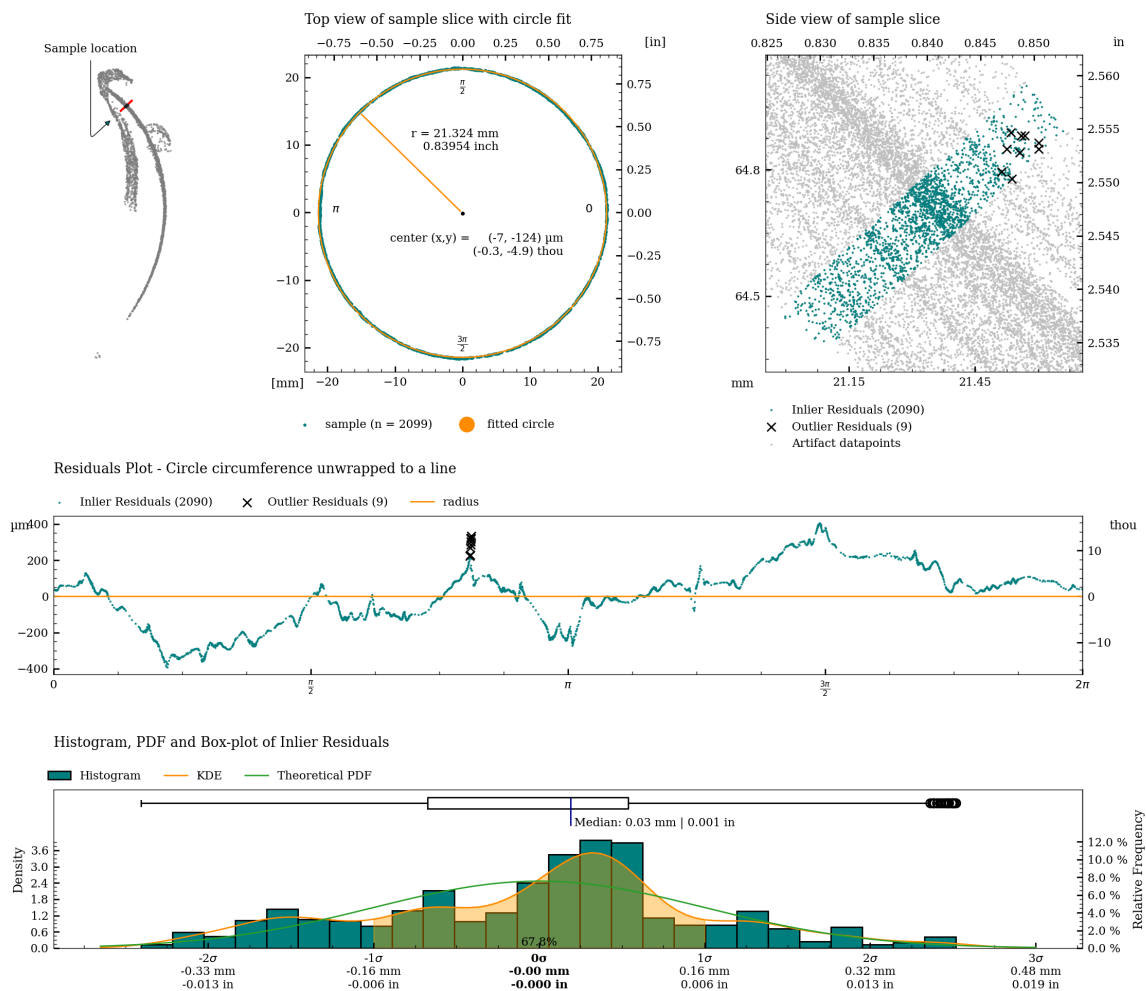
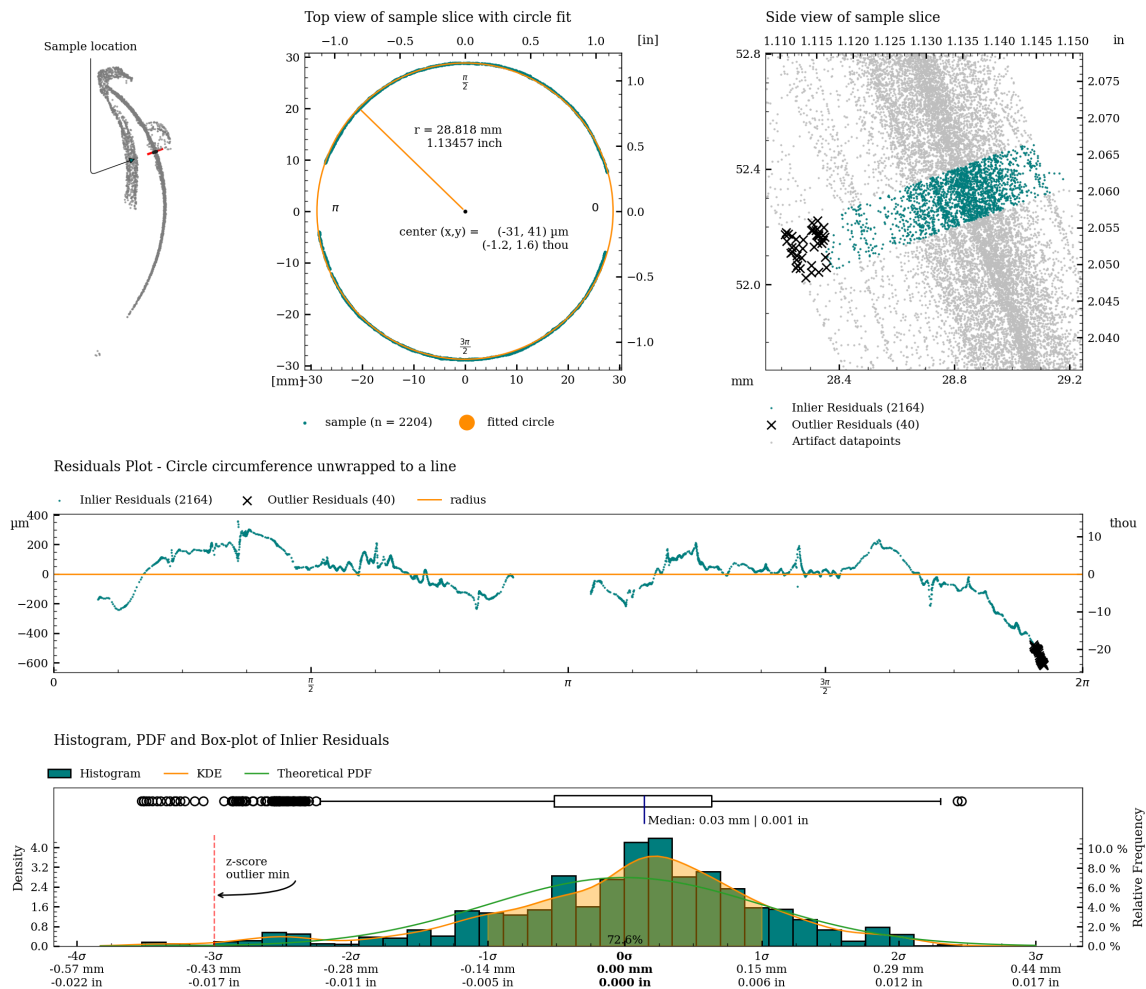
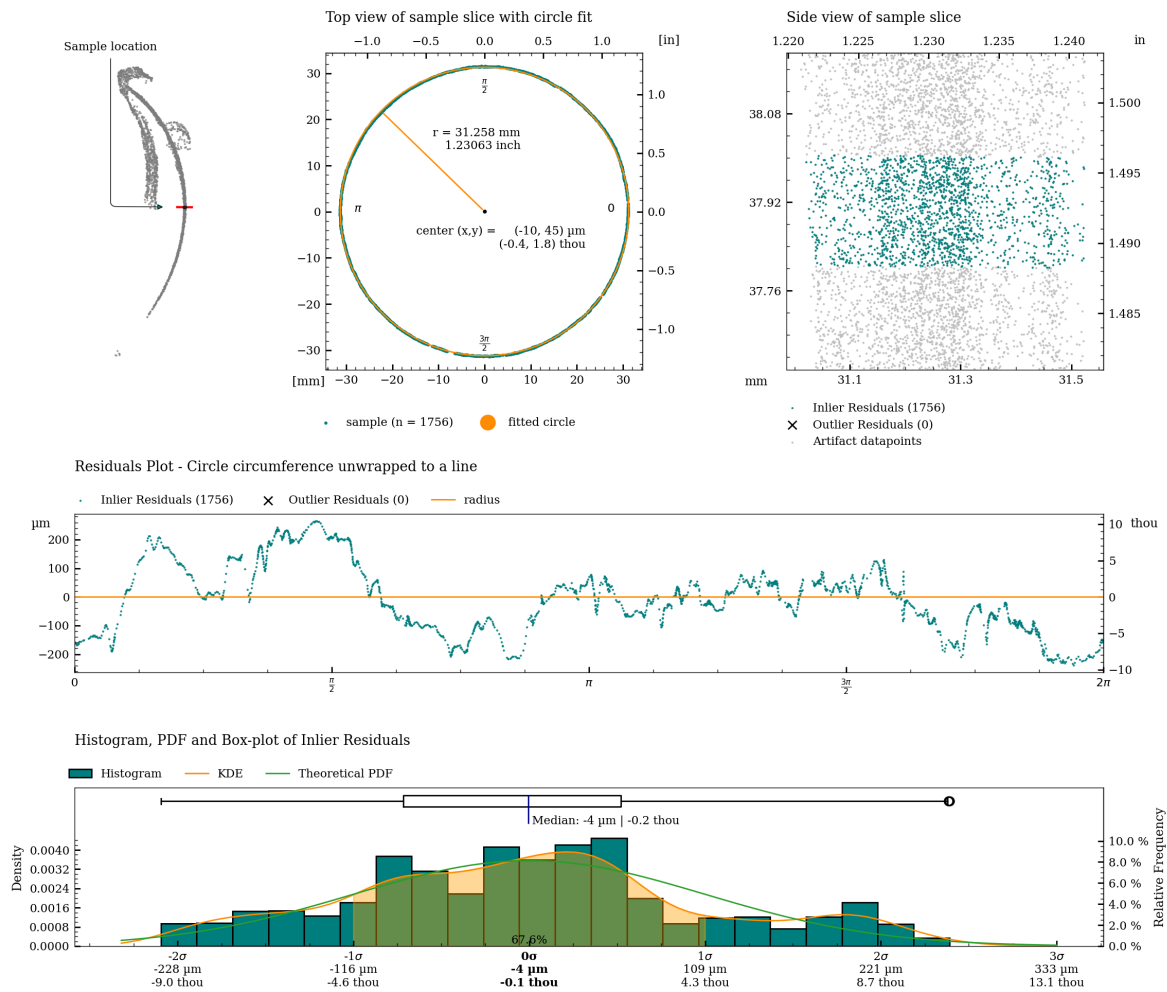


Figure 35: Detailed plot of concentricity measurement for c01.

Concentricity analysis of c02



Concentricity analysis of c03



Concentricity analysis of c04

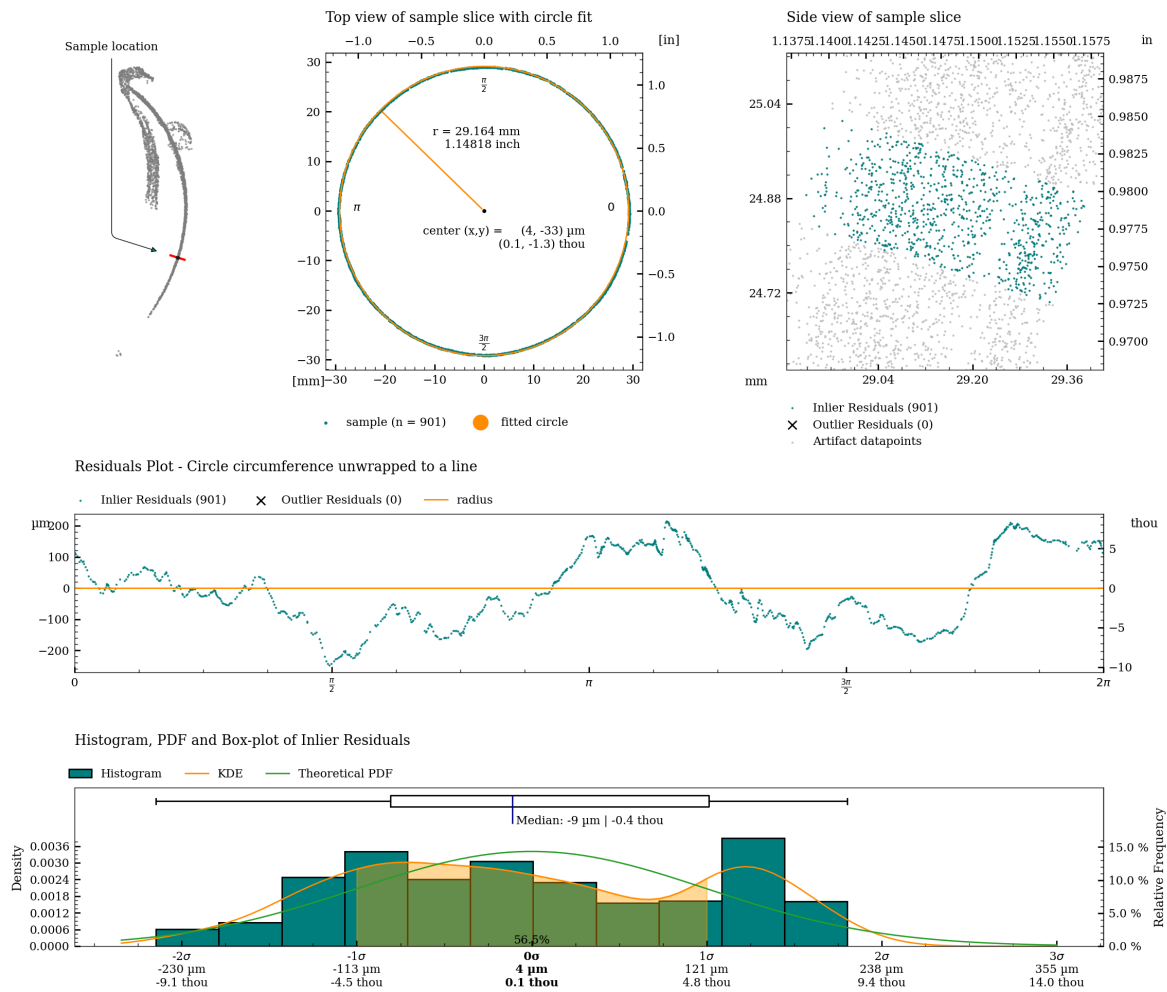
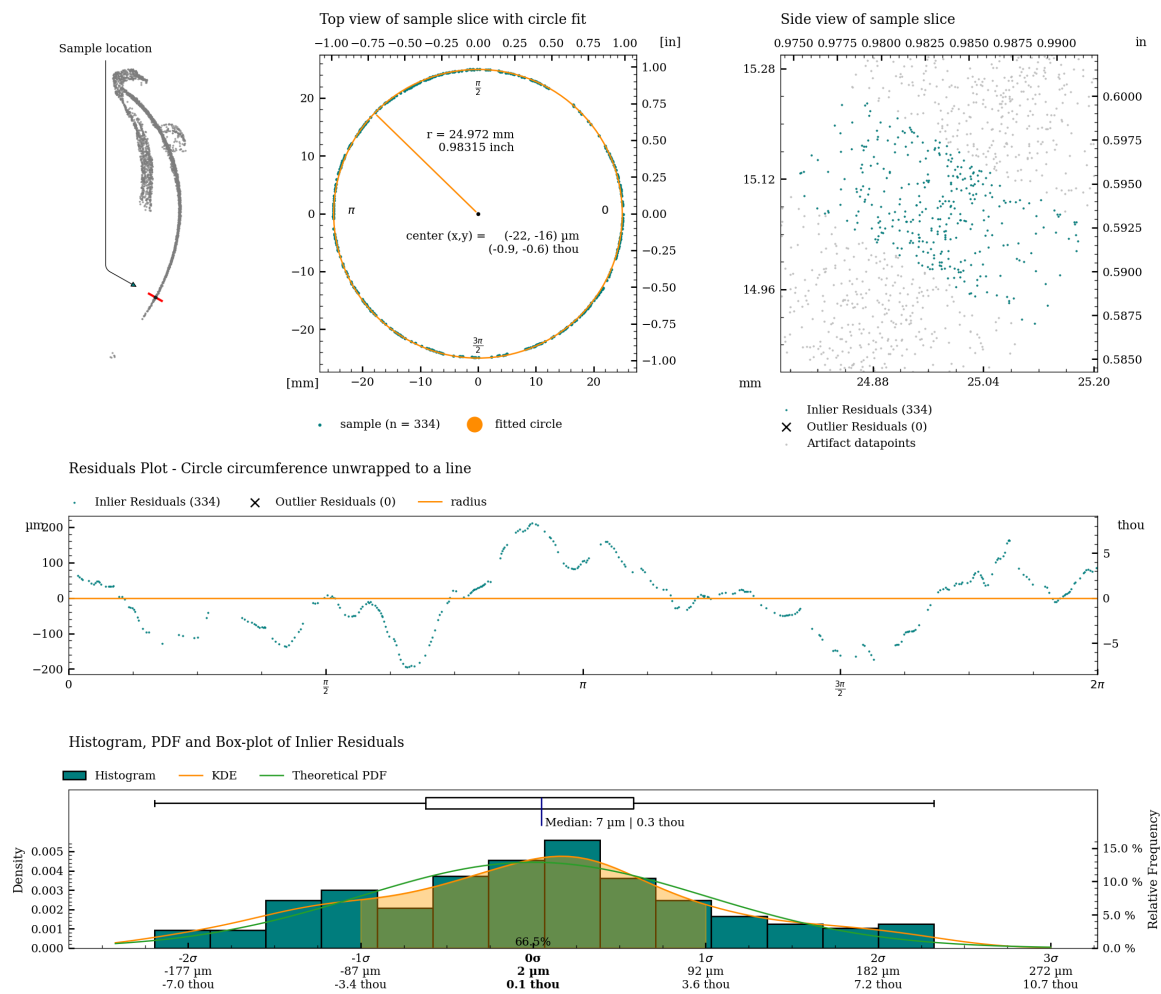


Figure 38: Detailed plot of concentricity measurement for c04.

Concentricity analysis of c05



Concentricity analysis of c06

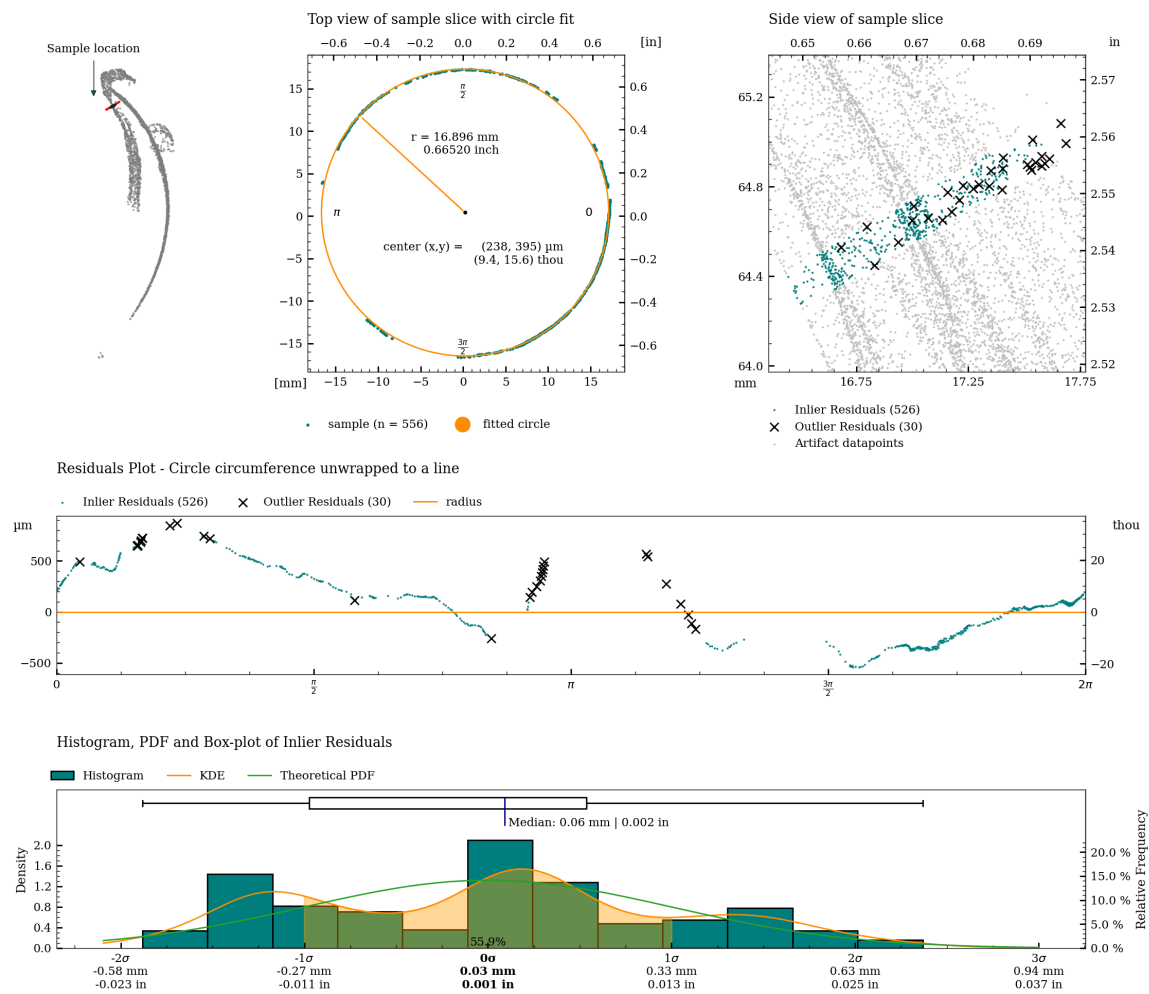


Figure 40: Detailed plot of concentricity measurement for c06.

Concentricity analysis of c06_s

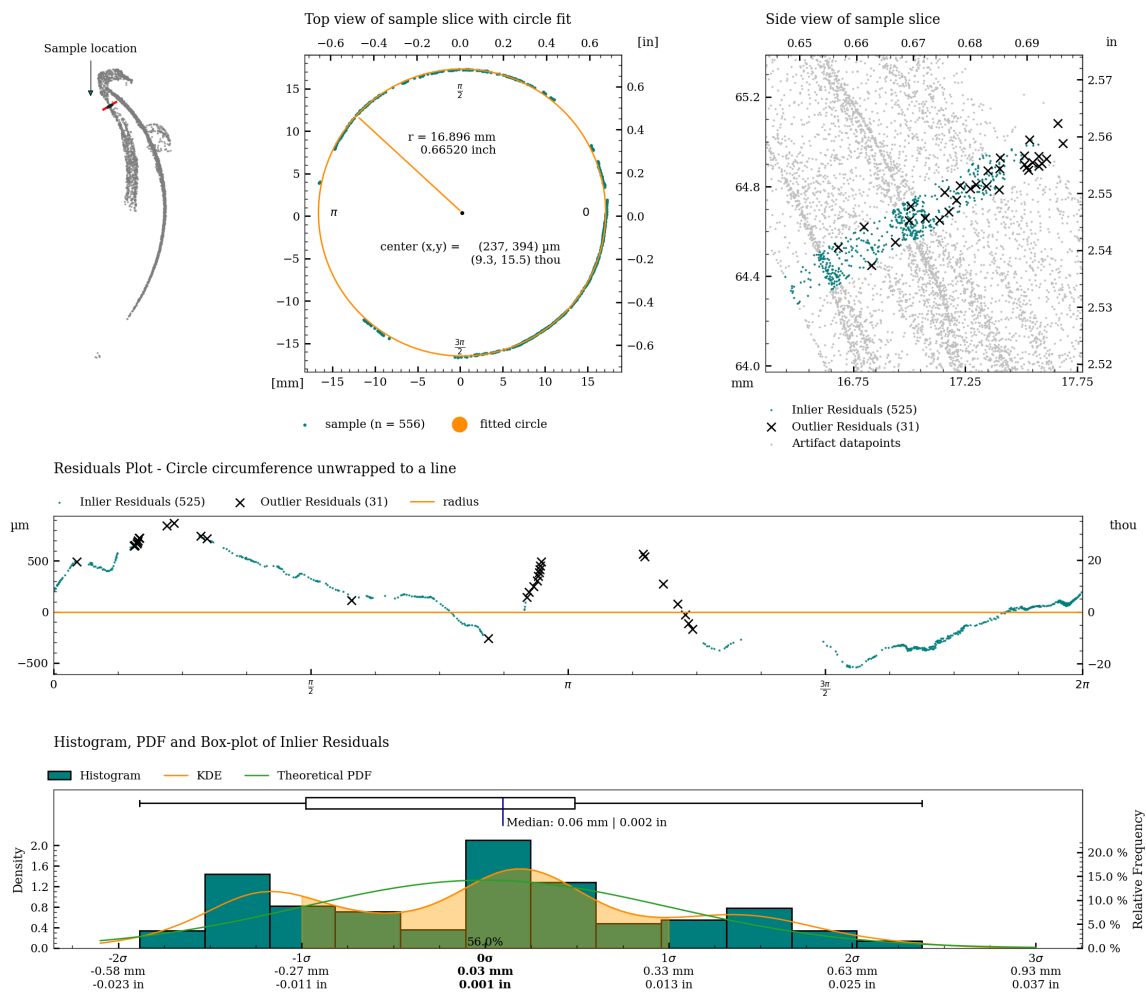


Figure 41: Detailed plot of concentricity measurement for c06_s.

Concentricity analysis of c07

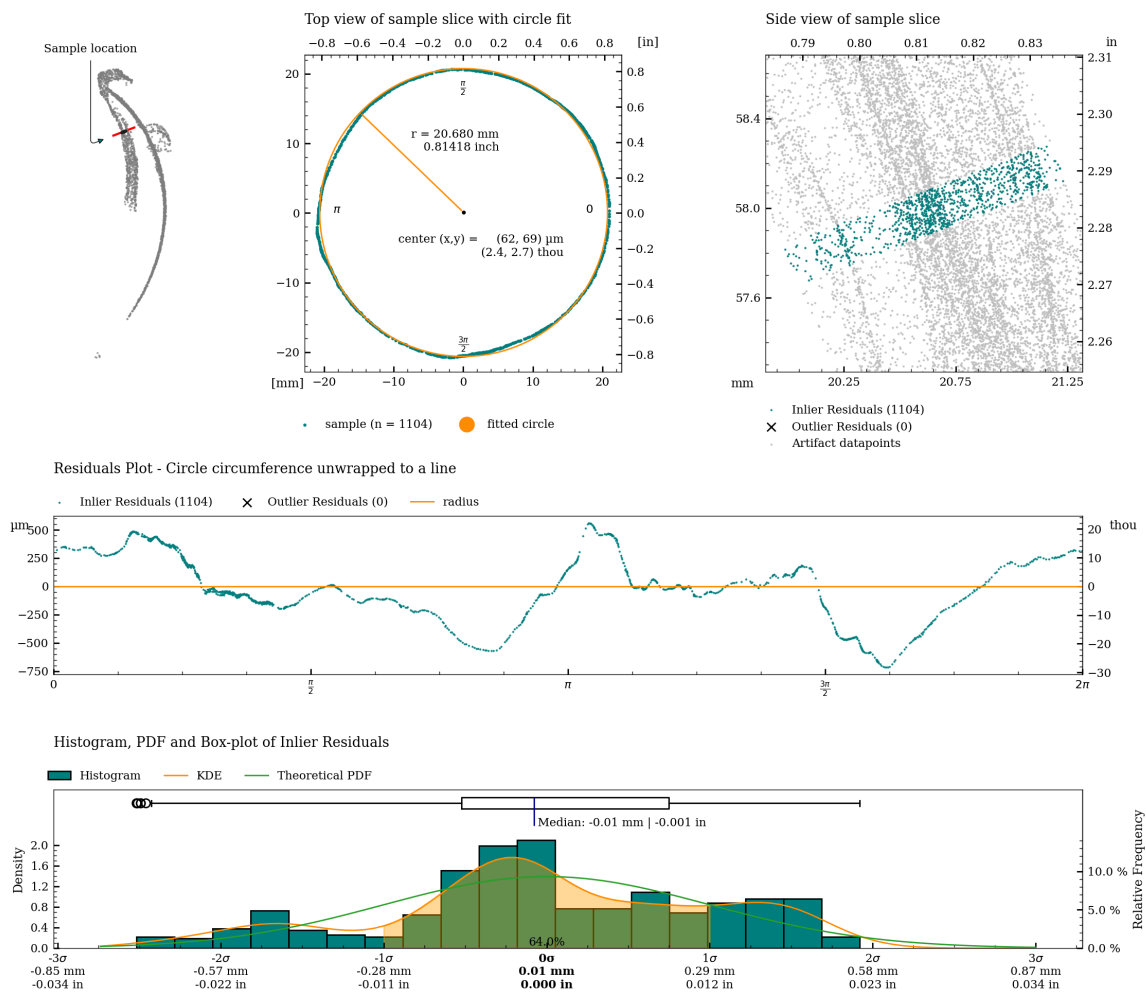


Figure 42: Detailed plot of concentricity measurement for c07.

Concentricity analysis of c07_s

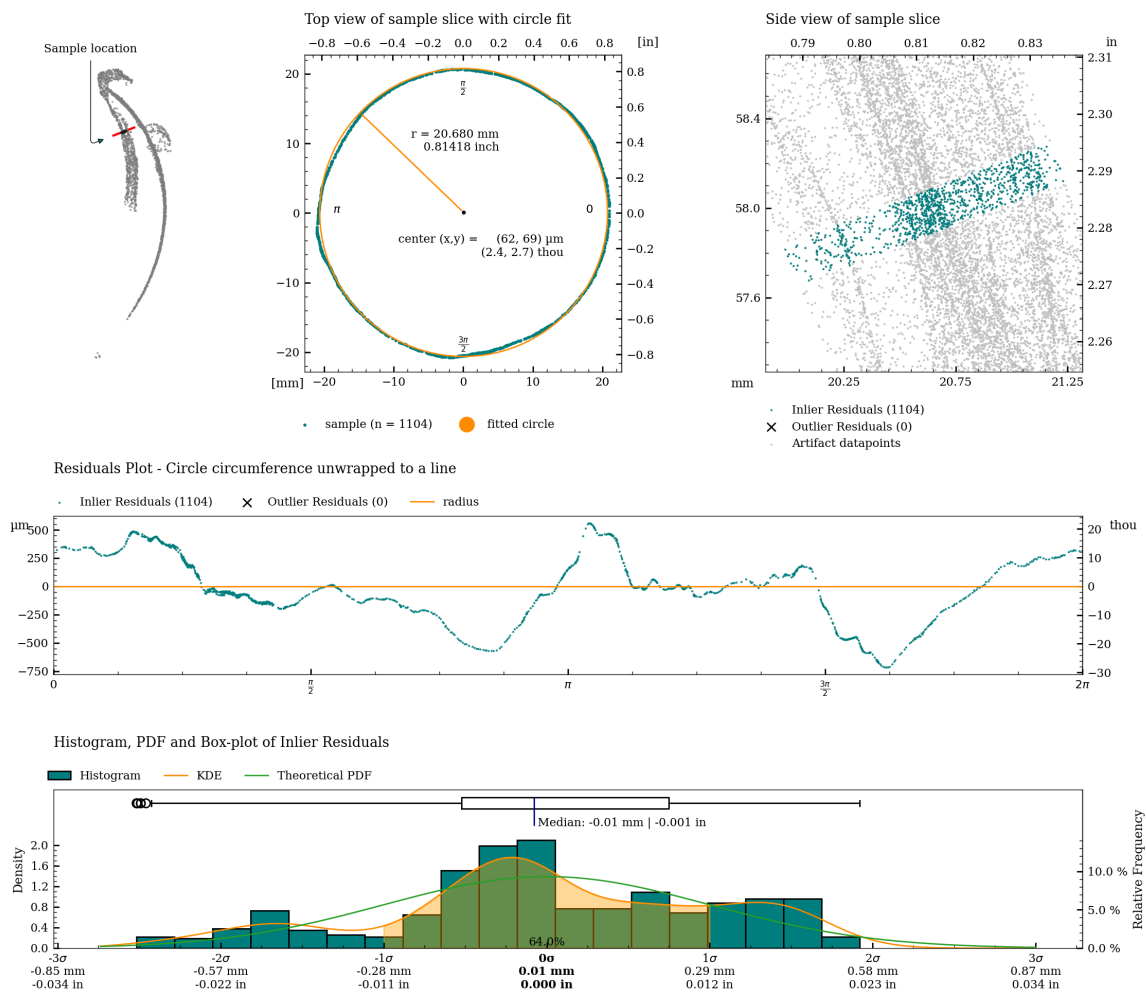


Figure 43: Detailed plot of concentricity measurement for c07_s.

Concentricity analysis of c08

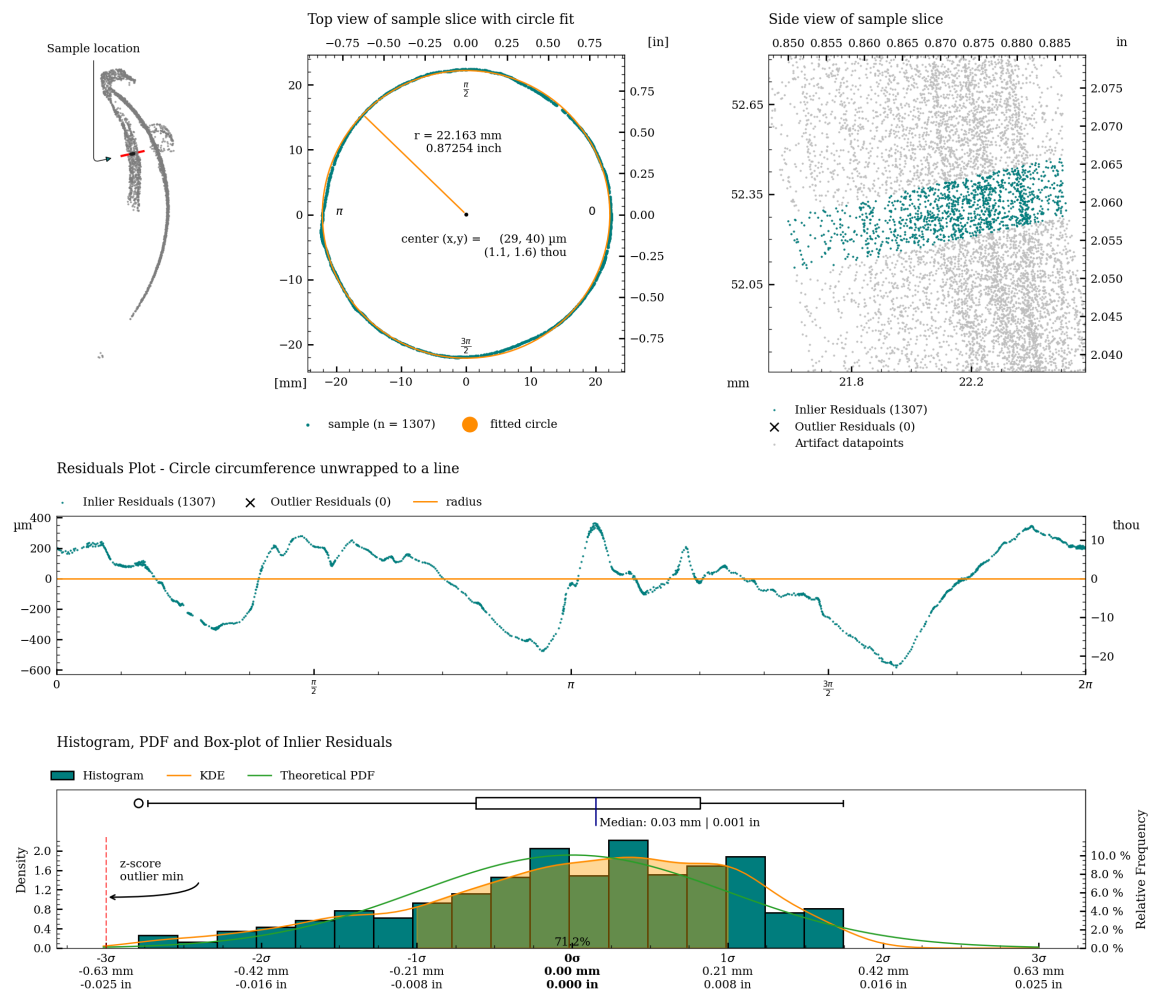


Figure 44: Detailed plot of concentricity measurement for c08.

Concentricity analysis of c08_s

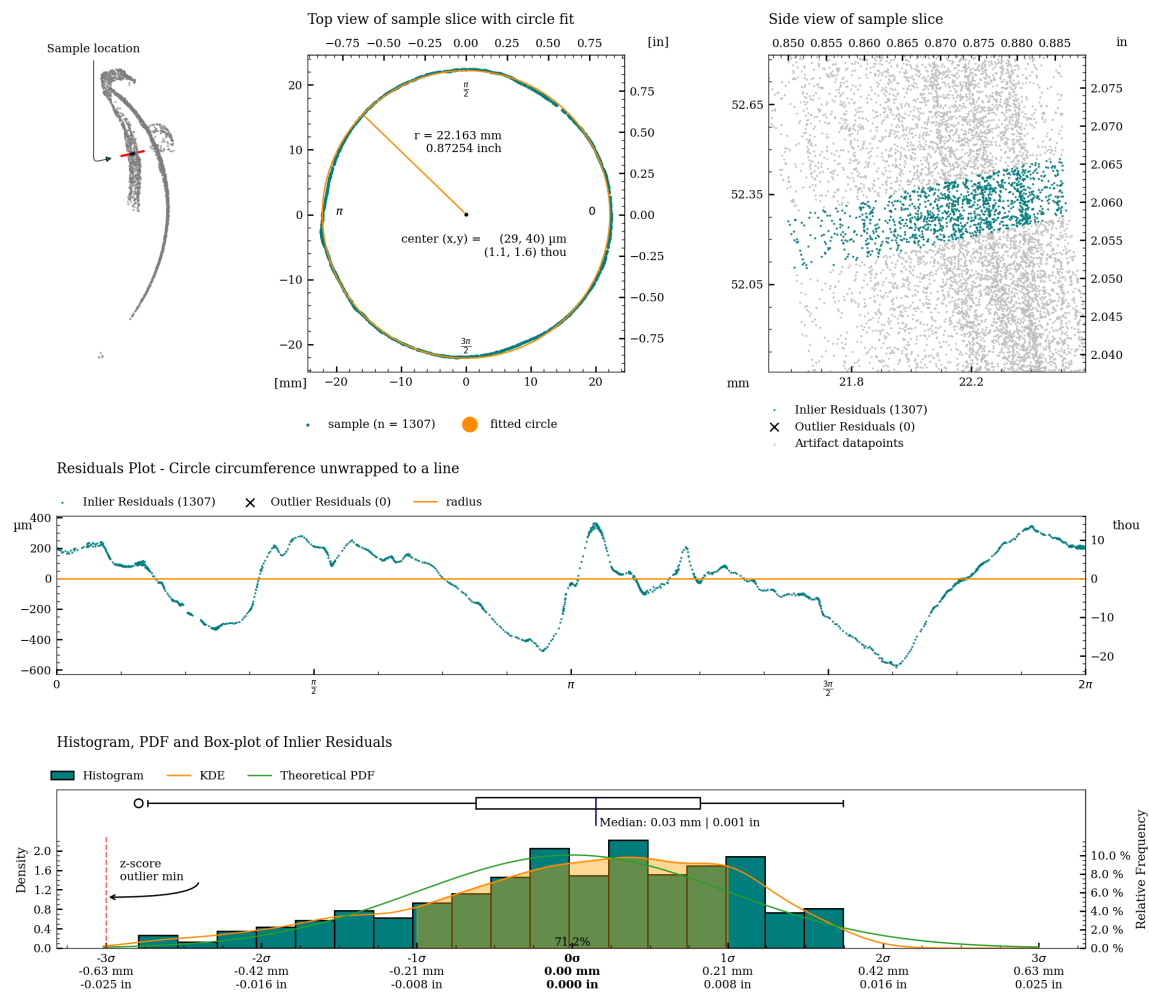


Figure 45: Detailed plot of concentricity measurement for c08_s.

Coaxiality

Coaxiality refers to the straightness and consistency of a central line running through the center of the vase. It measures how aligned the core of the vase remains along its vertical axis.

The coaxiality measurements are calculated using RANSAC (Random sample consensus) algorithm for outlier detection on least squares circle regression on cross-sections of the vessel (excluding potential handles), to estimate the best fit circle centers for each slice of the vessel. A best-fit line connects these centers, showing whether the vessels’s shape twists or remains straight. This concept helps describe the symmetry and structural uniformity in a visual and analytical way.

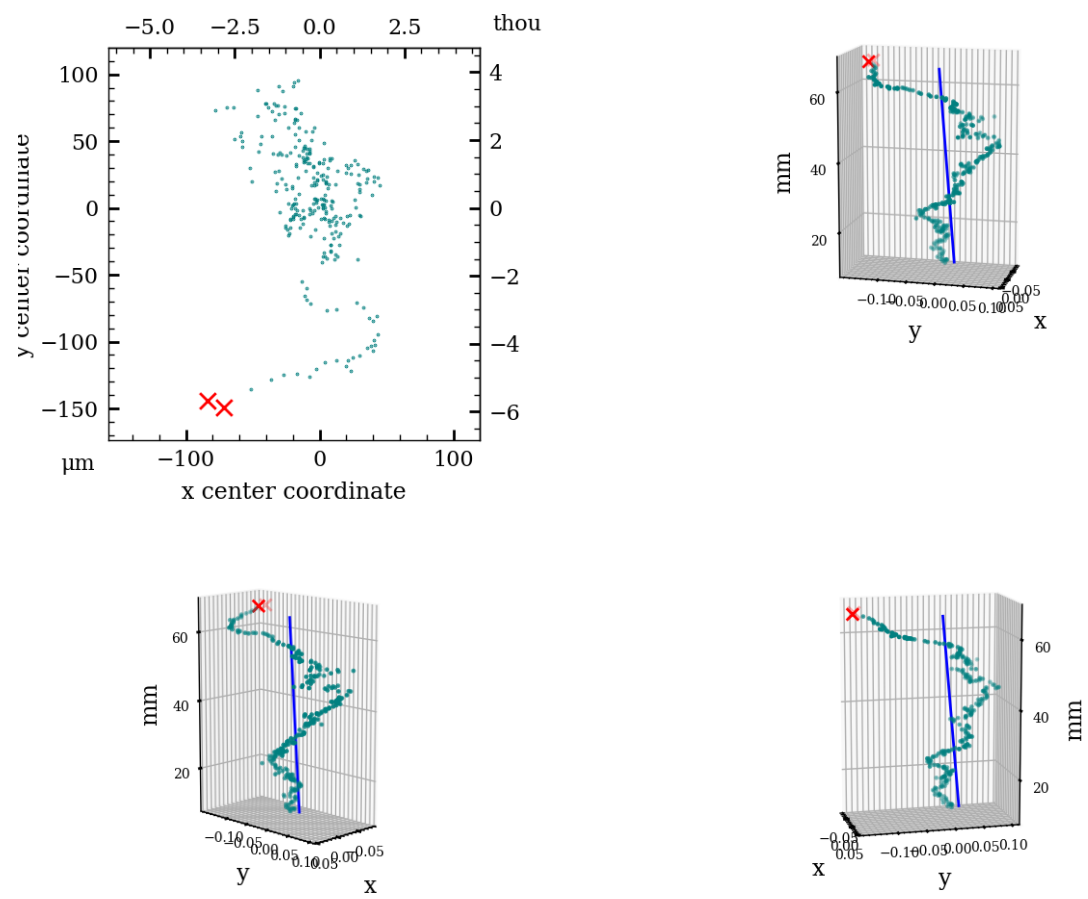
Coaxiality is measured for:

- The exterior surface (excluding handles)
- The interior surface

| | Exterior | | Interior | | Interior separate | |
|---|-----------------------|----------|-----------------------|-----------|-----------------------|-----------|
| Analyzed Slices | 275 | | 118 | | 118 | |
| Median sample size | 1731 | | 1158 | | 1148 | |
| Slice Height | 200 μm | 7.9 thou | 200 μm | 7.9 thou | 200 μm | 7.9 thou |
| Statistics with Z-axis as Reference | | | | | | |
| Median Absolute Deviation (MAD) | 37 μm | 1.4 thou | 839 μm | 33.0 thou | 117 μm | 4.6 thou |
| Standard Deviation (SD) | 33 μm | 1.3 thou | 384 μm | 15.1 thou | 190 μm | 7.5 thou |
| Root Mean Square Deviation (RMSD) | 56 μm | 2.2 thou | 841 μm | 33.1 thou | 283 μm | 11.1 thou |
| Statistics with Best Fit Central Axis as Reference | | | | | | |
| Best fit Central Axis Equation (in metric coordinate system with unit [mm]) | x = -0.001 + t0.00008 | | x = -4.868 + t0.07488 | | x = -0.066 + t0.00229 | |
| | y = 0.026 + t0.00051 | | y = -0.430 + t0.00107 | | y = 0.275 + t-0.00355 | |
| | z = 0.000 + t-1.00000 | | z = 0.000 + t0.99719 | | z = 0.000 + t0.99999 | |
| Axis tilt | 0.005° | | 4.266° | | 0.131° | |
| Median Absolute Deviation (MAD) | 37 μm | 1.5 thou | 155 μm | 6.1 thou | 102 μm | 4.0 thou |
| Standard Deviation (SD) | 29 μm | 1.1 thou | 153 μm | 6.0 thou | 178 μm | 7.0 thou |
| Root Mean Square Deviation (RMSD) | 54 μm | 2.1 thou | 257 μm | 10.1 thou | 258 μm | 10.2 thou |

Table 4: Coaxiality analysis of vessel MV015c.

Coaxiality plots, exterior surface



Coaxiality residuals from fitted axis, exterior surface

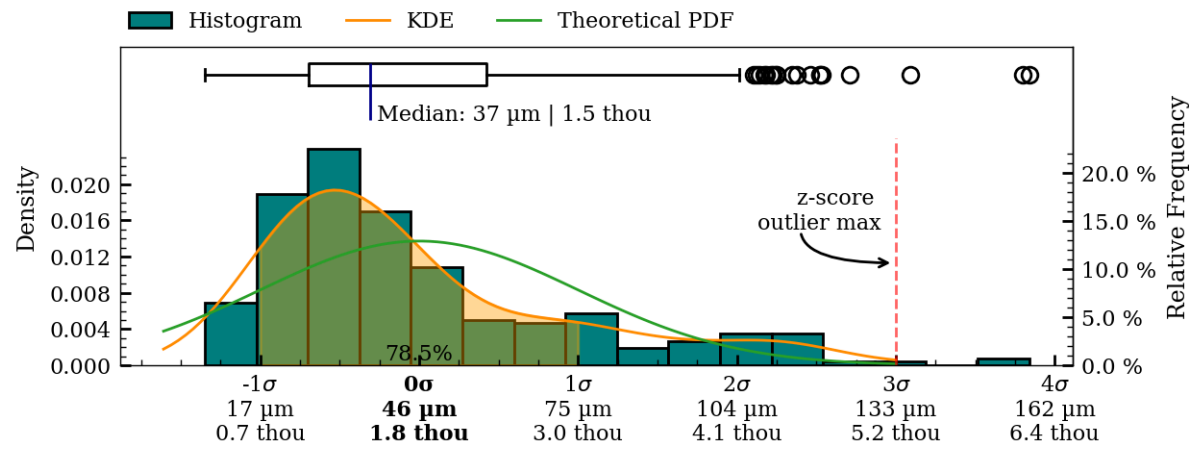
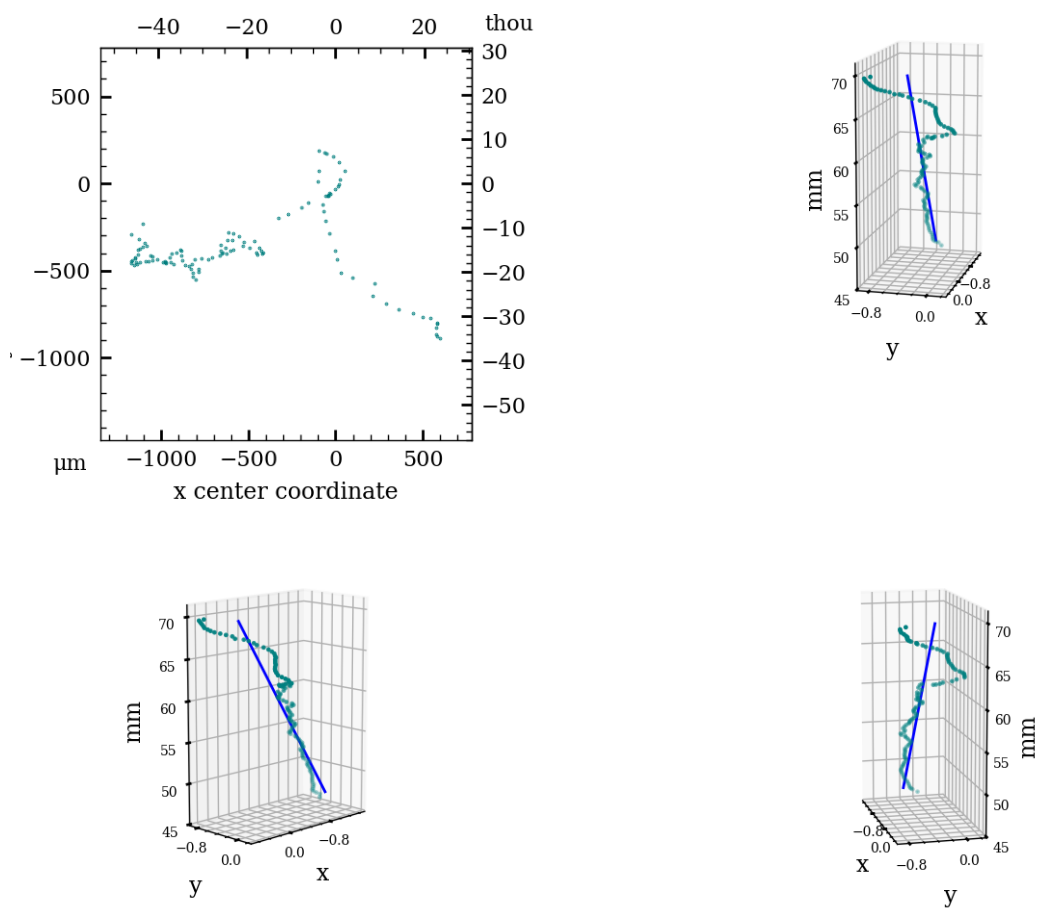


Figure 46: Coaxiality residual plots of exterior surface, MV015c.

Coaxiality plots, interior surface



Coaxiality residuals from fitted axis, interior surface

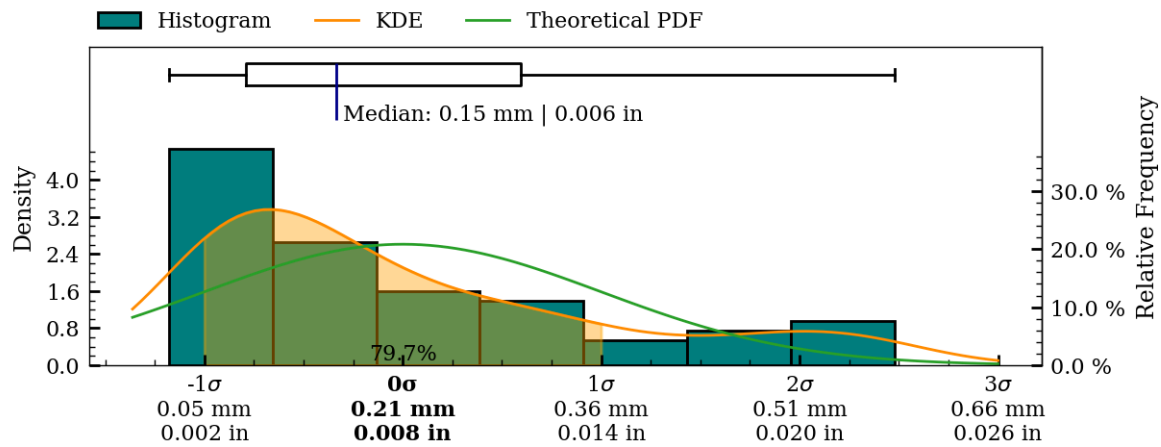
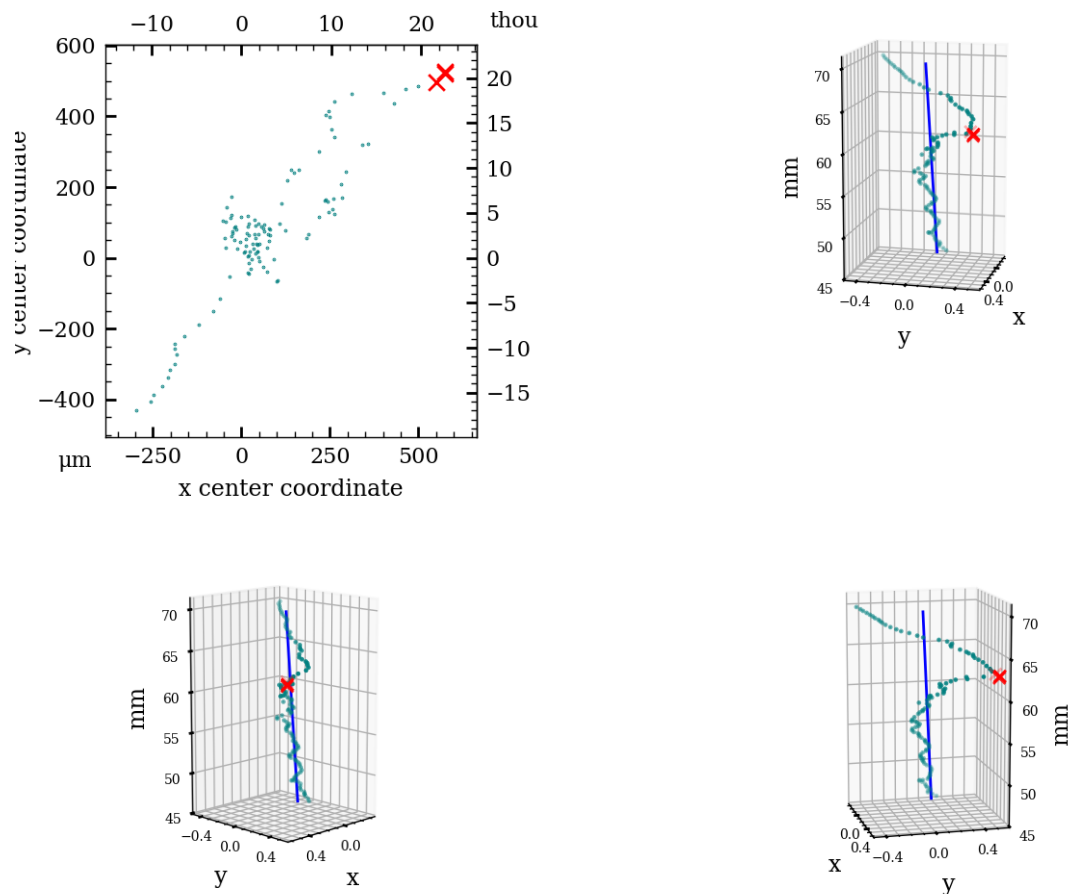


Figure 47: Coaxiality residual plots of interior surface, MV015c.

Coaxiality plots, interior separately aligned surface



Coaxiality residuals from fitted axis, interior separately aligned surface

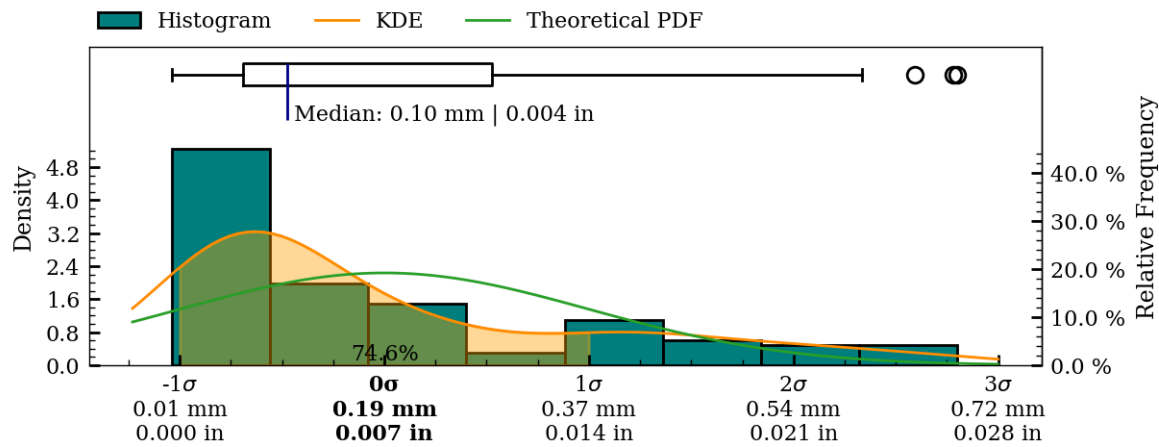


Figure 48: Coaxiality residual plots of interior_separate surface, MV015c.

Surface Variability

To illustrate the overall surface deviations of the object, a surface variability heatmap has been created. This heatmap provides an accessible overview of the topography of the manufacturing precision and surface structure of the object.

The surface variability measurements are created by fitting a number of higher-order polynomials to the two-dimensional folded profile of the scan data. This process creates an idealized mathematical representation of actual surface curvature of object, and as such provides a continuous model representation of the actual object. It is important to note that only such a non-discretized representation is sufficient to avoid introducing inconsistently varying errors in the mapping of the final surface deviation results, that the rendered heatmaps are based on.

To produce the final surface variability map, the distance from each scanned vertex to the fitted polynomial is calculated and used as the mapping function input, for applying colours to the surface of the object.

It is important to note that this variability map does not describe deviations from the original *intended* shape of the artifact (if any), as this shape (the *intended design*, so to speak) will have been lost to time. It does however provide a very informative visualization of the texture and structure of the surface and very importantly, *does* highlight potential manufacturing-relevant patterns in the surface texture (if present). Such patterns are, as an example, clearly evident on the interior surface of artifact PV001.

Exterior surface

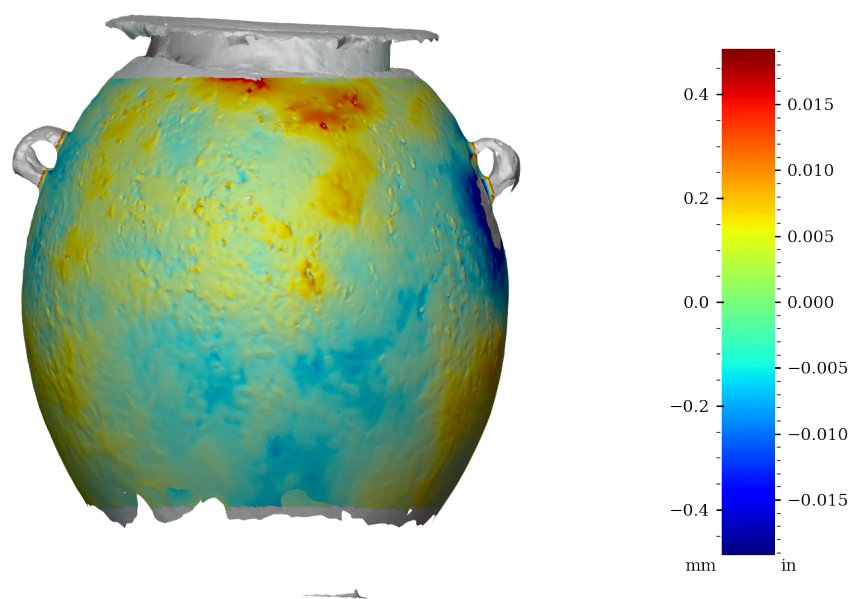


Figure 49: Surface variability heatmap of MV015c, front view

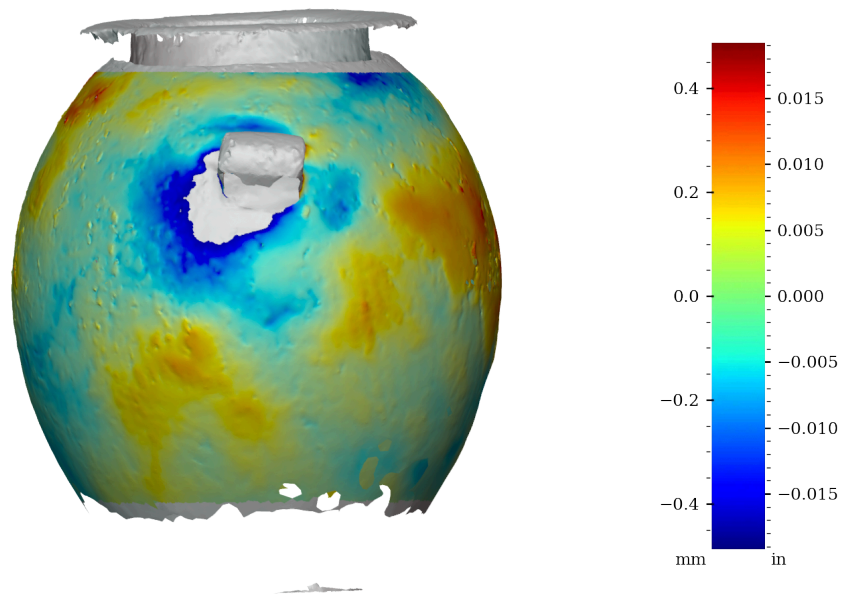


Figure 50: Surface variability heatmap of MV015c, rotated 90°

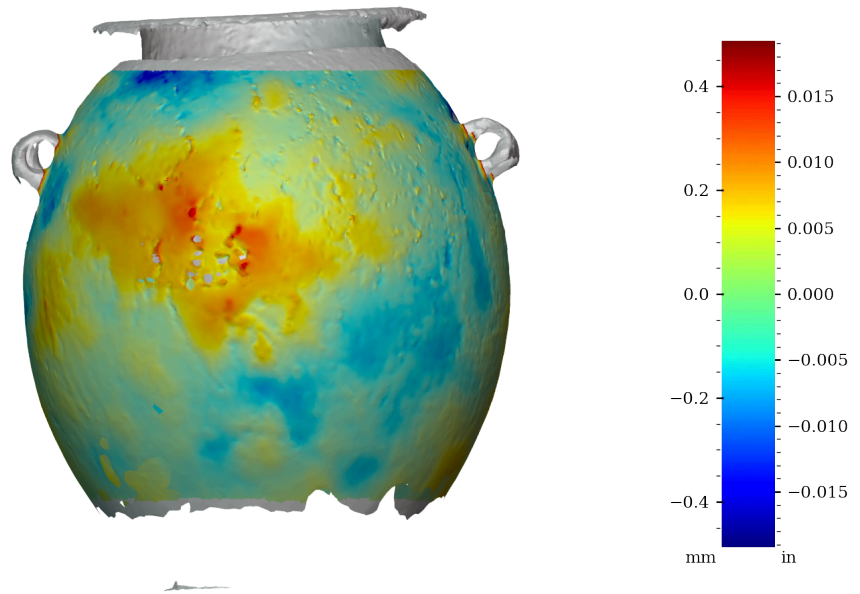


Figure 51: Surface variability heatmap of MV015c, rotated 180°

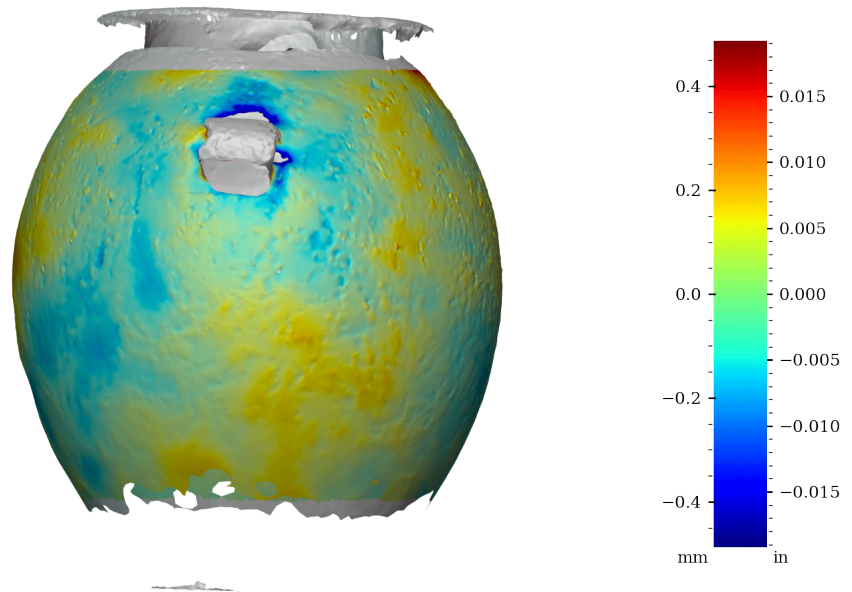


Figure 52: Surface variability heatmap of MV015c, rotated 270°

Interior surface

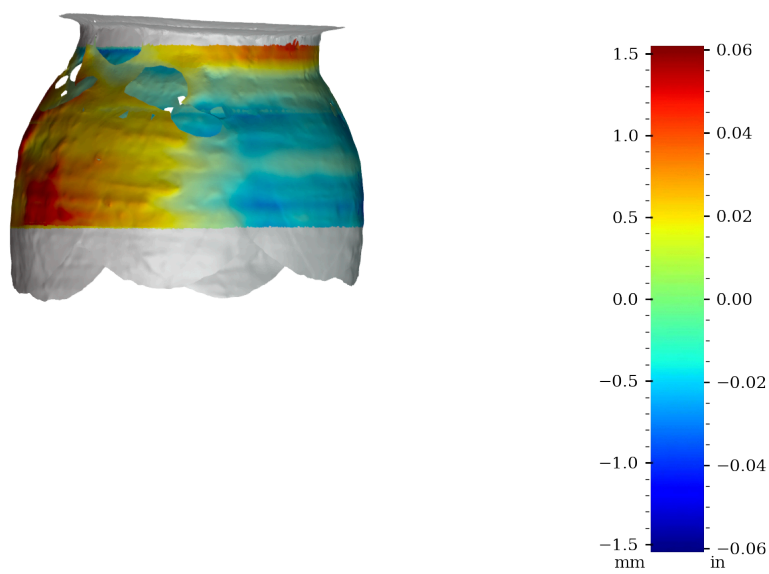


Figure 53: Surface variability heatmap of MV015c, front view

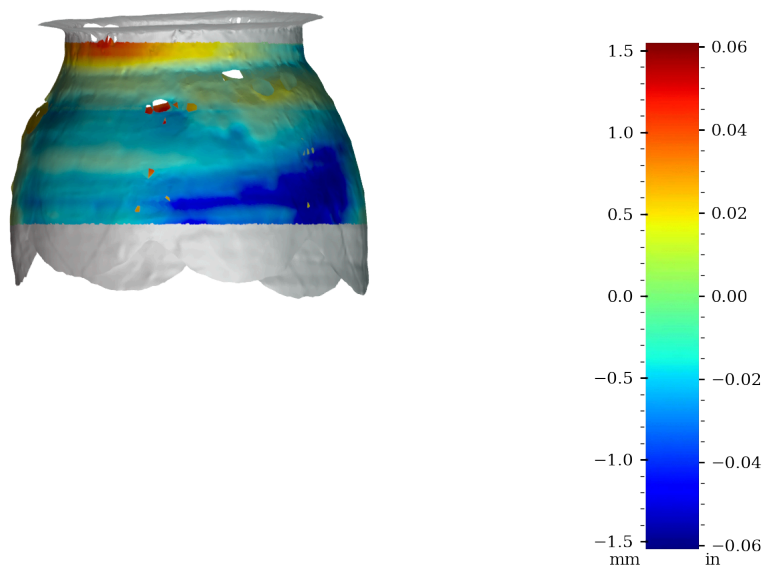


Figure 54: Surface variability heatmap of MV015c, rotated 90°

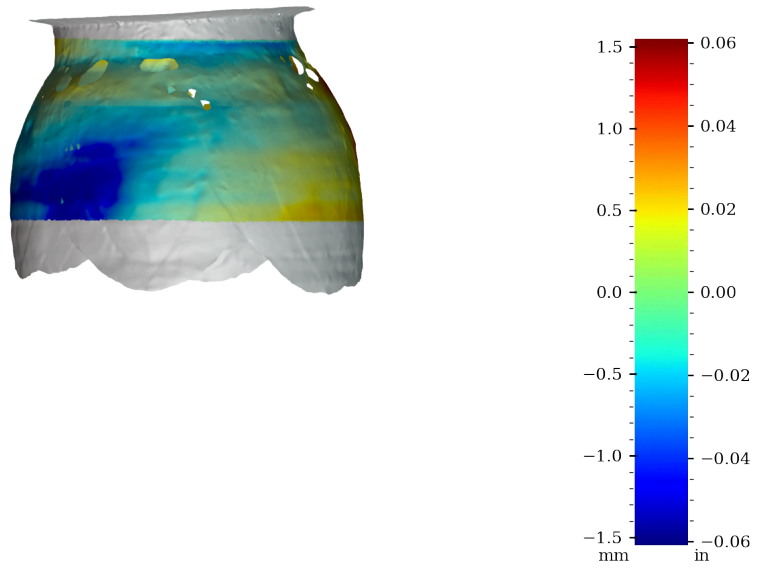


Figure 55: Surface variability heatmap of MV015c, rotated 180°

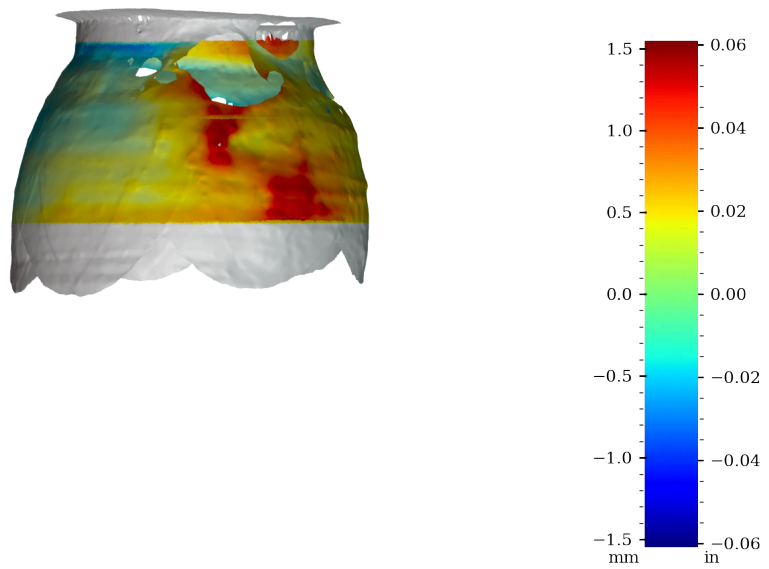


Figure 56: Surface variability heatmap of MV015c, rotated 270°

Interior surface aligned separately

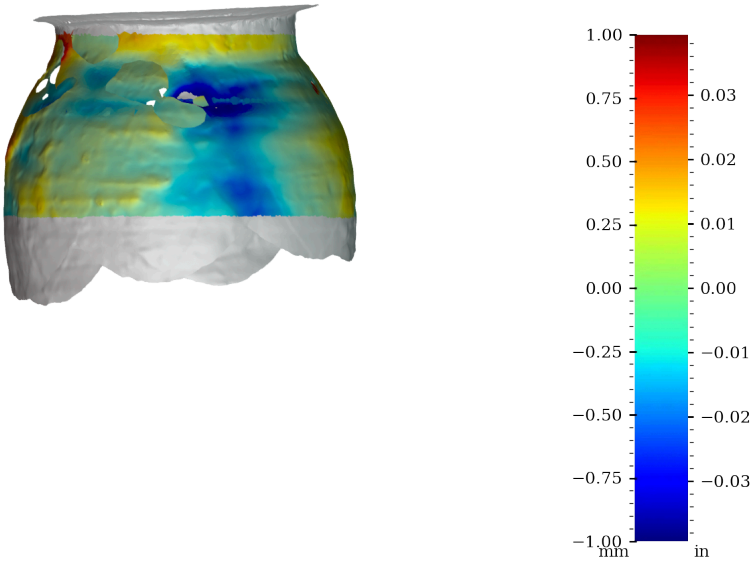


Figure 57: Surface variability heatmap of MV015c, front view

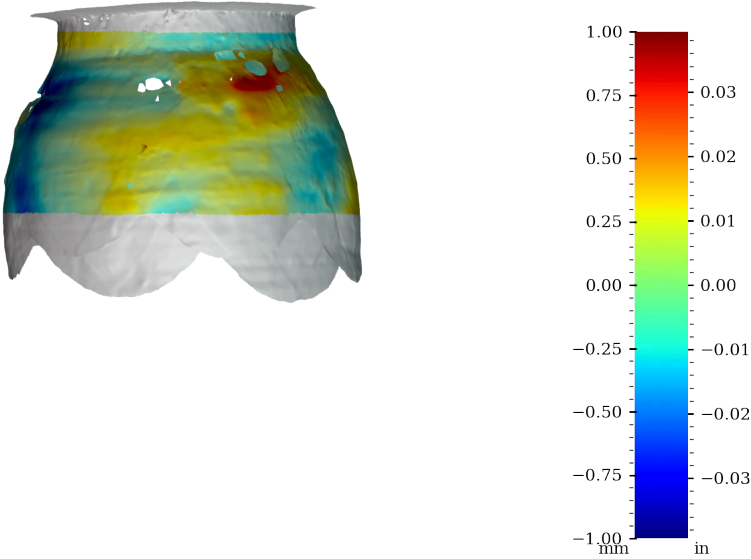


Figure 58: Surface variability heatmap of MV015c, rotated 90°

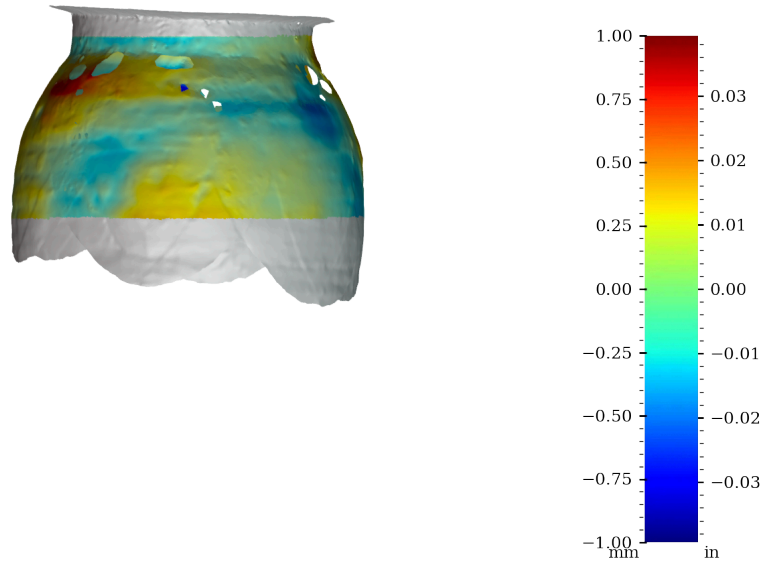


Figure 59: Surface variability heatmap of MV015c, rotated 180°

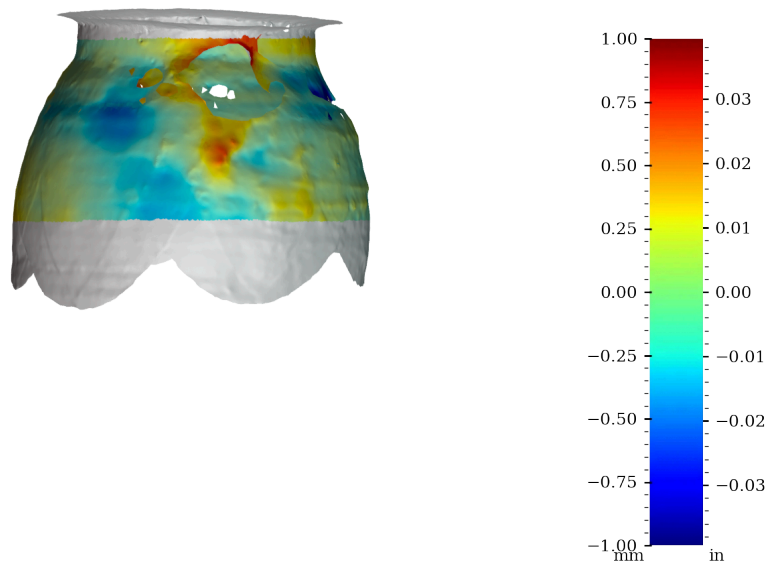


Figure 60: Surface variability heatmap of MV015c, rotated 270°

Surface variability statistics

| Area | MSD | RMSD | SD | Median AD | Range | Min | Max | Sample size |
|-------------------|-----------------|--------|--------|-----------|--------|---------|--------|-------------|
| | mm ² | mm | mm | mm | mm | mm | mm | |
| Exterior | 0.0194 | 0.139 | 0.090 | 0.049 | 1.283 | -0.765 | 0.518 | 496062 |
| Interior | 0.5218 | 0.722 | 0.387 | 0.305 | 3.088 | -1.547 | 1.542 | 140033 |
| Interior separate | 0.0812 | 0.285 | 0.177 | 0.107 | 2.175 | -1.168 | 1.007 | 137576 |
| | in ² | in | in | in | in | in | in | |
| Exterior | 0.000030 | 0.0055 | 0.0035 | 0.0019 | 0.0505 | -0.0301 | 0.0204 | 496062 |
| Interior | 0.000809 | 0.0284 | 0.0152 | 0.0120 | 0.1216 | -0.0609 | 0.0607 | 140033 |
| Interior separate | 0.000126 | 0.0112 | 0.0070 | 0.0042 | 0.0856 | -0.0460 | 0.0396 | 137576 |

Table 5: Surface variability statistics, MV015c

Table 5 shows the statistics of the distance from the scan vertices to the best fit object model. These statistics are briefly explained below.

Histogram, KDE and Box-plot of measured surface variability - exterior surface

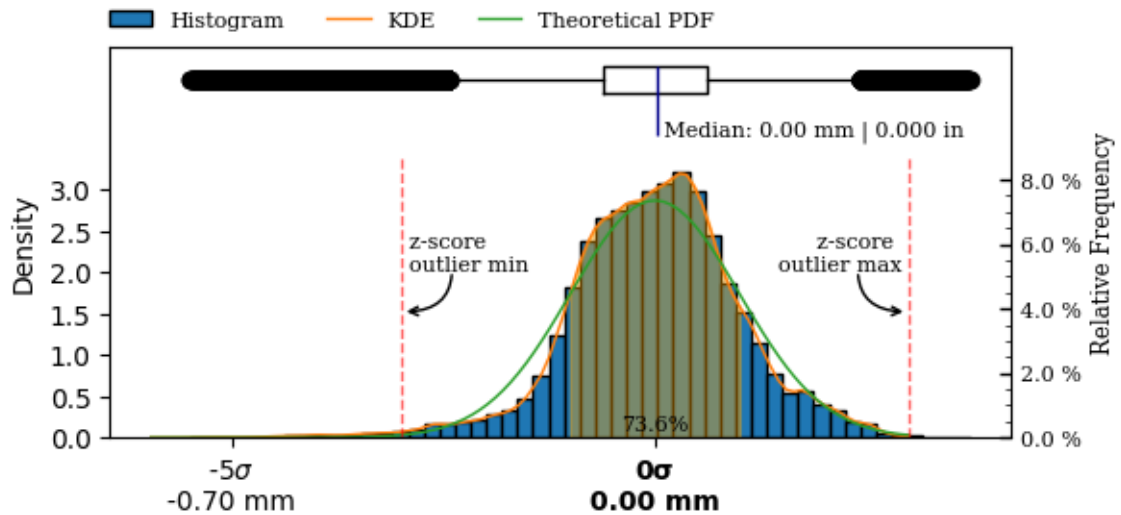


Figure 61: Exterior surface variability boxplot, kds and histogram.

Histogram, KDE and Box-plot of measured surface variability - interior surface

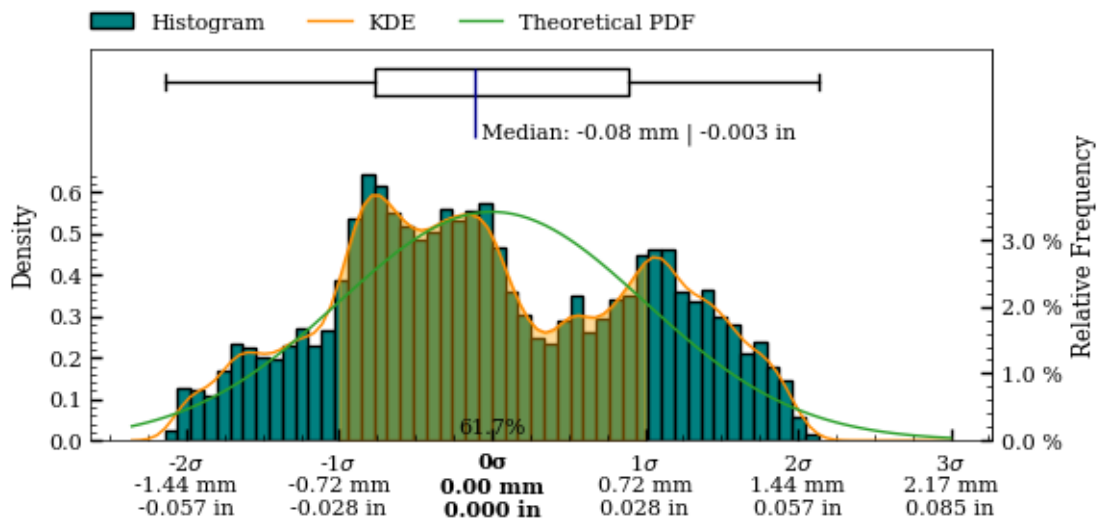


Figure 62: Interior surface variability boxplot, kds and histogram.

Histogram, KDE and Box-plot of measured surface variability - interior separately aligned surface

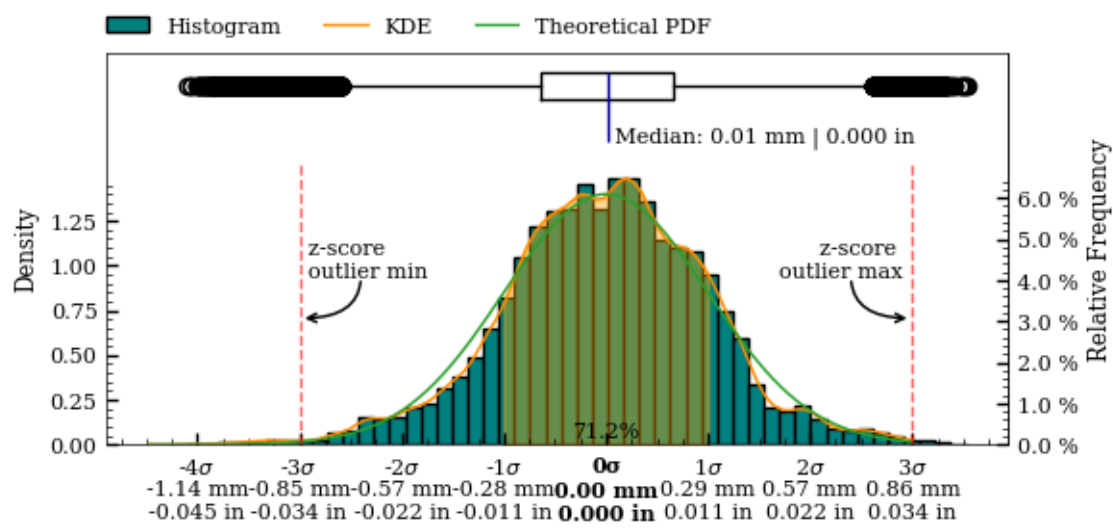


Figure 63: Interior separately aligned surface variability boxplot, kds and histogram.

Precision Score Of The Artifact

To enable valid comparison of the manufacturing precision of different artifacts, a metric that robustly quantifies the overall precision of the object is required. The considerations for such a metric will be explored in this section.

Based on these considerations, a *Precision Score* metric will be defined.

For an object to be described as having been manufactured with high precision, several qualities must be present *concurrently*, and throughout the *entire* geometry of the final object. A given object may exhibit high levels of one or more *components* of precision, but be lacking in others. For example:

- An object may present high levels of coaxiality, but lack circularity.
- An object may exhibit good circularity, but show imperfections in the surface structure.
- An object may be smoothed to perfection *without* any circularity or coaxiality.
- An object may exhibit high levels of all of the above metrics in *some* areas, but not in others.

Therefore, a precision score metric **must** account for *all* aspects of the individual, underlying precision metrics (circularity, concentricity, coaxiality and surface variability) throughout the *entire* surface area of the object.

The composite high order polynomial model, used to generate the surface variability map (described in Surface Variability, p. 48) is the best continuous mathematical representation of the object available to us (lacking any original design plans, as would normally be available in metrological analysis). This idealized model encompasses all of the above component metrics.

In the creation of the model, all scan data-points are taken into account (excluding areas with extensive damage), making it the best possible idealized representation we can achieve. When this model has been accurately created, the deviation between the model and the scanned data-points can be calculated over the non-discretized polynomials, *without* the need for an “original” CAD model (and importantly, unless such a CAD model *actually* corresponded to the original design intent, it would be an insufficient comparison basis).

Within the context of defining a valid, overall precision metric, this approach satisfies the incorporation of all of the necessary metrics:

- **Circularity:** Because the reconstructed polynomial model is revolved around the Z-plane, the idealized representation is perfectly circular, and thus incorporates the circularity component.
- **Concentricity and coaxiality:** Because the Z-axis (datum axis) is the center axis of the model, it incorporates the concentricity and coaxiality components.
- **Surface variability:** Because the model is continuous and non-discretized, it can be used accurately for all points of the scan data, and incorporates the surface variability component.

The level of precision ultimately achieved in a physical object does not share a linear relationship with its manufacturing requirements. Since continuously higher levels of final precision becomes progressively harder to achieve, an overall precision metric must take this relationship into account.

A robust statistical metric that satisfies this requirement is the *Mean Squared Deviation* (MSD or MSE). Here specifically, we can utilize the mean square of the deviations between the model (\hat{y}) and the data-points (y_i).

Combining all of the above considerations, we can express a well-defined *Precision Score* metric, that provides an immediately accessible way to understand the overall precision of an object, while being statistically valid. Since the Mean Squared Deviation tends towards zero as the overall precision increases, the inverse of the Mean Squared Deviation is taken to obtain a precision score metric that increases as precision increases¹²:

$$\text{Precision Score} = \frac{n}{\sum_{i=1}^n (y_i - \hat{y})^2}$$

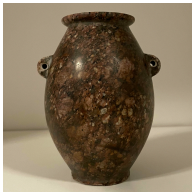
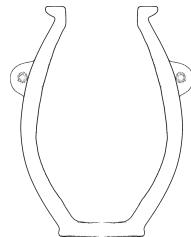

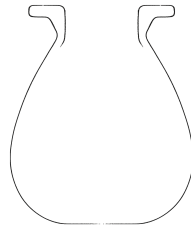

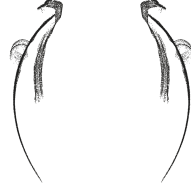

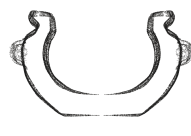


¹²The precision score unit is $\frac{1}{\text{mm}^2}$

The precision score of MV015c have been calculated separately for:

- Precision score, exterior surface: 52
- Precision score, separately aligned interior surface: 12
- Precision score, interior surface: 1.92
- Precision score, full surface: 31

The precision score of a Zeiss 1.00000 inch reference sphere have been calculated to 43,943 (RMSE = 0.00477 mm / 0.00010 in). The scan was obtained by Max Fomitchev-Zamilov using a Keyence VL –500 scanner with a rated accuracy of 10 microns. The precision analysis of the reference sphere scan indicates at the maximum possible precision score obtainable.

Table 6 shows the precision score of this artifact (MV015c), compared to the two most precise, and the two least precise vessels currently analyzed.

| Artifact | | Material | Precision Score | Link to Report |
|---|---|---|--|--------------------|
|  |  | PV001 Red Granite | 1980 Full: 1177 Exterior: 1980 Interior separate: 798 Interior: 722 | Report Publication |
|  |  | PV006 Dark grey granite | 621 Full: 610 Exterior: 621 Interior separate: 479 Interior: 152 | Report Publication |
|  |  | MV015c Black & White Syenite, perhaps Hornblende Diorite | 52 Full: 31 Exterior: 52 Interior separate: 12 Interior: 1.92 | Report Publication |
|  |  | RV003 Marble breccia | 1.46 Full: 1.49 Exterior: 1.46 Interior separate: 1.53 Interior: 0.54 | Report Publication |
|  |  | MV010 Calcite (Egyptian Alabaster) | 1.17 Full: 1.32 Exterior: 1.17 Interior separate: 11 Interior: 0.17 | Report Publication |

Analysis Roadmap

While the current iteration of this work already provides valuable results, continued future additions and improvements will enhance their utility further. This section details planned iterative updates and improvements, to both the reports themselves, and to the underlying methodology and software they are created with.

Alignment Section

- Detailed exploration of different circle regression algorithms
- If handles are present on the vessel, exploring alignment of the vessels so the handle positions match each other
- Add optimization of the perpendicular surface deviation, with the best results of the coaxial alignment
- Align by minimizing circularity results (of rotated sample slice, to compensate for sample height distortions)

Measurements of Precision

- Section detailing how measurements perpendicular to the surface curvature are obtained
- Detailed surface area analysis, exploring the residual patterns throughout subsequent sample slices of the artifact surface
- Wall thickness deviation color map
- Robust outlier identification on circularity, to better handle analysis of damaged areas of the artifacts in addition to removal of interior crystalline structure points present in CT scans
- Layout updates to the charts and tables

Visibility of Outliers and Damaged Sections

- Identification and marking of damaged parts
- Visualization of outliers on the artifact surface

Exploration of Mathematical Primitives

- Analysis of selected curvatures and flat surfaces on the vessel in both the horizontal and vertical planes
 - Circles
 - Parabolas
 - Ellipsoids
 - Hyperbolas
 - Cones
- Implementation of robust regressions models suitable for this domain, based on RANSAC.

Metrics on Primary Features

- Measurements of features in the horizontal plane
- Measurements of features in the vertical plane
- Measurements of angles
- Measurements of volume

Exploration of Potential Design Ratios

- π , φ , e , 1, 2, 3, 4 etc.

Raw Dataset Attachments

- Including all measurement and sample coordinates as CSV-files embedded in the report
- Including an STL file of the aligned object alongside the report, for easier external replication and validation of the research results

Appendix A - Comparison Of Circularity Measurements (Z-plane vs. surface-perpendicular)

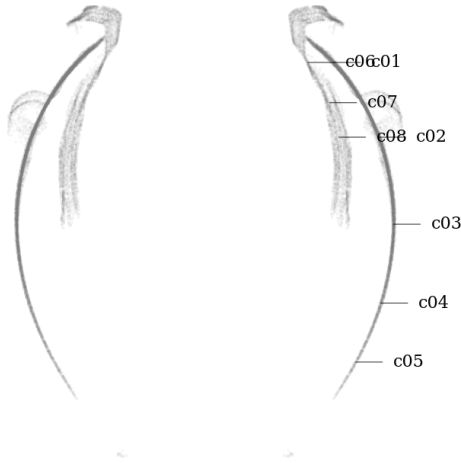


Figure 64: Circularity measurement sample locations, full mesh aligned to exterior surface

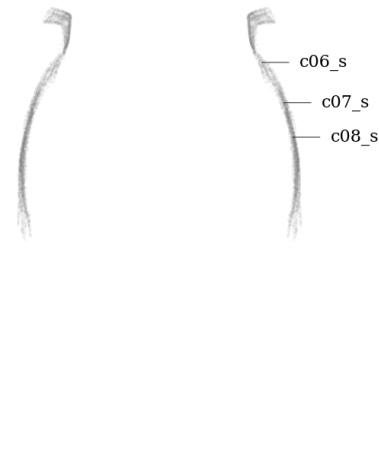


Figure 65: Circularity measurement sample location, separately aligned interior mesh

Samples perpendicular to the surface curvature

| Tag | Area | Measured deviation ⁸ | Residuals | | | | Sample size | Slice | | |
|-------|---------------|---------------------------------|-----------|-------------------|-------------------|-------|-------------|--------|----------|----------------------|
| | | | Range | RMSD ⁹ | MAD ¹⁰ | SD | | Height | Z coord. | Radius ¹¹ |
| | | mm | mm | mm | mm | mm | | mm | mm | mm |
| c01 | exterior | Ø42.631±0.411 | 0.796 | 0.163 | 0.060 | 0.099 | 2099 | 0.200 | 64.672 | 21.316 |
| c02 | exterior | Ø57.616±0.608 | 0.976 | 0.161 | 0.053 | 0.108 | 2204 | 0.200 | 52.303 | 28.808 |
| c03 | exterior | Ø62.507±0.269 | 0.503 | 0.112 | 0.046 | 0.068 | 1756 | 0.200 | 37.904 | 31.254 |
| c04 | exterior | Ø58.321±0.244 | 0.463 | 0.117 | 0.051 | 0.060 | 901 | 0.200 | 24.858 | 29.160 |
| c05 | exterior | Ø49.929±0.218 | 0.406 | 0.090 | 0.034 | 0.054 | 334 | 0.200 | 15.082 | 24.965 |
| c06 | interior sep. | Ø34.082±0.745 | 1.411 | 0.324 | 0.187 | 0.191 | 556 | 0.200 | 64.672 | 17.041 |
| c06_s | interior sep. | Ø34.082±0.745 | 1.411 | 0.324 | 0.187 | 0.191 | 556 | 0.200 | 64.672 | 17.041 |
| c07 | interior sep. | Ø41.386±0.727 | 1.275 | 0.287 | 0.123 | 0.175 | 1104 | 0.200 | 58.007 | 20.693 |
| c07_s | interior sep. | Ø41.386±0.727 | 1.275 | 0.287 | 0.123 | 0.175 | 1104 | 0.200 | 58.007 | 20.693 |
| c08 | interior sep. | Ø44.340±0.589 | 0.945 | 0.209 | 0.080 | 0.123 | 1307 | 0.200 | 52.303 | 22.170 |
| c08_s | interior sep. | Ø44.340±0.589 | 0.945 | 0.209 | 0.080 | 0.123 | 1307 | 0.200 | 52.303 | 22.170 |

Table 7: Detailed circularity measurements at selected samples in z-plane, vessel MV015c.

Samples in the Z-plane

| Tag | Area | Measured deviation ⁸ | Residuals | | | | Sample size | Slice | | |
|-------|---------------|---------------------------------|-----------|-------------------|-------------------|-------|-------------|--------|----------|----------------------|
| | | | Range | RMSD ⁹ | MAD ¹⁰ | SD | | Height | Z coord. | Radius ¹¹ |
| | | mm | mm | mm | mm | mm | | mm | mm | mm |
| c01 | exterior | Ø42.686±0.642 | 1.273 | 0.226 | 0.095 | 0.142 | 3705 | 0.200 | 64.672 | 21.343 |
| c02 | exterior | Ø57.692±0.731 | 1.176 | 0.172 | 0.057 | 0.122 | 2511 | 0.200 | 52.303 | 28.846 |
| c03 | exterior | Ø62.509±0.268 | 0.503 | 0.112 | 0.046 | 0.068 | 1751 | 0.200 | 37.904 | 31.254 |
| c04 | exterior | Ø58.306±0.271 | 0.536 | 0.126 | 0.054 | 0.065 | 992 | 0.200 | 24.858 | 29.153 |
| c05 | exterior | Ø49.959±0.262 | 0.523 | 0.112 | 0.049 | 0.068 | 441 | 0.200 | 15.082 | 24.980 |
| c06 | interior sep. | Ø33.981±1.072 | 1.815 | 0.408 | 0.193 | 0.248 | 756 | 0.200 | 64.672 | 16.991 |
| c06_s | interior sep. | Ø33.981±1.072 | 1.815 | 0.408 | 0.193 | 0.248 | 756 | 0.200 | 64.672 | 16.991 |
| c07 | interior sep. | Ø41.313±0.778 | 1.419 | 0.320 | 0.155 | 0.199 | 1269 | 0.200 | 58.007 | 20.656 |
| c07_s | interior sep. | Ø41.313±0.778 | 1.419 | 0.320 | 0.155 | 0.199 | 1269 | 0.200 | 58.007 | 20.656 |
| c08 | interior sep. | Ø44.393±0.624 | 0.962 | 0.215 | 0.087 | 0.130 | 1397 | 0.200 | 52.303 | 22.196 |
| c08_s | interior sep. | Ø44.393±0.624 | 0.962 | 0.215 | 0.087 | 0.130 | 1397 | 0.200 | 52.303 | 22.196 |

Table 8: Detailed circularity measurements at selected samples perpendicular to vessel curvature, vessel MV015c.

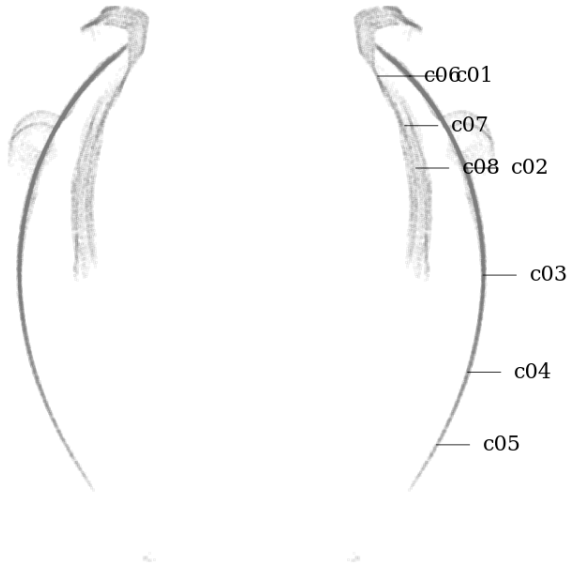


Figure 66: Circularity measurement sample locations, full mesh aligned to exterior surface

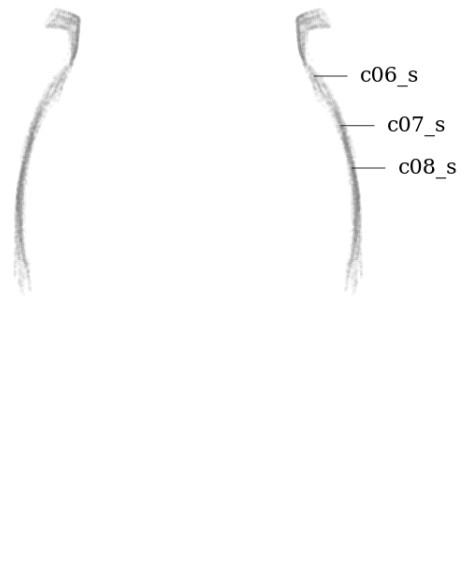


Figure 67: Circularity measurement sample location, separately aligned interior mesh

Samples perpendicular to the surface curvature

| Tag | Area | Measured deviation ⁸ | Residuals | | | | Sample size | Slice | | |
|-------|---------------|---------------------------------|-----------|-------------------|-------------------|--------|-------------|--------|----------|----------------------|
| | | | Range | RMSD ⁹ | MAD ¹⁰ | SD | | Height | Z coord. | Radius ¹¹ |
| | | in | in | in | in | in | | in | in | in |
| c01 | exterior | Ø1.6784±0.0162 | 0.0314 | 0.0064 | 0.0024 | 0.0039 | 2099 | 0.0079 | 2.5461 | 0.8392 |
| c02 | exterior | Ø2.2684±0.0239 | 0.0384 | 0.0063 | 0.0021 | 0.0043 | 2204 | 0.0079 | 2.0592 | 1.1342 |
| c03 | exterior | Ø2.4609±0.0106 | 0.0198 | 0.0044 | 0.0018 | 0.0027 | 1756 | 0.0079 | 1.4923 | 1.2305 |
| c04 | exterior | Ø2.2961±0.0096 | 0.0182 | 0.0046 | 0.0020 | 0.0024 | 901 | 0.0079 | 0.9786 | 1.1480 |
| c05 | exterior | Ø1.9657±0.0086 | 0.0160 | 0.0036 | 0.0014 | 0.0021 | 334 | 0.0079 | 0.5938 | 0.9829 |
| c06 | interior sep. | Ø1.3418±0.0293 | 0.0555 | 0.0128 | 0.0074 | 0.0075 | 556 | 0.0079 | 2.5461 | 0.6709 |
| c06_s | interior sep. | Ø1.3418±0.0293 | 0.0555 | 0.0128 | 0.0074 | 0.0075 | 556 | 0.0079 | 2.5461 | 0.6709 |
| c07 | interior sep. | Ø1.6294±0.0286 | 0.0502 | 0.0113 | 0.0048 | 0.0069 | 1104 | 0.0079 | 2.2838 | 0.8147 |
| c07_s | interior sep. | Ø1.6294±0.0286 | 0.0502 | 0.0113 | 0.0048 | 0.0069 | 1104 | 0.0079 | 2.2838 | 0.8147 |
| c08 | interior sep. | Ø1.7457±0.0232 | 0.0372 | 0.0082 | 0.0031 | 0.0048 | 1307 | 0.0079 | 2.0592 | 0.8728 |
| c08_s | interior sep. | Ø1.7457±0.0232 | 0.0372 | 0.0082 | 0.0031 | 0.0048 | 1307 | 0.0079 | 2.0592 | 0.8728 |

Table 9: Detailed circularity measurements at selected samples in z-plane, vessel MV015c.

Samples in the Z-plane

| Tag | Area | Measured deviation ⁸ | Residuals | | | | Sample size | Slice | | |
|-------|---------------|---------------------------------|-----------|-------------------|-------------------|--------|-------------|--------|----------|----------------------|
| | | | Range | RMSD ⁹ | MAD ¹⁰ | SD | | Height | Z coord. | Radius ¹¹ |
| | | in | in | in | in | in | | in | in | in |
| c01 | exterior | Ø1.6805±0.0253 | 0.0501 | 0.0089 | 0.0037 | 0.0056 | 3705 | 0.0079 | 2.5461 | 0.8403 |
| c02 | exterior | Ø2.2714±0.0288 | 0.0463 | 0.0068 | 0.0022 | 0.0048 | 2511 | 0.0079 | 2.0592 | 1.1357 |
| c03 | exterior | Ø2.4610±0.0106 | 0.0198 | 0.0044 | 0.0018 | 0.0027 | 1751 | 0.0079 | 1.4923 | 1.2305 |
| c04 | exterior | Ø2.2955±0.0107 | 0.0211 | 0.0049 | 0.0021 | 0.0026 | 992 | 0.0079 | 0.9786 | 1.1478 |
| c05 | exterior | Ø1.9669±0.0103 | 0.0206 | 0.0044 | 0.0019 | 0.0027 | 441 | 0.0079 | 0.5938 | 0.9835 |
| c06 | interior sep. | Ø1.3378±0.0422 | 0.0715 | 0.0160 | 0.0076 | 0.0098 | 756 | 0.0079 | 2.5461 | 0.6689 |
| c06_s | interior sep. | Ø1.3378±0.0422 | 0.0715 | 0.0160 | 0.0076 | 0.0098 | 756 | 0.0079 | 2.5461 | 0.6689 |
| c07 | interior sep. | Ø1.6265±0.0306 | 0.0559 | 0.0126 | 0.0061 | 0.0078 | 1269 | 0.0079 | 2.2838 | 0.8132 |
| c07_s | interior sep. | Ø1.6265±0.0306 | 0.0559 | 0.0126 | 0.0061 | 0.0078 | 1269 | 0.0079 | 2.2838 | 0.8132 |
| c08 | interior sep. | Ø1.7477±0.0246 | 0.0379 | 0.0085 | 0.0034 | 0.0051 | 1397 | 0.0079 | 2.0592 | 0.8739 |
| c08_s | interior sep. | Ø1.7477±0.0246 | 0.0379 | 0.0085 | 0.0034 | 0.0051 | 1397 | 0.0079 | 2.0592 | 0.8739 |

Table 10: Detailed circularity measurements at selected samples perpendicular to vessel curvature, vessel MV015c.

Comparison of circularity on the full vessel surface

Metric

Samples perpendicular to the surface curvature

| Area | Range | | | Standard Deviation | | | RMSD | | | Slices | Slice height |
|-------------------|--------|-------|-------|--------------------|-------|-------|--------|-------|-------|--------|--------------|
| | Median | Min. | Max. | Median | Min. | Max. | Median | Min. | Max. | | |
| | mm | mm | mm | mm | mm | mm | mm | mm | mm | | mm |
| Exterior | 0.564 | 0.345 | 1.152 | 0.068 | 0.044 | 0.161 | 0.117 | 0.070 | 0.215 | 275 | 0.200 |
| Interior | 2.340 | 1.038 | 2.991 | 0.308 | 0.097 | 0.437 | 0.690 | 0.123 | 0.964 | 118 | 0.200 |
| Interior separate | 1.243 | 0.942 | 2.050 | 0.152 | 0.086 | 0.298 | 0.254 | 0.131 | 0.566 | 118 | 0.200 |

Table 11: Detailed circularity measurements at selected samples in z-plane, vessel MV015c.

Samples in the z-plane

| Area | Range | | | Standard Deviation | | | RMSD | | | Slices | Slice height |
|-------------------|--------|-------|-------|--------------------|-------|-------|--------|-------|-------|--------|--------------|
| | Median | Min. | Max. | Median | Min. | Max. | Median | Min. | Max. | | |
| | mm | mm | mm | mm | mm | mm | mm | mm | mm | | mm |
| Exterior | 0.585 | 0.413 | 1.430 | 0.070 | 0.052 | 0.169 | 0.121 | 0.099 | 0.264 | 274 | 0.200 |
| Interior | 2.606 | 1.591 | 3.048 | 0.388 | 0.146 | 0.579 | 0.771 | 0.213 | 0.965 | 116 | 0.200 |
| Interior separate | 1.354 | 0.944 | 2.422 | 0.169 | 0.104 | 0.363 | 0.266 | 0.145 | 0.637 | 116 | 0.200 |

Table 12: Detailed circularity measurements at selected samples perpendicular to vessel curvature, vessel MV015c.

Imperial

Samples perpendicular to the surface curvature

| Area | Range | | | Standard Deviation | | | RMSD | | | Slices | Slice height |
|-------------------|--------|-------|-------|--------------------|-------|-------|--------|-------|-------|--------|--------------|
| | Median | Min. | Max. | Median | Min. | Max. | Median | Min. | Max. | | |
| | in | in | in | in | in | in | in | in | in | | in |
| Exterior | 0.564 | 0.345 | 1.152 | 0.068 | 0.044 | 0.161 | 0.117 | 0.070 | 0.215 | 275 | 0.200 |
| Interior | 2.340 | 1.038 | 2.991 | 0.308 | 0.097 | 0.437 | 0.690 | 0.123 | 0.964 | 118 | 0.200 |
| Interior separate | 1.243 | 0.942 | 2.050 | 0.152 | 0.086 | 0.298 | 0.254 | 0.131 | 0.566 | 118 | 0.200 |

Table 13: Detailed circularity measurements at selected samples in z-plane, vessel MV015c.

Samples in the z-plane

| Area | Range | | | Standard Deviation | | | RMSD | | | Slices | Slice height |
|-------------------|--------|-------|-------|--------------------|-------|-------|--------|-------|-------|--------|--------------|
| | Median | Min. | Max. | Median | Min. | Max. | Median | Min. | Max. | | |
| | in | in | in | in | in | in | in | in | in | | in |
| Exterior | 0.585 | 0.413 | 1.430 | 0.070 | 0.052 | 0.169 | 0.121 | 0.099 | 0.264 | 274 | 0.200 |
| Interior | 2.606 | 1.591 | 3.048 | 0.388 | 0.146 | 0.579 | 0.771 | 0.213 | 0.965 | 116 | 0.200 |
| Interior separate | 1.354 | 0.944 | 2.422 | 0.169 | 0.104 | 0.363 | 0.266 | 0.145 | 0.637 | 116 | 0.200 |

Table 14: Detailed circularity measurements at selected samples perpendicular to vessel curvature, vessel MV015c.

Circularity analysis of exterior surface - perpendicular to surface curvature

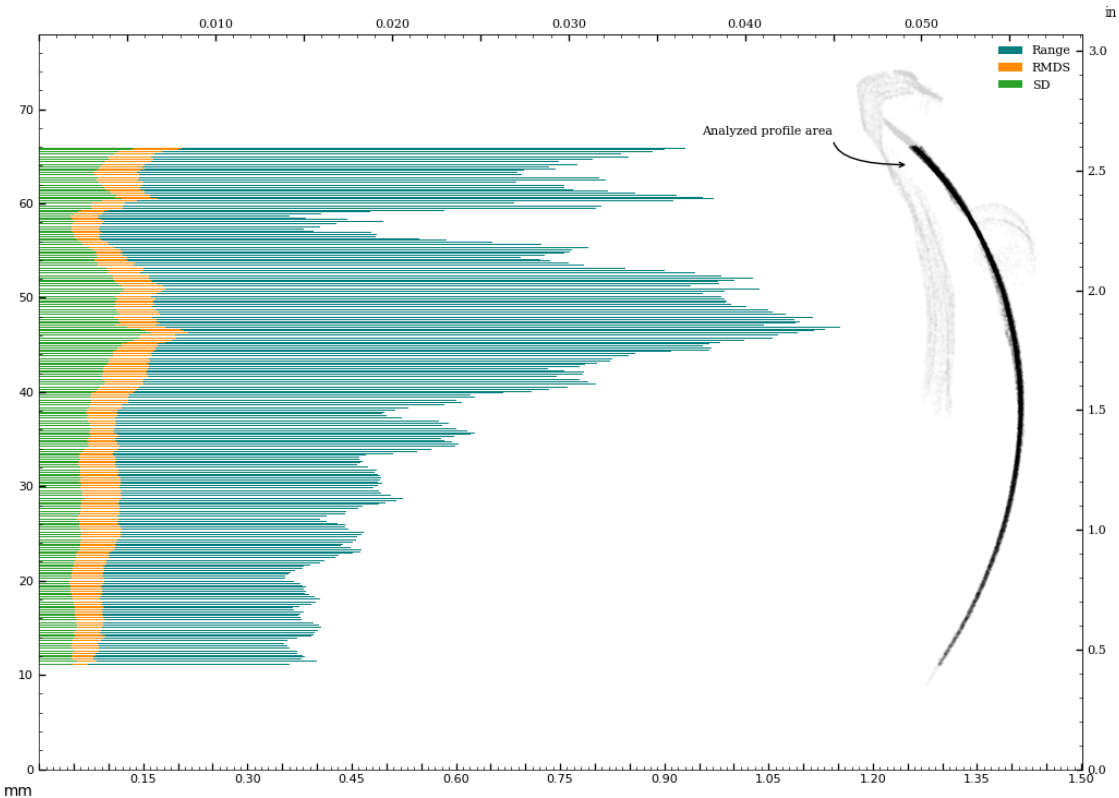


Figure 68: Circularity of exterior surface - perpendicular to surface curvature.

Circularity analysis of exterior surface - in z-plane

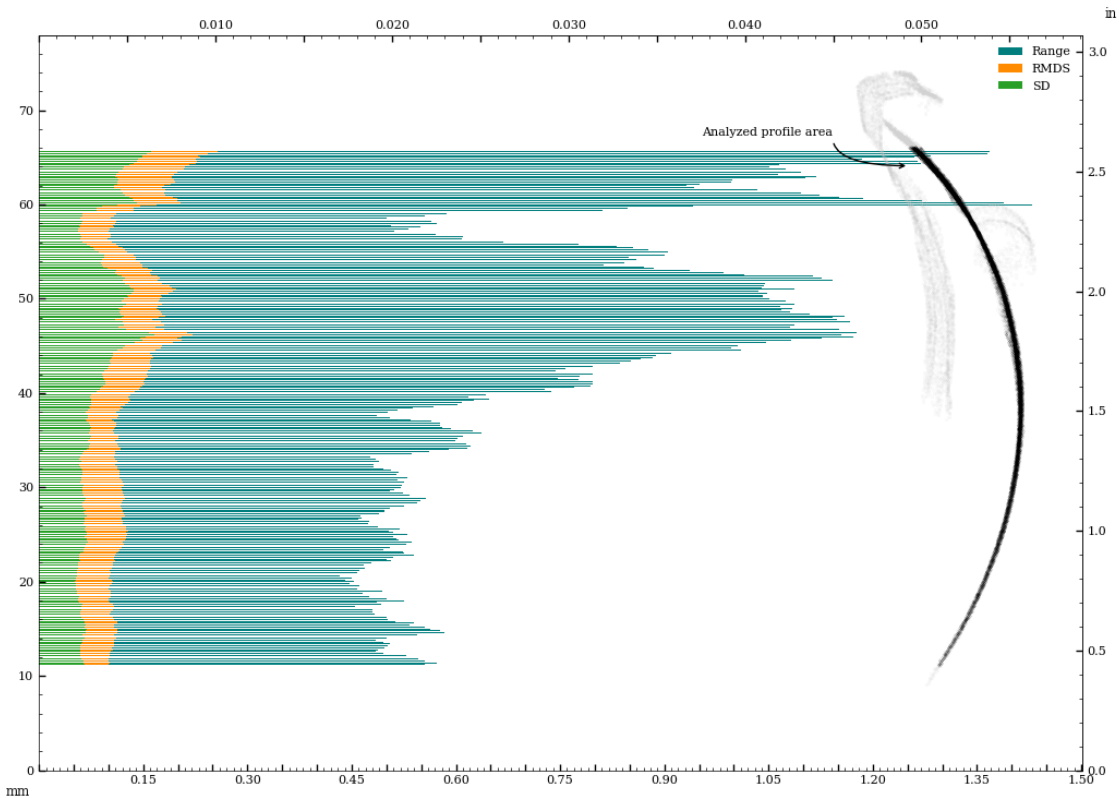


Figure 69: Circularity of exterior surface - in z-plane.

Circularity analysis of exterior surface, perpendicular to surface curvature, Standard Deviation and Root Mean Squared Deviation

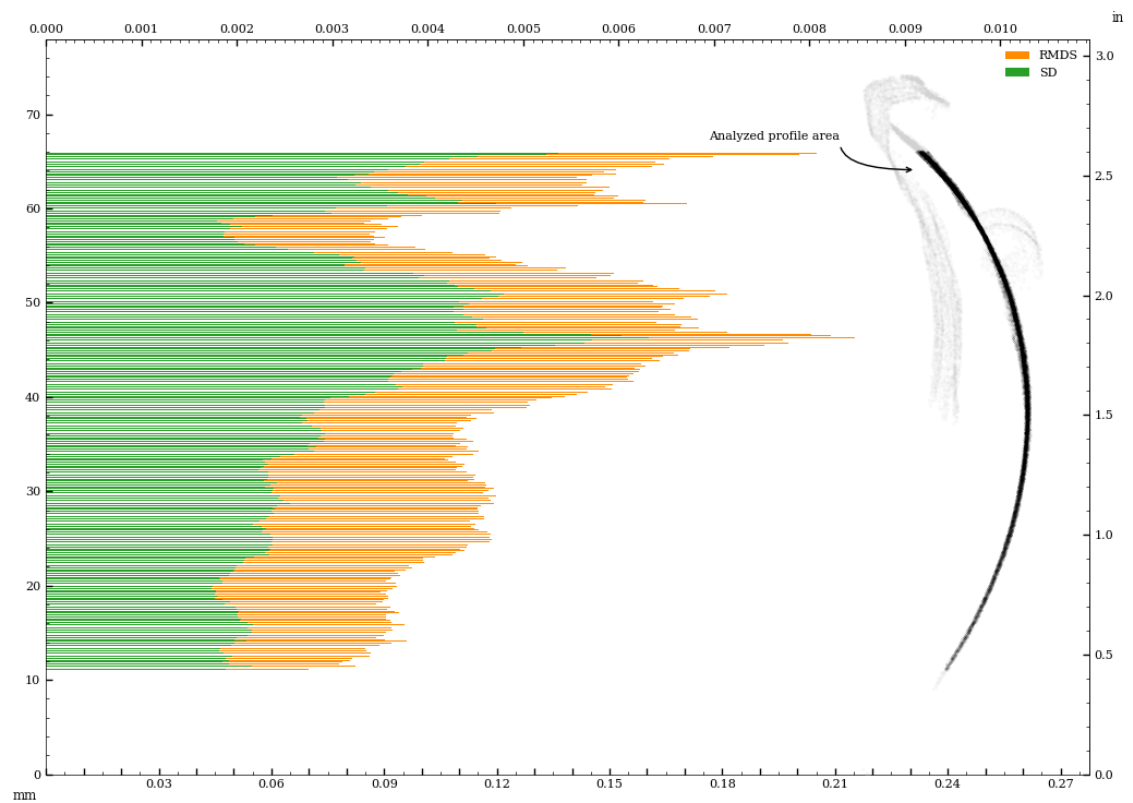


Figure 70: Vessel circularity of exterior surface, perpendicular to surface curvature, standard deviation and median absolute deviation.

Circularity analysis of exterior surface, in z-plane, Standard Deviation and Root Mean Squared Deviation

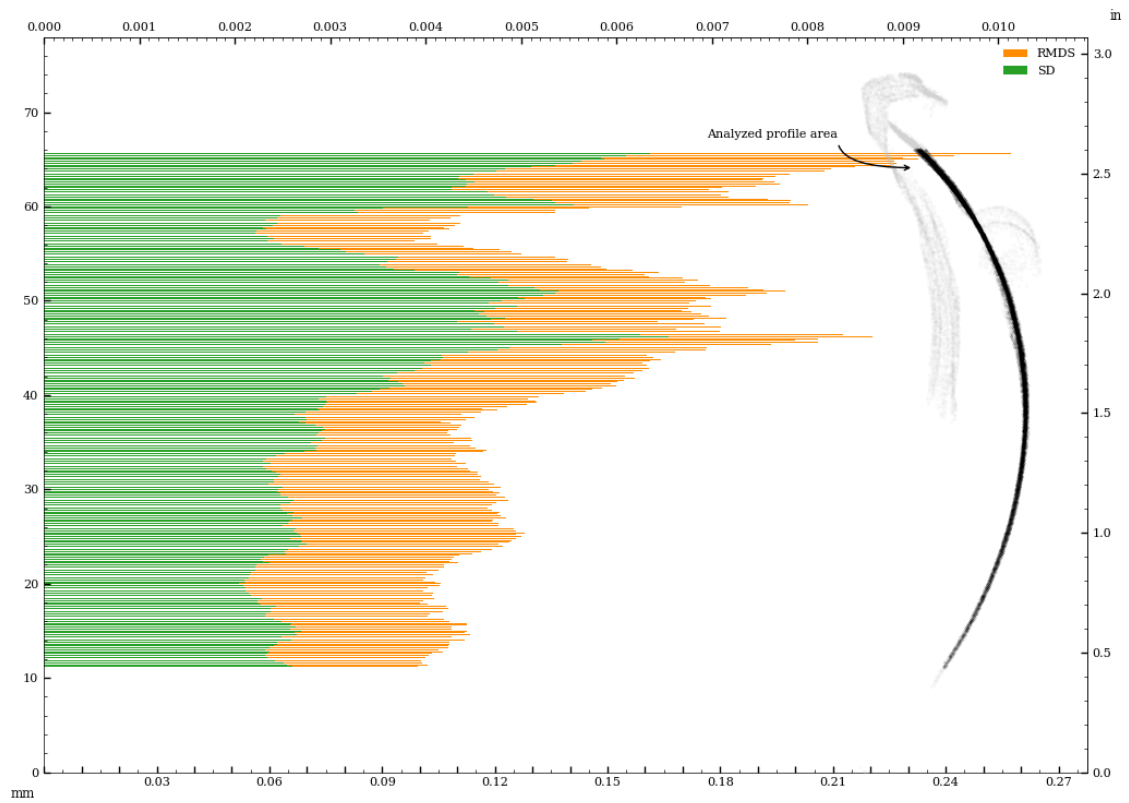


Figure 71: Vessel circularity of exterior surface, in z-plane, standard deviation and median absolute deviation.

Circularity analysis of interior surface - perpendicular to surface curvature

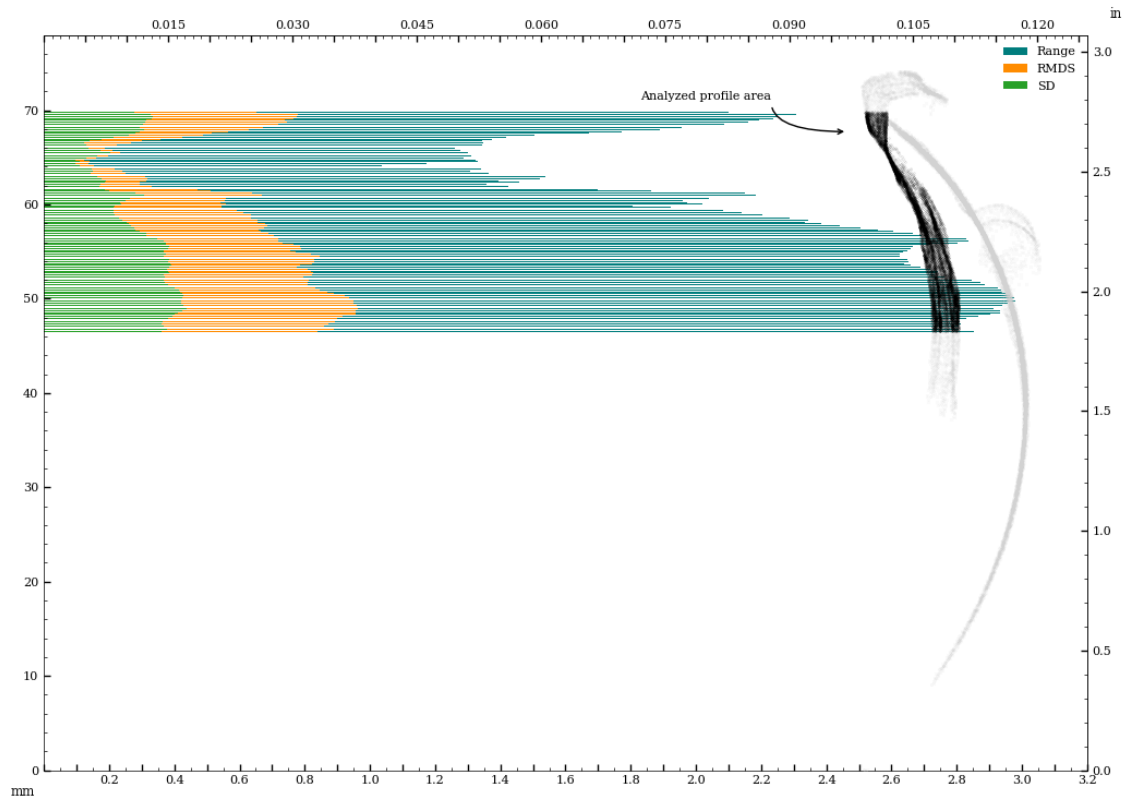


Figure 72: Circularity of interior surface - perpendicular to surface curvature.

Circularity analysis of interior surface - in z-plane

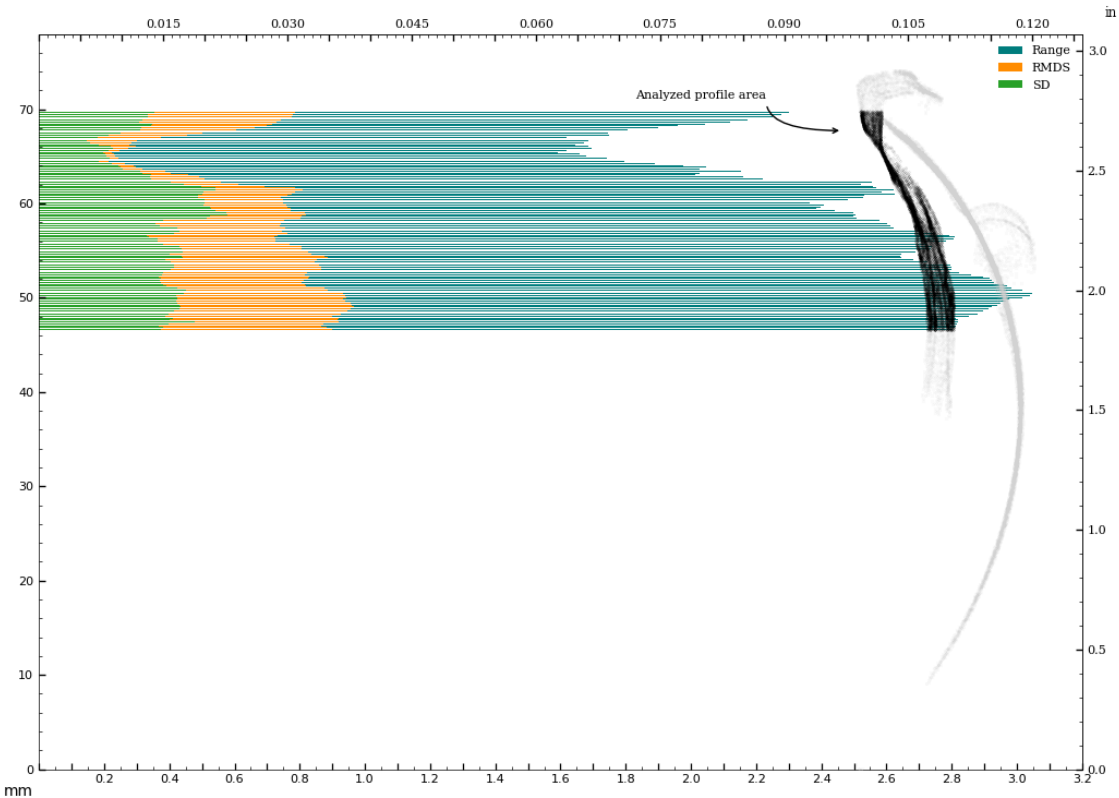


Figure 73: Circularity of interior surface - in z-plane.

Circularity analysis of interior surface, perpendicular to surface curvature, Standard Deviation and Root Mean Squared Deviation

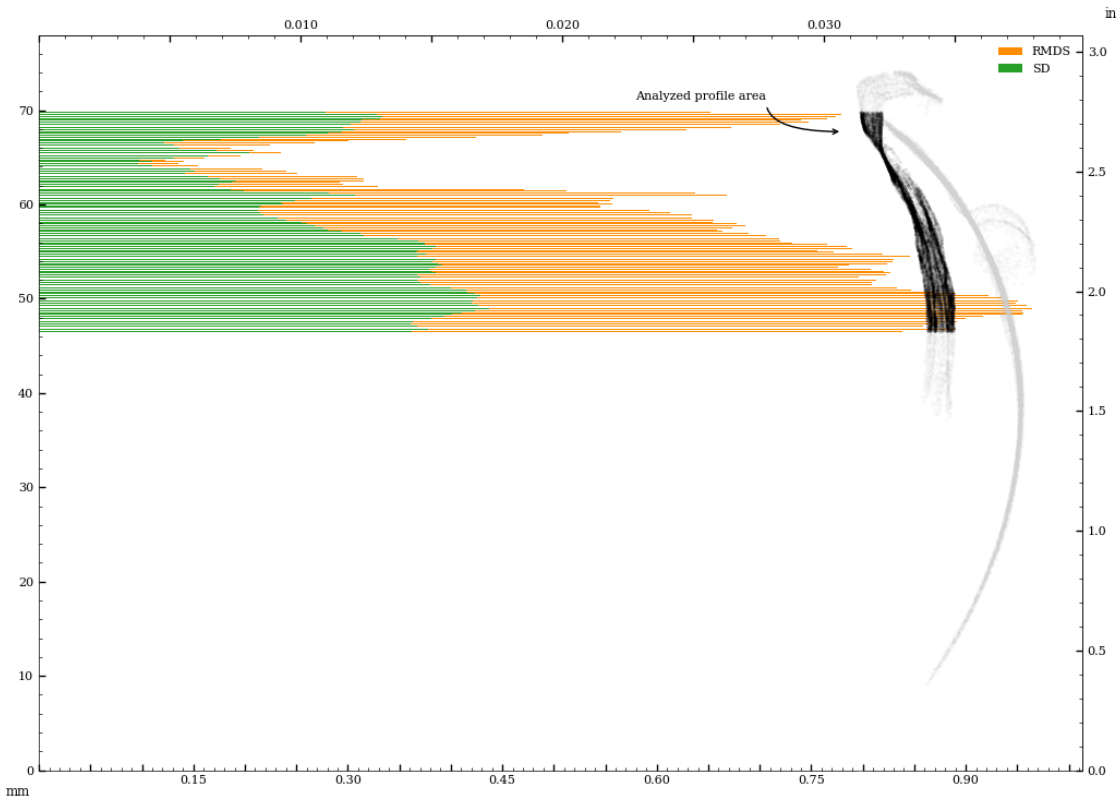


Figure 74: Vessel circularity of interior surface, perpendicular to surface curvature, standard deviation and median absolute deviation.

Circularity analysis of interior surface, in z-plane, Standard Deviation and Root Mean Squared Deviation

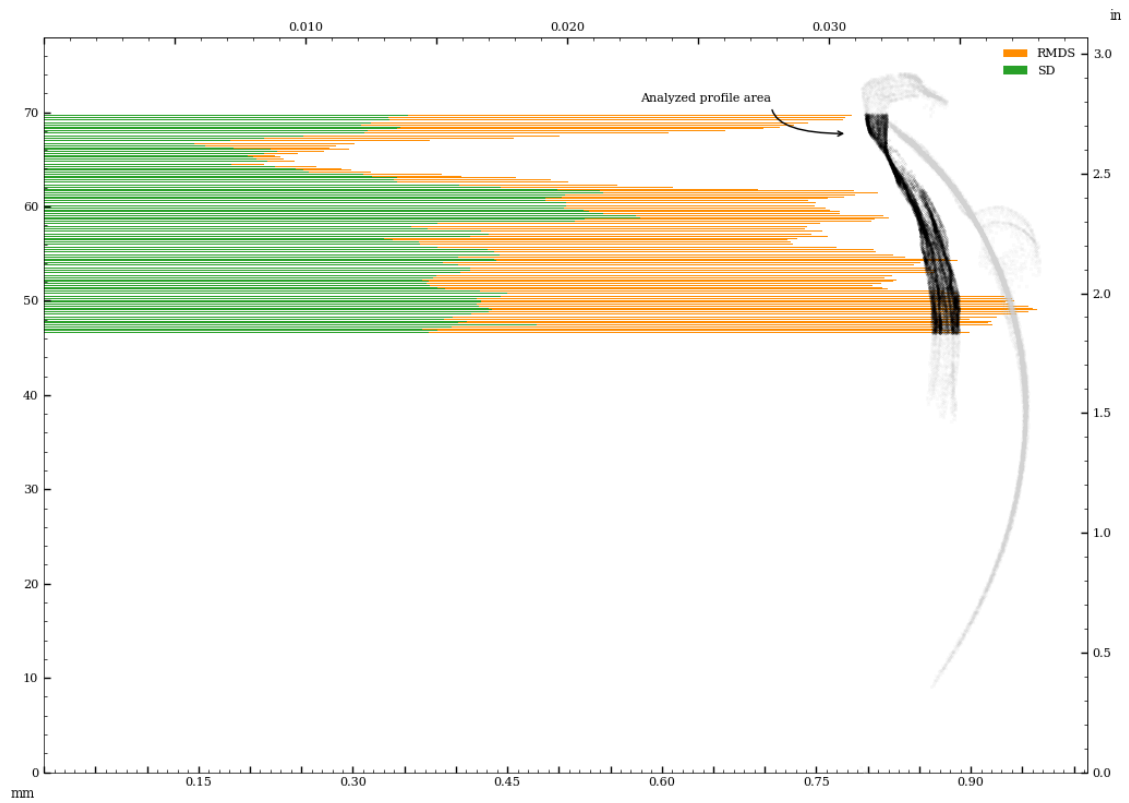


Figure 75: Vessel circularity of interior surface, in z-plane, standard deviation and median absolute deviation.

Circularity analysis of interior separately aligned surface - perpendicular to surface curvature

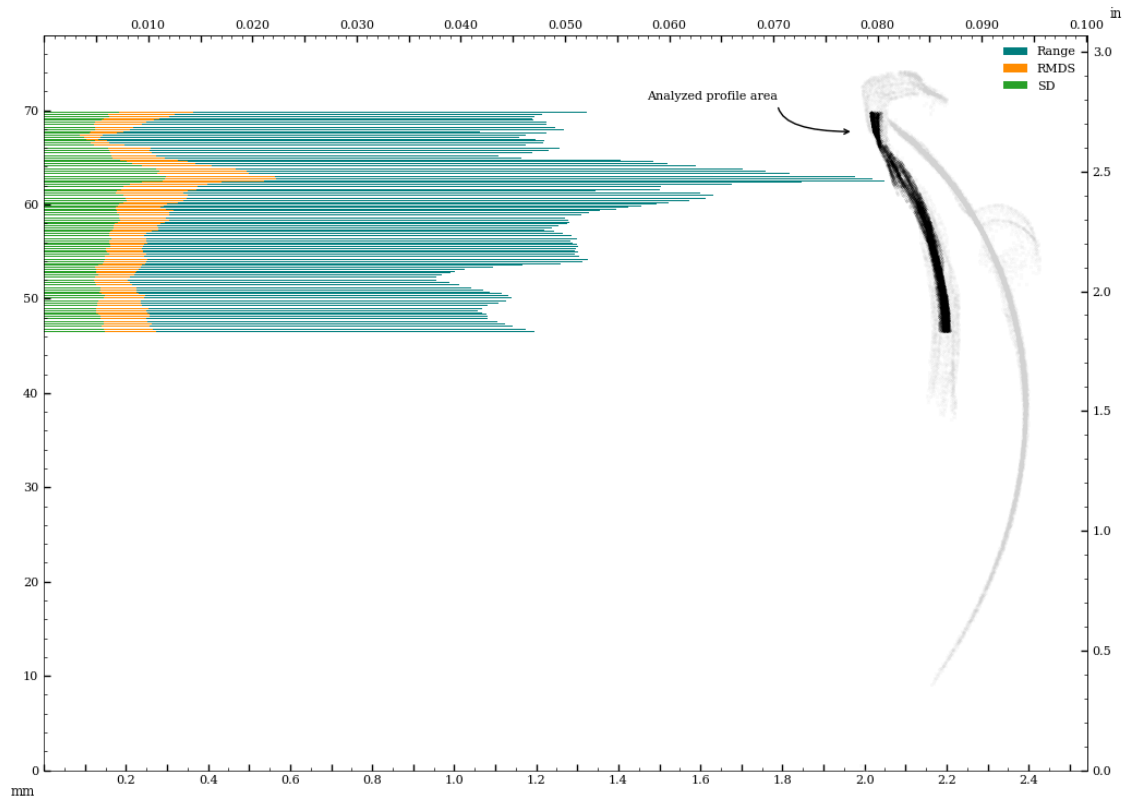


Figure 76: Circularity of interior_separate surface - perpendicular to surface curvature.

Circularity analysis of interior separately aligned surface - in z-plane

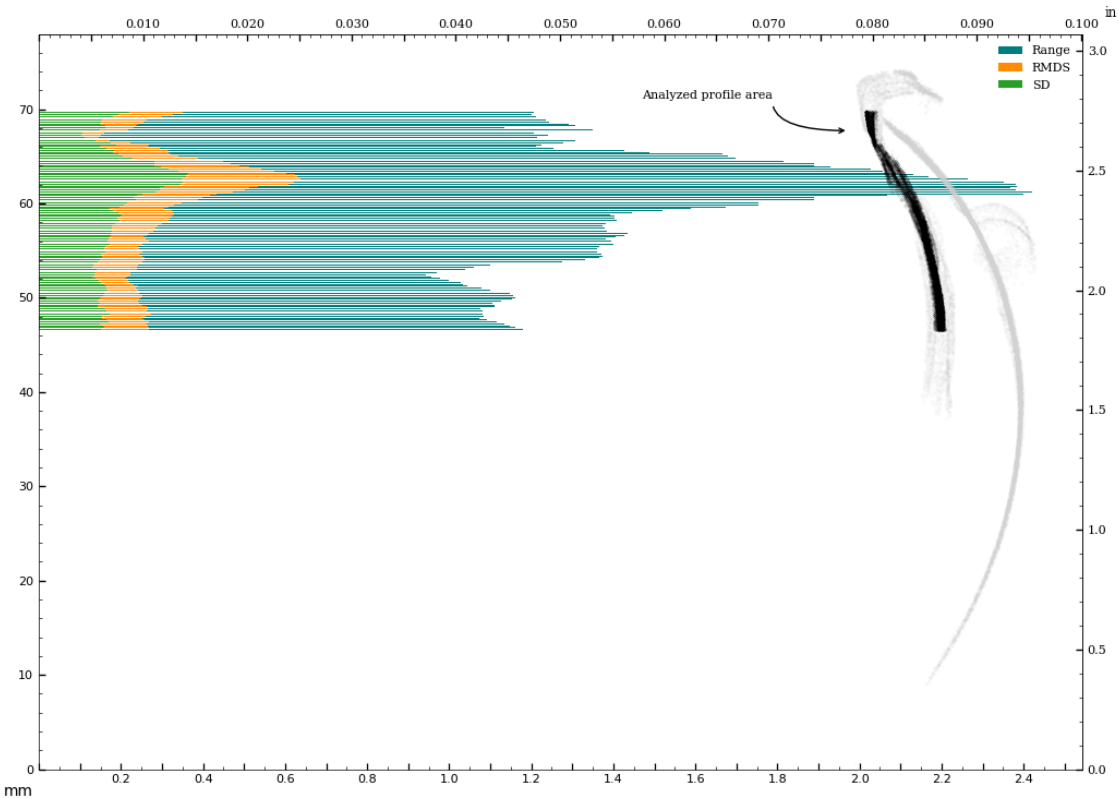


Figure 77: Circularity of interior_separate surface - in z-plane.

Circularity analysis of interior separately aligned surface, perpendicular to surface curvature, Standard Deviation and Root Mean Squared Deviation

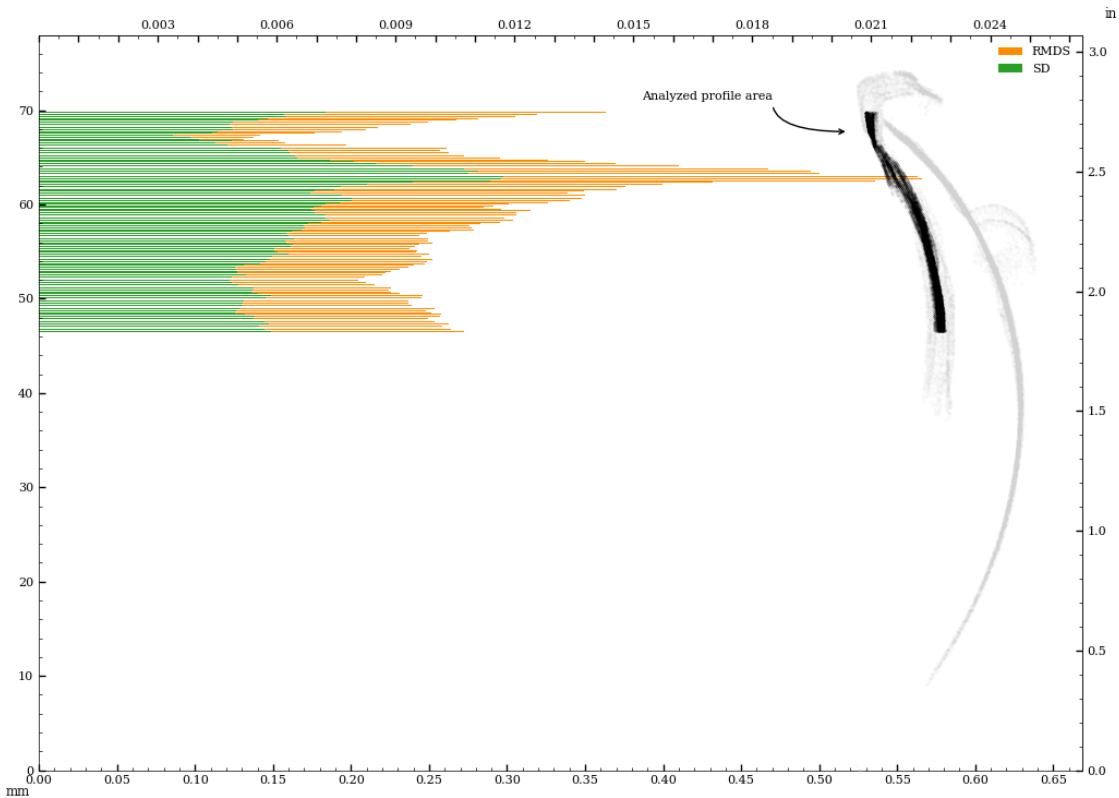


Figure 78: Vessel circularity of interior_separate surface, perpendicular to surface curvature, standard deviation and median absolute deviation.

Circularity analysis of interior separately aligned surface, in z-plane, Standard Deviation and Root Mean Squared Deviation

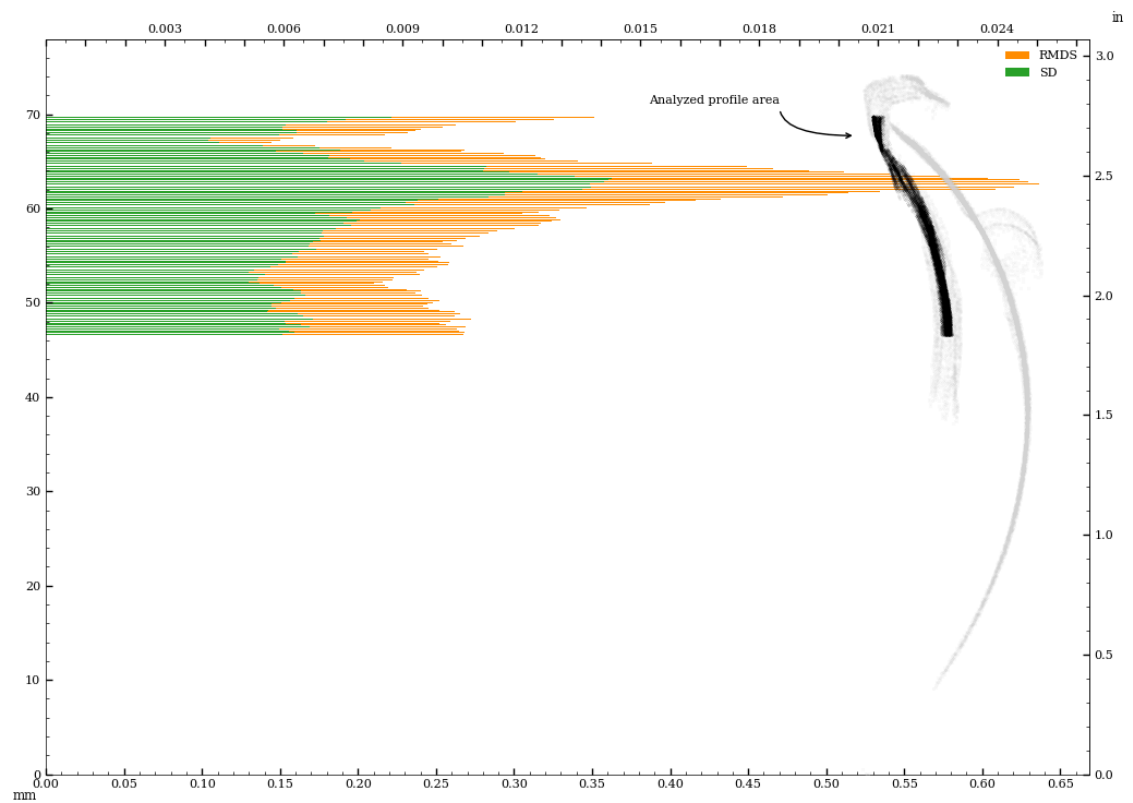


Figure 79: Vessel circularity of interior_separate surface, in z-plane, standard deviation and median absolute deviation.

Appendix B - Comparison Of Concentricity Measurements (Z-plane vs. surface-perpendicular)

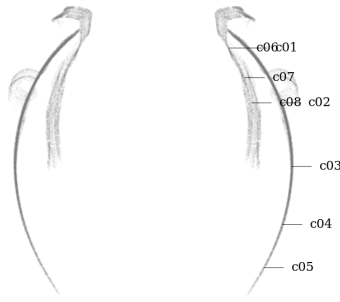


Figure 80: Circularity measurement sample locations, full mesh aligned to exterior surface

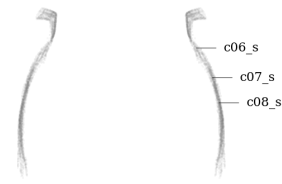


Figure 81: Circularity measurement sample location, separately aligned interior mesh

Concentricity measurements perpendicular to surface curvature

| Tag | Reference | Deviation | Sample size | Circle fit residuals analysis for sample listed in Tag column | | | | | | |
|-------|-----------|-----------|-------------|---|---------------|-----------|--------------|---------|------------|--------------|
| | | | | Range full | Range inliers | RMSD full | RMDS inliers | SD full | SD inliers | Center (x,y) |
| | | mm | | mm | mm | mm | mm | mm | mm | µm |
| c01 | z-axis | 0.229 | 3705 | 1.845 | 1.843 | 0.394 | 0.393 | 0.222 | 0.221 | −14, −229 |
| c02 | z-axis | 0.055 | 2511 | 1.205 | 0.935 | 0.180 | 0.163 | 0.119 | 0.102 | −26, 49 |
| c03 | z-axis | 0.046 | 1751 | 0.549 | 0.549 | 0.127 | 0.127 | 0.078 | 0.078 | −11, 45 |
| c04 | z-axis | 0.042 | 992 | 0.635 | 0.635 | 0.138 | 0.138 | 0.074 | 0.074 | 4, −42 |
| c05 | z-axis | 0.036 | 441 | 0.544 | 0.544 | 0.117 | 0.117 | 0.071 | 0.071 | −30, −20 |
| c06 | z-axis | 0.659 | 756 | 3.156 | 2.973 | 0.861 | 0.831 | 0.482 | 0.450 | 364, 550 |
| c06_s | z-axis | 0.659 | 756 | 3.156 | 2.973 | 0.861 | 0.831 | 0.482 | 0.450 | 364, 550 |
| c07 | z-axis | 0.111 | 1269 | 1.503 | 1.503 | 0.359 | 0.359 | 0.222 | 0.222 | 65, 89 |
| c07_s | z-axis | 0.111 | 1269 | 1.503 | 1.503 | 0.359 | 0.359 | 0.222 | 0.222 | 65, 89 |
| c08 | z-axis | 0.058 | 1397 | 1.009 | 1.009 | 0.225 | 0.225 | 0.126 | 0.126 | 41, 41 |
| c08_s | z-axis | 0.058 | 1397 | 1.009 | 1.009 | 0.225 | 0.225 | 0.126 | 0.126 | 41, 41 |
| c01 | c06 | 0.865 | | | | | | | | −378, −778 |
| c02 | c08 | 0.067 | | | | | | | | −67, 8 |

Concentricity measurements in z-plane

| Tag | Reference | Deviation | Sample size | Circle fit residuals analysis for sample listed in Tag column | | | | | | |
|-------|-----------|-----------|-------------|---|---------------|-----------|--------------|---------|------------|--------------|
| | | | | Range full | Range inliers | RMSD full | RMDS inliers | SD full | SD inliers | Center (x,y) |
| | | mm | | mm | mm | mm | mm | mm | mm | µm |
| c01 | z-axis | 0.229 | 3705 | 1.845 | 1.843 | 0.394 | 0.393 | 0.222 | 0.221 | −14, −229 |
| c02 | z-axis | 0.055 | 2511 | 1.205 | 0.935 | 0.180 | 0.163 | 0.119 | 0.102 | −26, 49 |
| c03 | z-axis | 0.046 | 1751 | 0.549 | 0.549 | 0.127 | 0.127 | 0.078 | 0.078 | −11, 45 |
| c04 | z-axis | 0.042 | 992 | 0.635 | 0.635 | 0.138 | 0.138 | 0.074 | 0.074 | 4, −42 |
| c05 | z-axis | 0.036 | 441 | 0.544 | 0.544 | 0.117 | 0.117 | 0.071 | 0.071 | −30, −20 |
| c06 | z-axis | 0.659 | 756 | 3.156 | 2.973 | 0.861 | 0.831 | 0.482 | 0.450 | 364, 550 |
| c06_s | z-axis | 0.659 | 756 | 3.156 | 2.973 | 0.861 | 0.831 | 0.482 | 0.450 | 364, 550 |
| c07 | z-axis | 0.111 | 1269 | 1.503 | 1.503 | 0.359 | 0.359 | 0.222 | 0.222 | 65, 89 |
| c07_s | z-axis | 0.111 | 1269 | 1.503 | 1.503 | 0.359 | 0.359 | 0.222 | 0.222 | 65, 89 |
| c08 | z-axis | 0.058 | 1397 | 1.009 | 1.009 | 0.225 | 0.225 | 0.126 | 0.126 | 41, 41 |
| c08_s | z-axis | 0.058 | 1397 | 1.009 | 1.009 | 0.225 | 0.225 | 0.126 | 0.126 | 41, 41 |
| c01 | c06 | 0.865 | | | | | | | | −378, −778 |
| c02 | c08 | 0.067 | | | | | | | | −67, 8 |

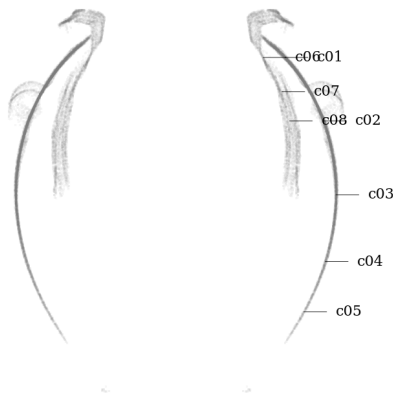


Figure 82: Circularity measurement sample locations, full mesh aligned to exterior surface

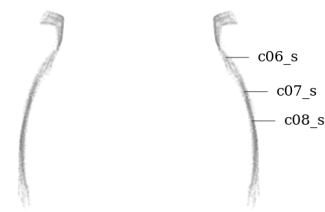


Figure 83: Circularity measurement sample location, separately aligned interior mesh

Concentricity measurements perpendicular to surface curvature

| Tag | Reference | Deviation | Sample size | Circle fit residuals analysis for sample listed in Tag column | | | | | | |
|-------|-----------|-----------|-------------|---|---------------|-----------|--------------|---------|------------|--------------|
| | | | | Range full | Range inliers | RMSD full | RMDS inliers | SD full | SD inliers | Center (x,y) |
| | | in | | in | in | in | in | in | in | thou |
| c01 | z-axis | 0.0090 | 3705 | 0.0726 | 0.0726 | 0.0155 | 0.0155 | 0.0087 | 0.0087 | −0.6, −9.0 |
| c02 | z-axis | 0.0022 | 2511 | 0.0475 | 0.0368 | 0.0071 | 0.0064 | 0.0047 | 0.0040 | −1.0, 1.9 |
| c03 | z-axis | 0.0018 | 1751 | 0.0216 | 0.0216 | 0.0050 | 0.0050 | 0.0031 | 0.0031 | −0.4, 1.8 |
| c04 | z-axis | 0.0017 | 992 | 0.0250 | 0.0250 | 0.0054 | 0.0054 | 0.0029 | 0.0029 | 0.2, −1.6 |
| c05 | z-axis | 0.0014 | 441 | 0.0214 | 0.0214 | 0.0046 | 0.0046 | 0.0028 | 0.0028 | −1.2, −0.8 |
| c06 | z-axis | 0.0259 | 756 | 0.1242 | 0.1170 | 0.0339 | 0.0327 | 0.0190 | 0.0177 | 14.3, 21.6 |
| c06_s | z-axis | 0.0259 | 756 | 0.1242 | 0.1170 | 0.0339 | 0.0327 | 0.0190 | 0.0177 | 14.3, 21.6 |
| c07 | z-axis | 0.0044 | 1269 | 0.0592 | 0.0592 | 0.0141 | 0.0141 | 0.0087 | 0.0087 | 2.6, 3.5 |
| c07_s | z-axis | 0.0044 | 1269 | 0.0592 | 0.0592 | 0.0141 | 0.0141 | 0.0087 | 0.0087 | 2.6, 3.5 |
| c08 | z-axis | 0.0023 | 1397 | 0.0397 | 0.0397 | 0.0089 | 0.0089 | 0.0050 | 0.0050 | 1.6, 1.6 |
| c08_s | z-axis | 0.0023 | 1397 | 0.0397 | 0.0397 | 0.0089 | 0.0089 | 0.0050 | 0.0050 | 1.6, 1.6 |
| c01 | c06 | 0.0341 | | | | | | | | −14.9, −30.6 |
| c02 | c08 | 0.0027 | | | | | | | | −2.6, 0.3 |

Concentricity measurements in z-plane

| Tag | Reference | Deviation | Sample size | Circle fit residuals analysis for sample listed in Tag column | | | | | | |
|-------|-----------|-----------|-------------|---|---------------|-----------|--------------|---------|------------|--------------|
| | | | | Range full | Range inliers | RMSD full | RMDS inliers | SD full | SD inliers | Center (x,y) |
| | | in | | in | in | in | in | in | in | thou |
| c01 | z-axis | 0.0090 | 3705 | 0.0726 | 0.0726 | 0.0155 | 0.0155 | 0.0087 | 0.0087 | −0.6, −9.0 |
| c02 | z-axis | 0.0022 | 2511 | 0.0475 | 0.0368 | 0.0071 | 0.0064 | 0.0047 | 0.0040 | −1.0, 1.9 |
| c03 | z-axis | 0.0018 | 1751 | 0.0216 | 0.0216 | 0.0050 | 0.0050 | 0.0031 | 0.0031 | −0.4, 1.8 |
| c04 | z-axis | 0.0017 | 992 | 0.0250 | 0.0250 | 0.0054 | 0.0054 | 0.0029 | 0.0029 | 0.2, −1.6 |
| c05 | z-axis | 0.0014 | 441 | 0.0214 | 0.0214 | 0.0046 | 0.0046 | 0.0028 | 0.0028 | −1.2, −0.8 |
| c06 | z-axis | 0.0259 | 756 | 0.1242 | 0.1170 | 0.0339 | 0.0327 | 0.0190 | 0.0177 | 14.3, 21.6 |
| c06_s | z-axis | 0.0259 | 756 | 0.1242 | 0.1170 | 0.0339 | 0.0327 | 0.0190 | 0.0177 | 14.3, 21.6 |
| c07 | z-axis | 0.0044 | 1269 | 0.0592 | 0.0592 | 0.0141 | 0.0141 | 0.0087 | 0.0087 | 2.6, 3.5 |
| c07_s | z-axis | 0.0044 | 1269 | 0.0592 | 0.0592 | 0.0141 | 0.0141 | 0.0087 | 0.0087 | 2.6, 3.5 |
| c08 | z-axis | 0.0023 | 1397 | 0.0397 | 0.0397 | 0.0089 | 0.0089 | 0.0050 | 0.0050 | 1.6, 1.6 |
| c08_s | z-axis | 0.0023 | 1397 | 0.0397 | 0.0397 | 0.0089 | 0.0089 | 0.0050 | 0.0050 | 1.6, 1.6 |
| c01 | c06 | 0.0341 | | | | | | | | −14.9, −30.6 |
| c02 | c08 | 0.0027 | | | | | | | | −2.6, 0.3 |